USGS
science for a changing world

The Las Vegas Formation

Professional Paper 1839

U.S. Department of the Interior
U.S. Geological Survey

Cover. Buff-colored deposits sit against the backdrop of the Las Vegas Range in the northern Las Vegas Valley. Once thought to be remnants of a large pluvial lake, these sediments actually record the presence of extensive paleowetlands that supported a diverse flora and fauna. Throughout the Quaternary, the wetlands expanded and contracted in response to abrupt changes in climate. These dynamic ecosystems are preserved in the geologic record as the Las Vegas Formation. (Photograph by Eric Scott, Cogstone Resource Management, Inc., used with permission)

The Las Vegas Formation

By Kathleen B. Springer, Jeffrey S. Pigati, Craig R. Manker, and Shannon A. Mahan

Professional Paper 1839

U.S. Department of the Interior
U.S. Geological Survey

U.S. Department of the Interior
RYAN K. ZINKE, Secretary

U.S. Geological Survey
James F. Reilly II, Director

U.S. Geological Survey, Reston, Virginia: 2018

Suggested citation:
Springer, K.B., Pigati, J.S., Manker, C.R., and Mahan, S.A., 2018, The Las Vegas Formation: U.S. Geological Survey Professional Paper 1839, 62 p., https://doi.org/10.3133/pp1839.

Library of Congress Cataloging-in-Publication Data

Names: Springer, Kathleen B., author. | Geological Survey (U.S.), issuing body.
Title: The Las Vegas Formation / by Kathleen B. Springer [and three others].
Other titles: U.S. Geological Survey professional paper ; 1839.
Description: Reston, Virginia : U.S. Department of the Interior, U.S. Geological Survey, 2018. | Series: Professional paper ; 1839 | Includes bibliographical references.
Identifiers: LCCN 2018029677 | ISBN 9781411342378 (paperback)
Subjects: LCSH: Formations (Geology)--Nevada--Las Vegas Valley. | Sediments (Geology)--Nevada--Las Vegas Valley. | Geology, Stratigraphic--Pleistocene. | Geology, Stratigraphic--Holocene.
Classification: LCC QE697 .S67 2018 | DDC 557.93/13--dc23 | SUDOC I 19.16:1839
LC record available at https://lccn.loc.gov/2018029677

ISSN 1044-9612 (print)
ISSN 2330-7102 (online)
ISBN 978-1-4113-4237-8

Acknowledgments

This study was inspired by our colleague and friend C. Vance Haynes, Jr., the vanguard of desert wetland research. This manuscript is a product of more than a decade of work investigating the deposits in the upper Las Vegas Wash. Early on, the Bureau of Land Management understood the significance of this important fossil-bearing sequence of "white dirt" and had the foresight to fund our work. In part, that recognition, and the science that came from their support, eventually led to the area being designated as Tule Springs Fossil Beds National Monument. We gratefully thank Gayle Marrs-Smith, Field Manager of the Bureau of Land Management's Southern Nevada District Office, and Scott Foss, Bureau of Land Management Senior Paleontologist, for their vision, assistance, and support of this work with funding through Federal Assistance Agreement L08AC13098 (to Kathleen Springer). We also extend great appreciation to the National Park Service and the leadership of Tule Springs Fossil Beds National Monument for their support of our ongoing work there, because the fossils are cool, but the rocks rock.

We thank Dan Muhs, Marith Reheis, Buddy Schweig, Randy Schumann, Keith Kirk, and Janet Slate (all U.S. Geological Survey) and Mark Springer (University of California, Riverside) for their constructive reviews of this manuscript. We also thank Paco van Sistine (U.S. Geological Survey) for assistance with figures 1 and 3. This project was funded in part by the U.S. Geological Survey's Land Change Science Program through the Paleohydrology of Desert Wetlands project.

Contents

Figures

Tables

Conversion Factors

International System of Units to U.S. customary units

Multiply	By	To obtain
	Length	
centimeter (cm)	0.3937	inch (in.)
micrometer (µm)	0.03937	mil
meter (m)	3.281	foot (ft)
	Density	
gram per cubic centimeter (g/cm^3)	62.4220	pound per cubic foot (lb/ft^3)

Temperature in degrees Celsius (°C) may be converted to degrees Fahrenheit (°F) as

$$°F = (1.8 \times °C) + 32$$

Abbreviations

>	greater than
%	percent
‰	part per thousand
^{14}C	radiocarbon
^{13}C	stable carbon isotope
^{18}O	oxygen isotope
ABA	acid-base-acid
ABOX	acid-base-wet oxidation
AMS	accelerator mass spectrometry
cal	calibrated
CO_2	carbon dioxide
D-O	Dansgaard-Oeschger
E	easting
GWD	groundwater discharge
Gy	gray (unit of measure for luminescence dose)
H_2O_2	hydrogen peroxide
HCl	hydrochloric acid
ID	identification
IR	infrared
IRSL	infrared-stimulated luminescence
K	potassium
ka	kilo-annum (thousands of years before present)
m	meter
MIS	marine isotope stage
N	northing
no.	number
OSL	optically stimulated luminescence
P	probability of the calibrated age falling within the reported range as calculated by CALIB v.7.1html
ppm	part per million
Th	thorium
TL	thermoluminescence
U	uranium
VPDB	Vienna Pee Dee Belemnite

The Las Vegas Formation

By Kathleen B. Springer,[1] Jeffrey S. Pigati,[1] Craig R. Manker,[2] and Shannon A. Mahan[1]

Abstract

The Las Vegas Formation was established in 1965 to designate the distinctive light-colored, fine-grained, fossil-bearing sedimentary deposits exposed in and around the Las Vegas Valley, Nevada. In a coeval designation, the sediments were subdivided into informal units with stratigraphic and chronologic frameworks that have persisted in the literature. Use of the Las Vegas Formation name over the past half century has been hampered because of the lack of a robust definition and characterization of the entire lithostratigraphic sequence, its geographic distribution, and chronology. This study evaluates and describes deposits attributed to the Las Vegas Formation with detailed stratigraphy, sedimentology, and field relations. A large suite of radiocarbon and luminescence ages facilitates revision and temporal expansion of the geochronology. In all, we characterize 17 informal geologic units within the formation, each dating to a unique period of geologic time, with stratigraphically ascending members X, A, B, D, and E and attendant beds in members B, D, and E. The age of the Las Vegas Formation spans at least the middle Pleistocene to early Holocene (from approximately 573 to 8.53 kilo-annum [thousands of years before present]) and is related to past episodes of groundwater discharge in the Las Vegas Valley. The contextual information derived from this new framework is dually noteworthy because the sediments entomb one of the most significant Pleistocene vertebrate faunas in the American Southwest, the Tule Springs local fauna, and represent a paleohydrologic system that responded dynamically to abrupt changes in climate throughout the late Quaternary. Characterizing the nature of these important deposits stabilizes the nomenclature, promotes the continued use of the informal units within the formation, and facilitates studies of similar deposits associated with desert wetland ecosystems elsewhere in the southwestern United States.

Introduction

The upper Las Vegas Wash, located in the northern Las Vegas Valley, Nevada, has exposed prominent and distinctive light-colored, fine-grained sediments along its length. These sediments occupied much of the Las Vegas Valley prior to extensive urbanization of the cities of Las Vegas and North Las Vegas (Longwell and others, 1965; Haynes, 1967; Bingler, 1977; Matti and Bachhuber, 1985; Matti and others, 1987, 1993; Bell and others, 1998, 1999; Page and others, 2005; Ramelli and others, 2011, 2012). Today, exposures are restricted primarily to the upper Las Vegas Wash and Corn Creek flat areas, coincident with the boundaries of Tule Springs Fossil Beds National Monument, and also extend north and west to Indian Springs and Cactus Springs (fig. 1).

Early Investigations

Geologist Chester Longwell named these deposits the Las Vegas Formation, describing them as "light-colored deposits of clay and silt" (Longwell and others, 1965, p. 50) with "abundant lenses of water-worn gravel" (Longwell and others, 1965, p. 52). The presence of fossil mollusks and vertebrate megafauna led him to assign a Pleistocene age to the deposits, which he mapped as Quaternary lacustrine (Ql) (Longwell, 1946; Longwell and others, 1965). Within the fine-grained sediments, he also described extensive cut-and-fill features that he interpreted as representing aggrading streams with wide flood plains that were likely exploited by Pleistocene megafauna. He observed thin, horizontal bedding within the sedimentary sequence and, together with the nature and abundance of fossil mollusk shells, concluded that the Las Vegas Formation represented shallow lakes that once occupied the valley (Longwell, 1946). As supporting evidence, he noted that two large alluvial fans, one emanating from the Spring Mountains and the other from the Sheep Range (fig. 1), could have coalesced and formed a barrier to overland flow, creating a series of shallow lake basins and flood plains in the valley.

Prior to Longwell and others (1965), both Rose (1938) and Longwell (1946) proposed that the fine-grained deposits of the Las Vegas Valley may have close genetic and temporal affinities with the Chemehuevi Formation, which is exposed along the main stem of the Colorado River. Similar to the Las Vegas Formation, Longwell and colleagues interpreted the Chemehuevi Formation as having been deposited in a lake that once filled the Colorado River Valley, and based on the composition of vertebrate fossils and abundant invertebrates, also assigned it a Pleistocene age (Longwell, 1946, 1963; Longwell and others, 1965). The lacustrine origin of the Chemehuevi

[1]U.S. Geological Survey.

[2]California State Polytechnic University.

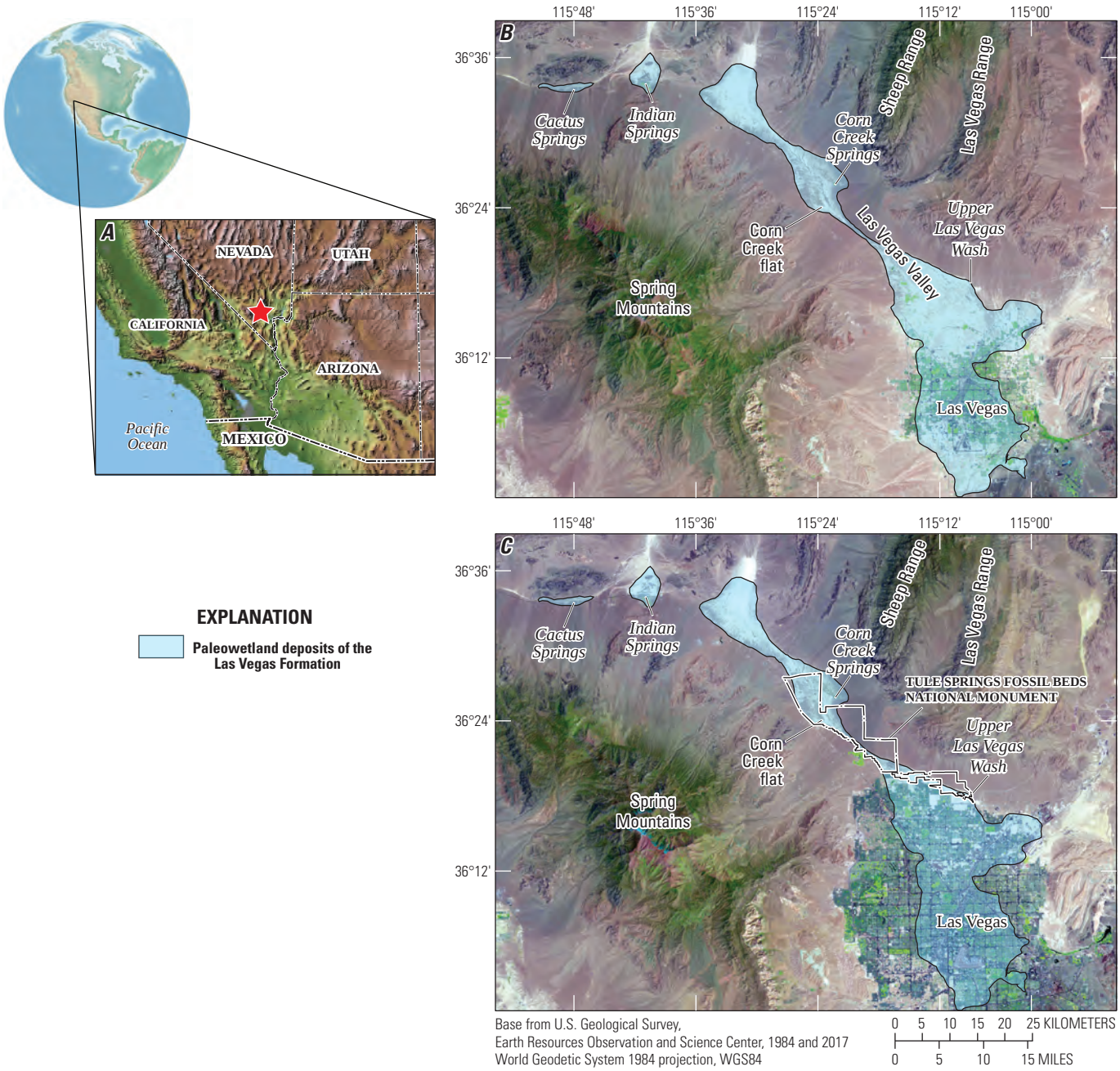

Figure 1. Location and geographic extent of the Las Vegas Formation. *A*, Site location map for the Las Vegas Valley of southern Nevada (red star). *B*, Landsat image from 1984 showing the geographic extent of the paleowetland deposits attributed to the Las Vegas Formation that were exposed throughout most of the valley (Longwell and others, 1965; Page and others, 2005). *C*, Landsat image from 2017 showing the substantial loss of the deposits to urban expansion in the intervening decades. The last contiguous vestiges of the formation are protected in Tule Springs Fossil Beds National Monument on the northern end of the Las Vegas metropolitan area, the boundary of which is shown in panel *C*. Additional deposits attributed to the formation are located at Indian Springs and Cactus Springs to the northwest. Landsat images are courtesy of the U.S. Geological Survey's Earth Resources Observation and Science Center.

deposits was ascribed to natural damming of the Colorado River, in contrast to the Las Vegas Formation, which was interpreted to be the result of the onset of more humid climatic conditions in the desert during times of Pleistocene glaciation (Longwell and others, 1965). Based on these lines of evidence, Longwell reasoned that the Las Vegas Formation was distinctive enough to be mapped separately from other Quaternary units in the region, but he did not go so far as to differentiate individual units within the newly named formation.

Longwell and others (1965) designated the type section along the upper Las Vegas Wash in the northeast quarter of T. 19 S., R. 60 E. and also noted that the geographic distribution of the Las Vegas Formation included "several large areas along Las Vegas Valley, from the vicinity of Las Vegas to a point several miles west of Indian Springs [with] extensions of outcrop areas…northward into the wide valleys east and west of the Pintwater Range" (Longwell and others, 1965, p. 50). In addition, these researchers observed that deposits strikingly similar to those in the Las Vegas Valley are exposed in parts of Pahrump Valley to the west. Because of a lack of detailed geologic mapping at the time, however, they chose to exclude those deposits from the Las Vegas Formation.

Geologist C. Vance Haynes, Jr., followed these early investigations by establishing detailed stratigraphic and chronologic frameworks for the sediments as part of a multidisciplinary study in 1962–63 called the Tule Springs Expedition (Wormington and Ellis, 1967). The primary objective of the expedition was to determine whether or not humans and Pleistocene animals were contemporaneous in the valley and, if so, during what period of geological time. Since the early 1900s, the Tule Springs area in the upper Las Vegas Wash has garnered widespread interest arising from the discovery of human cultural artifacts and vertebrate megafauna. From the 1930s to the 1960s, numerous archaeologic and paleontologic expeditions were mounted from natural history museums throughout the United States to investigate the early peopling of North America (for example, Simpson, 1933; Harrington, 1955; Harrington and Simpson, 1961). As part of the Tule Springs Expedition, Haynes directed geological investigations with the aid of massive trenches dug by heavy equipment.

Haynes (1967) subdivided the sedimentary sequence into eight stratigraphically informal units and stated they were included in the Las Vegas Formation of Longwell and others (1965). He designated the ascending units X and A through G, denoted subunits with subscript numerals (1, 2, and 3), and identified intervening buried soils as S1 through S6. The type exposure for Haynes' informal classification is located in the longest and deepest trench dug for the study—Trench K (Haynes, 1967, Trench K plate). Based on nearly 80 radiocarbon (^{14}C) ages, the degree of soil development, and physical characteristics of the sediments, he concluded that units A–E were Pleistocene in age and units F and G were deposited during the Holocene (fig. 2; app. 1). In addition, he referred to fine-grained deposits in the Las Vegas Valley older than unit A as unit X (shown by map unit Qx). Haynes' classification (1967), with its pioneering stratigraphy and chronology, has persisted in the literature, and his unit designations have been correlated to similar deposits throughout the eastern Mojave Desert and southern Great Basin (Quade, 1986; Quade and Pratt, 1989; Quade and others, 1995, 1998, 2003; Pigati and others, 2011), with the recognition that they represent ancient desert wetland ecosystems.

Desert Wetlands

Desert wetlands are common features in arid lands worldwide; they form in broad valleys and basins where water tables approach or breach the ground surface (Pigati and others, 2014). They are expressed on the landscape in a variety of hydrologic settings, including seeps, marshes, wet meadows, spring pools, and flowing streams. Over time, eolian and alluvial sediments are trapped by dense vegetation and wet ground conditions, resulting in a unique combination of clastic sediments, chemical precipitates, and organic matter that are collectively referred to as groundwater discharge (GWD) deposits.

GWD deposits contain information on the timing and magnitude of past changes in local or regional hydrologic budgets and mark the position of past groundwater "high stands" on the landscape. Importantly, they can be distinguished from lake sediments by using sedimentologic and stratigraphic properties, geomorphic features, and microfaunal assemblages (ostracodes, gastropods, and diatoms) (Pigati and others, 2014). Within wetland settings, specific hydrologic regimes can be delineated based on the types of sediments left behind in the geologic record, as well as on floral and faunal assemblages. For example, geologist Jay Quade (Quade, 1986; Quade and Pratt, 1989; Quade and others, 1995) recognized several different sedimentary facies in both extant and paleowetland systems, including dry alluvial fan environments, phreatophyte flats (areas where groundwater has not breached the surface but is shallow enough that plants can tap into it), wet meadows and marshes, spring orifices, and outflow streams. In addition to sedimentological properties, Quade and other researchers have shown that ostracode and gastropod assemblages can be used to delineate different spring hydrologic regimes in both extant and fossil wetland systems (for example, Bequaert and Miller, 1973; Quade, 1986; Quade and Pratt, 1989; Forester, 1991; Quade and others, 2003; Pigati and others, 2011).

GWD deposits are relatively common in desert environments and, since they were first recognized in the mid-1980s, have been identified in all four major deserts of the American Southwest, the Atacama Desert of northern Chile, the Middle East, North Africa, Australia, and Tibet (see Pigati and others, 2014, and references therein). In the Mojave Desert alone, there are more than 130 different localities that exhibit some evidence of past groundwater discharge (Schmidt and McMackin, 2006; Bedford and others, 2010; Amoroso and Miller, 2012). Given their widespread distribution, GWD deposits represent a largely untapped source of valuable paleohydrologic and paleoclimatic information that can be examined and queried on a variety of spatial and temporal scales.

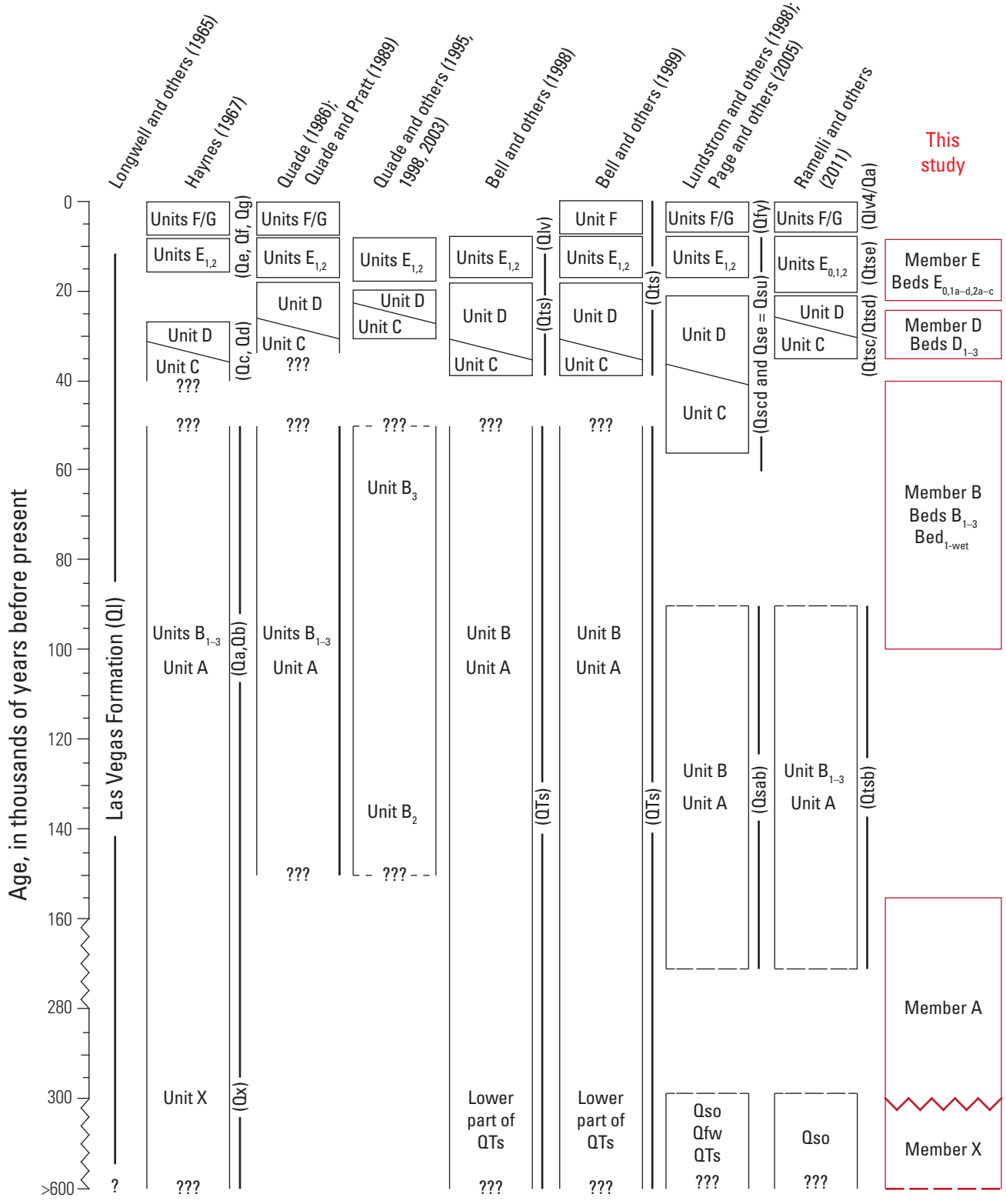

Figure 2. Interpretations of informal units within the Las Vegas Formation, as well as of younger, erosionally inset, limestone gravel units (such as units F and G of Haynes [1967]), as presented in various studies since the formation was defined by Longwell and others (1965). Unit designations made in those studies, as well as in this one, are shown in columns with map designations shown to the right. Positions of the unit boxes along the vertical axis are based on each study's inherited or constructed chronologies. The unit boxes use different types of boundaries to denote varying types of age control: solid horizontal lines for firm age control, solid diagonal lines when ages of different units overlap, dashed lines for age control with large uncertainties or ranges, and question marks for units with no age control.

Groundwater Discharge Deposits in the Las Vegas Valley

The Las Vegas Formation sediments were initially interpreted to be strictly lacustrine in origin (Hubbs and Miller, 1948; Maxey and Jamesson, 1948; Snyder and others, 1964; Longwell and others, 1965). Haynes (1967) determined that at least some of the sediments were deposited in ciénegas, or desert wetlands, specifically in spring pools and outflow streams, although he supported the existence of "Pluvial Lake Las Vegas" in the valley between approximately 35 and 20 kilo-annum (ka [thousands of years before present]) based on the spatial abundance of deposits that date to the last full glacial period. Mifflin and Wheat (1979) later proposed that stratigraphic and paleontologic evidence suggested that deposition of sediments attributed to the Las Vegas Formation occurred in paludal, or marshy, environments, rather than a series of shallow lakes.

Quade and colleagues provided additional evidence of extensive paleowetland systems in the Las Vegas Valley based on exposures in the northwestern part of the valley in the upper Las Vegas Wash, Corn Creek flat, Indian Springs, and Cactus Springs (Quade, 1986; Quade and Pratt, 1989; Quade and others, 1995). In these areas, they documented former desert wetland ecosystems and identified multiple depositional facies within the last full-glacial sedimentary sequence. In cross section, orthogonal to the valley axis, the facies are distributed from the valley bottom to upland alluvial fans and include shallow, spring-fed bodies of water in the center of the valley that supported marshes and adjacent wet meadows (represented by white silts and green clays), a broad phreatophyte flat (brown silts and fine sands), and an upland alluvial fan apron (coarse sands and gravels).

These and other studies (for example, Hay and others, 1986; Pigati and others, 2011) have recorded the presence of past episodes of groundwater discharge in the southern Great Basin and Mojave Desert in areas formerly reported as lacustrine. Most of these records show that springs and desert wetlands in the region expanded and contracted in response to hydrologic changes arising from past climate fluctuations on glacial to interglacial timescales. More recent studies have shown that wetlands in the Las Vegas Valley actually responded to abrupt changes in climate on millennial to submillennial timescales (Springer and others, 2015). These dynamic ecosystems supported a diverse flora and fauna throughout the late Pleistocene (Scott and Springer, 2016; Scott and others, 2017) and are preserved in the geologic record as the deposits distributed along the length of the valley that are, in totality, what Longwell and others (1965) assigned to the Las Vegas Formation.

Subsequent Mapping and Topical Studies

Quade and colleagues followed up on the initial work of Longwell and others (1965) and Haynes (1967) and correlated the informal units of Haynes (1967) to sites throughout the Las Vegas Valley, including Corn Creek flat and Cactus Springs (fig. 1), and elsewhere in the southern Great Basin and Mojave Deserts, including Valley Wells, Chicago Valley, and Piute Valley in California and Lathrop Wells, Ash Meadows, Pahrump Valley, Indian Springs Valley, Three Lakes Valley, and Coyote Springs Valley in Nevada (Quade, 1986; Quade and Pratt, 1989; Quade and others, 1995, 1998, 2003). These authors refined the chronology of the deposits using ^{14}C dating of a variety of materials, including carbonized wood, bulk organic matter, humic acids, and gastropod shells. They also demonstrated unequivocally that units B_2, D, E_1, and E_2 of Haynes (1967) were, in fact, deposited in association with spring discharge. Importantly, they showed that extant desert wetlands in several north-central Nevada valleys are appropriate modern analogs for the GWD deposits in the Las Vegas Valley (Quade and others, 1995).

Successive mapping investigations in the Las Vegas Valley (Longwell and others, 1965; Haynes, 1967; Bingler, 1977; Matti and Bachhuber, 1985; Matti and others, 1987, 1993; Bell and others, 1998, 1999; Lundstrom and others, 1998; Page and others, 2005; Ramelli and others, 2011, 2012) also recognized sediments attributed to the Las Vegas Formation and have generally used Haynes' informal stratigraphic framework (1967) while expanding the geographic distribution, lithologies, paleoenvironments, and chronology of the formation (fig. 2; apps. 1 and 2). Donovan (1996) diverged significantly from this framework, citing difficulties with working with the named lithostratigraphic units in the Las Vegas Valley, and suggested the use of allostratigraphic units, which are defined in terms of bounding discontinuities rather than lithology, as an alternative to describe the sediments in the Las Vegas Valley. His "Tule Springs Alloformation" combined all of the exposed Pleistocene sediments in the northwestern Las Vegas Valley into a single unit, with the fine-grained sediments of the Las Vegas Formation consisting of fine-grained facies and contemporaneous alluvial fan sediment consisting of coarse-grained facies. A "mixed" facies was also determined to occur locally between the two facies.

Bell and others (1998, 1999) incorporated Donovan's interpretation (1996) in their mapping of the North Las Vegas area to some degree. In their usage, QTs (undivided older fine-grained alluvium) included units A and B; Qts (fine-grained alluvium of Tule Springs) included units C, D, and (in part) E; and Qlv (mainstream alluvium of Las Vegas Wash) consisted of unit E_2 (fig. 2). More recent mapping efforts (Ramelli and others, 2011, 2012) and topical studies (Springer and others, 2015; Scott and Springer, 2016; Scott and others, 2017) have not adopted the alloformation approach but instead have augmented and expanded the original stratigraphic and chronologic frameworks of Haynes (1967).

This Study

Haynes' informal classification (1967) of the deposits of the Las Vegas Formation has persisted for decades. The current study builds upon that scaffolding by using recent advances in the identification and delineation of subunits within the formation, improved ^{14}C dating and new luminescence techniques, and the recognition of similar deposits outside the Las Vegas Valley. Detailed field investigations have resulted in the identification of several new units, and numerous new ^{14}C and luminescence ages have significantly refined and expanded the chronology of the stratigraphic sequence.

Although the North American Stratigraphic Code allows for formal redefinition or revision of a formation (North American Commission on Stratigraphic Nomenclature, 2005), that endeavor would be impractical in the case of the Las Vegas Formation because it would necessitate the assignment of at least 20 new names for the members and beds that we attribute to the formation. In our view, and in the interests of maintaining nomenclatural continuity, it is more sensible and efficacious to expand upon the informal classification of Haynes (1967). Therefore, this study utilizes his original framework, albeit greatly augmented and refined, and includes a hierarchy of informal members and beds based on lithologic characteristics and stratigraphic relations that were employed previously by Scott and Springer (2016), Scott and others, 2017, and Springer and others (2017a, b). Our objective is to stabilize the nomenclature and facilitate communication regarding the sediments that make up the Las Vegas Formation, as well as to promote the continued use of these informal units by the scientific community, which will have great utility in future geologic, paleontologic, and climate studies of paleowetland deposits throughout the southwestern United States.

Methods

Standard stratigraphic and sedimentologic field practices and techniques were employed during the course of this investigation. Multiple stratigraphic sections from the study area were measured and the lithologies described to build the composite stratigraphy of the Las Vegas Formation deposits. Materials for both ^{14}C and luminescence dating methods were collected and analyzed according to standard protocols, which resulted in the expanded chronologic framework of the Las Vegas Formation described herein.

Field Methods

A total of 52 stratigraphic sections throughout the upper Las Vegas Wash were described and measured; they were then used to construct a composite stratigraphy of the sediments that make up the Las Vegas Formation. At each section, we determined the sedimentologic properties at both the outcrop scale (for example, bedding, unit thickness, and structures) and hand-sample scale (for example, grain size, sorting, and color) and also established the stratigraphic boundaries of the units present at each location. Field textures were determined by using procedures described in the U.S. Department of Agriculture's 1951 Soil Survey Manual (U.S. Department of Agriculture, 1951), and dry sediment colors were determined using the Munsell Soil Color Chart (Munsell Color [Firm], 2010). Bulk sediment, tufa, and samples for ^{14}C and luminescence dating were collected and curated at the San Bernardino County Museum in Redlands, California (this collection currently resides at the Las Vegas Natural History Museum in Las Vegas, Nevada), and the U.S. Geological Survey in Denver, Colorado. All described sections were photodocumented, and their positions were recorded with handheld Global Positioning System units.

Radiocarbon Dating Methods

Radiocarbon dating of charred vascular plants (charcoal) and, to a lesser extent, small, terrestrial gastropod shells (Succineidae) was used to establish the chronologic framework of the Las Vegas Formation for approximately the past 40 ka (see fig. 3 for spatial coverage and table 1 for specific sampling locations). Charcoal is well known for producing reliable ^{14}C ages (Jull and Burr, 2015) and was the preferred target material for dating. Prior to analysis, PaleoResearch Institute in Golden, Colorado, identified a few aliquots of charcoal to genus level, but most were not identified (table 1). Previous work has shown the Succineidae shells also yield reliable ^{14}C ages regardless of the local habitat, environmental conditions, and geologic substrate (Pigati and others, 2010, 2013). Radiocarbon dating of Succineidae shells has been used previously to establish the chronology of sediments in desert wetland ecosystems in the southwestern United States (Pigati and others, 2009, 2011).

All charcoal samples were subjected to either the standard acid-base-acid treatment or acid-base-wet oxidation before combustion online in the presence of excess high-purity oxygen. Clean, dry gastropod shells were broken and examined under a dissecting microscope to ensure that the interior whorls were free of secondary carbonate and detritus. Shells that were free of detritus were treated with 30 percent hydrogen peroxide (H_2O_2) to remove organic matter and then etched with dilute hydrochloric acid (HCl) to remove as much as 30–50 percent of the total mass prior to hydrolysis. Several shells were selected at random for X-ray diffraction analysis to verify that only primary shell aragonite remained before preparation for ^{14}C analysis. None of the shells that were analyzed contained measurable quantities of secondary calcite. Shell carbonate was converted to carbon dioxide (CO_2) using American Chemical Society reagent grade 85 percent phosphoric acid (H_3PO_4) under vacuum at 50 °C until the reaction was visibly complete (typically around 1 hour).

For all samples, water and other contaminant gases (including sulfur oxides [SO_x], nitrogen oxides [NO_x], and halide species) were removed using a combination of cryogenic separation and high-temperature, fine-wire copper and silver wool traps. The resulting pure CO_2 gas was measured manometrically and split into two aliquots. One aliquot was converted to graphite using an iron catalyst and the standard hydrogen reduction process and submitted for ^{14}C analysis by accelerator mass spectrometry. For samples submitted to Beta Analytic, Inc. (Miami, Florida), the former U.S. Geological Survey radiocarbon lab in Reston, Virginia, and Aeon Laboratories, LLC (Tucson, Arizona), the second aliquot of purified CO_2 was submitted for stable carbon isotope ($\delta^{13}C$) analysis to correct the measured ^{14}C activity of the shell carbonate for isotopic fractionation. These laboratories are denoted by Beta, CAMS, and Aeon numbers, respectively, in table 1. The resulting ^{14}C ages were calibrated using the IntCal13 dataset and CALIB v.7.1html (Stuiver and Reimer, 1993; Reimer and others, 2013). Ages are presented in thousands of calibrated years before present (A.D. 1950), and uncertainties are given at the 95 percent (2σ) confidence level.

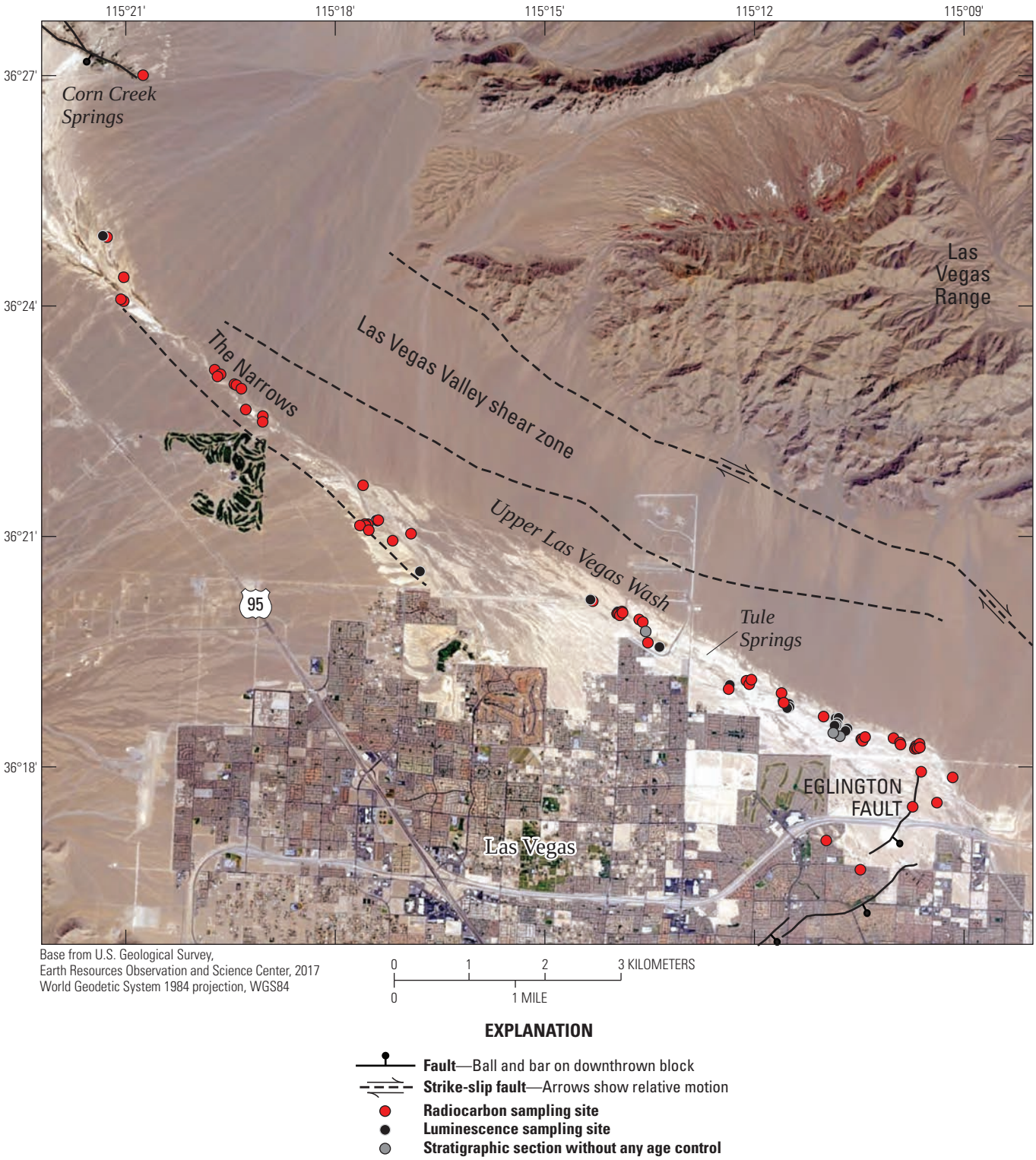

Figure 3. Landsat image from 2017 of the upper Las Vegas Wash showing major physiographic features and the spatial coverage of the radiocarbon and luminescence sampling sites and the stratigraphic sections that do not have any age control. Universal Transverse Mercator coordinates for all samples are given in tables 1 and 2. Landsat image courtesy of the U.S. Geological Survey's Earth Resource Observation and Science Center.

Table 1. Summary of sample information, radiocarbon (^{14}C) ages, and calibrated ages.

[Uncertainties for the calibrated ages are given at the 95 percent (2σ) confidence level, and all others are given at the 68 percent (1σ) confidence level. no., number; AMS, accelerator mass spectrometry; $\delta^{13}C$, stable carbon isotope; VPDB, Vienna Pee Dee Belemnite; ‰, part per thousand; ka, kilo-annum (thousands of years before present); cal, calibrated; P, probability of the calibrated age falling within the reported range as calculated by CALIB v.7.1html; ABA, acid-base-acid; HCl, hydrochloric acid; ABOX, acid-base-wet oxidation; >, greater than]

Sample no.	AMS no.	Section	Easting[1]	Northing[1]	Bed	Context	Material dated	Treatment	$\delta^{13}C_{VPDB}$ (‰)	^{14}C age (ka)	Age (cal ka)[2]	P
11KS2-8.1	Beta-294464	E_2-7	665039	4016945	E_{2c}	Black mat	Charcoal	ABA	–26.8	7.77±0.05	8.53±0.10	1.00
15JP11-22.1B	Aeon-2134	E_2-3	664239	4017550	E_{2c}	Black mat	Charcoal	ABA	*–25*[3]	8.68±0.04	9.62±0.08	1.00
10CM8-25.1	Beta-289513	E_2-2	666650	4018545	E_{2c}	Black mat	Charcoal[4a]	ABA	*–25*[3]	9.40±0.05	10.63±0.12	1.00
LVV-X-5	CAMS-165865	E_2-4	653593	4023954	E_{2b}	Black mat	Charcoal	ABA	–26.1	9.68±0.03	10.91±0.03	0.17
											11.14±0.06	0.83
09CM11-5.1	Beta-269140	E_2-1	664879	4019853	E_{2b}	Black mat	Organic sediment	ABA	–22.8	9.79±0.07	11.22±0.14	0.96
10CM3-11.1	Beta-279304	E_2-5	666258	4019211	E_{2a}	Black mat	Charcoal[4b]	ABA	–25.4	10.48±0.06	12.35±0.23	1.00
16CCS8-28.1A	Aeon-2311	E_2-6	647966	4033640	E_{2a}	Black mat	Organic sediment	ABA	*–25*[3]	10.87±0.06	12.77±0.09	1.00
LVV-X-7	CAMS-165864	E_2-4	653593	4023954	E_{2a}	Sediment	Succineidae	HCl	–6.7	10.99±0.03	12.85±0.12	1.00
LVV-X-4	CAMS-165866	E_2-4	653593	4023954	E_{2a}	Black mat	Charcoal	ABA	–24.5	11.03±0.04	12.90±0.12	1.00
10CM3-18.3	Beta-297878	E_1-12	666115	4018420	E_{1d}	Black mat	Charcoal	ABA	–25.5	11.53±0.05	13.37±0.09	1.00
LVV-X-3	CAMS-165867	E_2-4	653593	4023954	E_{1d}	Black mat	Charcoal	ABA	–25.4	11.68±0.04	13.50±0.07	1.00
03KS9-23.1	Beta-346502	E_1-9	649971	4027181	E_{1d}	Sediment	Charcoal	ABA	–26.3	11.88±0.06	13.69±0.14	1.00
12CM4-19.4A	Beta-320860	E_1-8	650108	4027087	E_{1c}	Black mat	Charcoal	ABA	–27.0	12.10±0.05	13.95±0.16	1.00
13MS3-11.1 (U)	Beta-346504	E_1-10	651107	4026213	E_{1c}	Black mat	Charcoal	ABA	–25.1	12.21±0.06	14.12±0.21	0.99
12CM4-18.1A	Aeon-970	E_1-11	647851	4028585	E_{1b}	Black mat	Charcoal	ABA	–27.3	12.28±0.05	14.27±0.25	1.00
12KS2-2.1	Beta-317293	E_1-6	650592	4026798	E_{1b}	Sediment	Charcoal	ABA	–26.3	12.32±0.07	14.39±0.34	1.00
LVV-X-1	CAMS-165868	E_2-4	653593	4023954	E_{1b}	Black mat	Charcoal	ABA	–24.9	12.37±0.04	14.42±0.28	1.00
10CM3-18.1A	Beta-279305	E_1-1	664885	4019852	E_{1b}	Black mat	Charcoal[4c]	ABA	–22.6	12.43±0.06	14.56±0.38	1.00
03CM10-9.1 (M)	Aeon-1179	E_1-3	654570	4023804	E_{1b}	Sediment	Charcoal	ABA	–26.5	12.42±0.13	14.59±0.50	1.00
12CM4-19.4B	Beta-320861	E_1-8	650108	4027087	E_{1a}	Black mat	Charcoal	ABA	–25.3	12.62±0.05	14.96±0.23	1.00
12CM4-18.1B	Aeon-971	E_1-11	647851	4028585	E_{1a}	Sediment	Charcoal	ABA	–27.6	12.73±0.06	15.14±0.23	1.00
16KS7-19.1A	Aeon-2308	E_1-13	650477	4026871	E_{1a}	Sediment	Charcoal	ABA	*–25*[3]	12.74±0.05	15.17±0.16	1.00
10CM4-22.1	Beta-279251	E_1-2	664958	4019904	E_{1a}	Black mat	Charcoal	ABA	–21.8	12.84±0.06	15.35±0.22	1.00

Table 1. Summary of sample information, radiocarbon (^{14}C) ages, and calibrated ages.—Continued

[Uncertainties for the calibrated ages are given at the 95 percent (2σ) confidence level, and all others are given at the 68 percent (1σ) confidence level. no., number; AMS, accelerator mass spectrometry; $\delta^{13}C$, stable carbon isotope; VPDB, Vienna Pee Dee Belemnite; ‰, part per thousand; ka, kilo-annum (thousands of years before present); cal, calibrated; P, probability of the calibrated age falling within the reported range as calculated by CALIB v.7.1html; ABA, acid-base-acid; HCl, hydrochloric acid; ABOX, acid-base-wet oxidation; >, greater than]

Sample no.	AMS no.	Section	Easting[1]	Northing[1]	Bed	Context	Material dated	Treatment	$\delta^{13}C_{VPDB}$ (‰)	^{14}C age (ka)	Age (cal ka)[2]	P
12CM4-19.2	Aeon-973	E_1-4	653434	4024815	E_{1a}	Black mat	Charcoal	ABA	–24.6	12.92±0.07	15.46±.025	1.00
12CM4-19.3	Beta-320859	E_1-7	650430	4026888	E_{1a}	Sediment	Charcoal	ABA	–24.0	13.04±0.05	15.59±0.24	1.00
12CM8-17.1	Aeon-1180	E_1-5	651111	4026089	E_{1a}	Sediment	Charcoal	ABA	–26.1	13.09±0.14	15.67±0.42	1.00
10CM3-18.1B	Beta-279306	E_1-1	664885	4019852	E_{1a}	Black mat	Charcoal[4d]	ABA	–25.7	13.39±0.06	16.10±0.21	1.00
15KS9-10.1	Aeon-2209	E_0-6	654196	4023801	E_0	Black mat	Charcoal	ABA	*–25*[3]	14.95±0.06	18.16±0.19	1.00
15JP11-20.2	CAMS-173741	E_0-4	659993	4021705	E_0	Black mat	Organic sediment	ABA	–22.2	15.54±0.04	18.80±0.11	1.00
10CM6-30-H-C1	Aeon-591	E_0-2	665593	4019918	E_0	Sediment	Charcoal	ABA	–21.9	15.79±0.05	19.04±0.14	1.00
SBCM 2-6-74	CAMS-175648	E_0-3	663037	4020771	E_0	Sediment	Succineidae	HCl	–85	16.18±0.06	19.52±0.22	1.00
09CM9-2.1	Beta-264965	E_0-1	665757	4019826	E_0	Sediment	Charcoal	ABA	–23.8	16.30±0.07	19.71±0.22	1.00
09CM9-2.1C	Beta-272512	E_0-1	665744	4019833	E_0	Sediment	Charcoal	ABA	–20.4	16.82±0.07	20.28±0.22	1.00
11KS4-17.1	Beta-297880	E_0-5	659765	4022211	E_0	Black mat	Charcoal	ABA	–23.1	17.30±0.08	20.87±0.26	1.00
10CM7-20.1	Beta-282792	E_0-5	659803	4022184	E_0	Black mat	Charcoal	ABA	–24.8	17.37±0.06	20.96±0.24	1.00
03TAH10-23.1 (II)	Aeon-953	B-3	659289	4022347	E_0	Black mat	Charcoal	ABA	–23.4	17.40±0.19	21.04±0.52	1.00
03Q11-18.1A	Aeon-2128	E_0-7	666149	4019815	E_0	Sediment	Succineidae	HCl	*–8*[3]	17.63±0.07	21.31±0.28	1.00
15KS11-18.1	Aeon-2129	E_0-8	659323	4022354	E_0	Sediment	Succineidae	HCl	*–8*[3]	18.18±0.07	22.05±0.23	1.00
16KS8-29.1A	Aeon-2315	E_0-9	658710	4022556	E_0	Sediment	Succineidae	HCl	*–8*[3]	18.73±0.08	22.62±0.21	1.00
16KS10-23.1A	Aeon-2321	E_0-10	666964	4019128	E_0	Sediment	Succineidae	HCl	*–8*[3]	19.11±0.12	23.04±0.38	1.00
04MRR1-22.2	Beta-252833	D-4	659277	4022354	D_3	Sediment	Organic sediment	ABA	–25.3	20.31±0.12	24.45±0.39	1.00
10JP11-16-P-M11	Aeon-703	D-4	659277	4022354	D_3	Sediment	*Physa* sp.[5]	HCl	–13.2	21.48±0.15	25.77±0.27	1.00
10JP11-16-P-M11	Aeon-702	D-4	659277	4022354	D_3	Sediment	*Fossaria* sp.[5]	HCl	–10.8	21.58±0.15	25.85±0.26	1.00
12CM4-19.1	Aeon-972	D-2	653764	4024064	D_2	Black mat	Charcoal	ABA	–22.9	23.39±0.15	27.58±0.23	1.00
12KS6-6.1	Aeon-1201	D-5	650719	4026341	D_2	Sediment	Succineidae	HCl	–8.1	24.74±0.28	28.80±0.64	1.00
17KS1-29.1A	Aeon-2387	D-9	647558	4029568	D_2	Sediment	Succineidae	HCl	*–8*[3]	24.85±0.19	28.93±0.44	1.00
09CM11-2.1	Beta-268971	D-3	662242	4021004	D_2	Black mat	Organic sediment	ABA	–23.8	25.95±0.17	30.18±0.52	1.00

Table 1. Summary of sample information, radiocarbon (^{14}C) ages, and calibrated ages.—Continued

[Uncertainties for the calibrated ages are given at the 95 percent (2σ) confidence level, and all others are given at the 68 percent (1σ) confidence level. no., number; AMS, accelerator mass spectrometry; $\delta^{13}C$, stable carbon isotope; VPDB, Vienna Pee Dee Belemnite; ‰, part per thousand; ka, kilo-annum (thousands of years before present); cal, calibrated; P, probability of the calibrated age falling within the reported range as calculated by CALIB v.7.1html; ABA, acid-base-acid; HCl, hydrochloric acid; ABOX, acid-base-wet oxidation; >, greater than]

Sample no.	AMS no.	Section	Easting[1]	Northing[1]	Bed	Context	Material dated	Treatment	$\delta^{13}C_{VPDB}$ (‰)	^{14}C age (ka)	Age (cal ka)[2]	P
11CM12-20.2A	Aeon-960	D-6	666152	4019764	D_2	Carbonate cap	Succineidae	HCl	–8.5	26.97±0.33	31.01±0.44	1.00
11CM12-20.2C	Aeon-961	D-6	666152	4019764	D_2	Carbonate cap	Succineidae	HCl	–7.6	27.02±0.33	31.05±0.43	1.00
09CM11-4.2	Beta-268972	D-3	662242	4021004	D_2	Black mat	Organic sediment	ABA	–22.1	27.85±0.18	31.68±0.47	1.00
10CM6-30-I-C2	Aeon-592	D-7	666103	4019772	D_1	Black mat	Charcoal	ABOX	–24.3	30.14±0.11	34.18±0.28	1.00
10CM6-30-I-C3	Aeon-593	D-7	666103	4019772	D_1	Black mat	Charcoal	ABOX	–27.4	30.93±0.09	34.83±0.24	1.00
09KS2-12.1	Beta-264964	D-7	666103	4019772	D_1	Black mat	Charcoal	ABA	–25.6	31.10±0.24	35.04±0.50	1.00
LVV-Y-1	Aeon-2063	D-3	662240	4020996	D_1	Sediment	Succineidae	HCl	–10.7	32.21±0.21	36.07±0.47	1.00
17KS5-24.1d	Aeon-2463	D-10	647736	4029085	D_1	Sediment	Succineidae	HCl	–12.2	33.20±0.24	37.44±0.83	1.00
12CM2-1.1	Aeon 954	B-7	664008	4020305	B_3	Black mat	Charcoal	ABA	–26.6	38.6±2.7	42.2±5.3	1.00
03CM11-6.11	Aeon 809	B-6	663100	4020559	B_2	Sediment	Charcoal	ABOX	–23.2	47.3±2.8	>50[6]	—
LVV-Y-2	Aeon-974	B-8	661853	4020784	B_2	Sediment	Charcoal	ABOX	–24.8	47.5±2.0	>50[6]	—

[1]Universal Transverse Mercator coordinates are all in zone 11S.

[2]Calibrated ages were determined using the IntCal13.14C dataset; limit 50.0 calendar ka. Calibrated ages are reported as the midpoint of the calibrated range. Uncertainties are calculated as the difference between the midpoint and either the upper or lower limit of the calibrated age range, whichever is greater (reported at the 95 percent confidence level; 2σ). Multiple ages are reported when the probability of a calibrated age range exceeds 0.05.

[3]$\delta^{13}C$ value not measured. Assumed values of –25‰ for charcoal and –8‰ for shells based on other samples from the Las Vegas Valley.

[4](a) *Prosopis*-type; (b) mix of *Picea*, cf. Asteraceae, and an unidentified hardwood; (c) mix of *Picea* and cf. *Juniperus*, *Prosopis*-type; and (d) cf. Asteraceae.

[5]Sample age corrected for local hard-water effect. See text for details.

[6]Sample ^{14}C age is beyond the limit of the IntCal13 dataset and therefore cannot be calibrated (Reimer and others, 2013).

Table 2. Summary of infrared-stimulated luminescence (IRSL) sample information and ages.

[Uncertainties for all dose parameters and ages are given at the 95 percent (2σ) confidence level. ID, identifier; %, percent; K, potassium; U, uranium; Th, thorium; ppm, part per million; Gy, gray (unit of measure for luminescence dose); ka, kilo-annum (thousands of years before present)]

Sample ID	Section	Easting[1]	Northing[1]	Member/ bed	Water content (%)[2]	K (%)	U (ppm)	Th (ppm)	Cosmic dose addition (Gy/ka)[3]	Total dose rate (Gy/ka)[4]	Equivalent dose (Gy)[4]	Age (ka)
OSL 22	D-8	653737	4024038	D_3 (top)	7 (35)	0.68±0.02	2.55±0.06	3.00±0.15	0.27±0.02	2.45±0.06	60±4	25±3
OSL 20	D-2	653764	4024064	D_3 (base)	1 (29)	1.03±0.03	2.28±0.06	7.80±0.24	0.19±0.01	2.87±0.08	75±3	26±2
OSL10	B-5	664317	4020174	B_3	1 (66)	1.08±0.02	1.83±0.06	4.81±0.09	0.22±0.04	2.41±0.06	107±15	44±6
OSL9	B-5	664317	4020174	B_2	3 (68)	1.01±0.02	2.02±0.06	4.57±0.09	0.19±0.02	2.38±0.08	111±10	47±4
OSL12	B-8	661875	4020878	B_2	0 (64)	1.04±0.03	1.81±0.08	4.88±0.25	0.15±0.02	2.31±0.14	112±7	48±4
OSL8	B-5	664317	4020174	B_1	2 (61)	0.76±0.02	1.66±0.06	3.70±0.08	0.17±0.02	1.90±0.06	115±19	61±10
OSL5	B-4	663221	4020539	B_1	5 (25)	0.88±0.02	1.70±0.06	4.36±0.09	0.11±0.02	2.37±0.06	227±9	96±5
OSL4	A-1	664555	4020071	A	1 (110)	0.76±0.02	1.87±0.06	3.16±0.08	0.16±0.02	1.62±0.06	296±21	183±15
OSL15	A-5	663075	4020598	A	1 (40)	0.33±0.02	0.84±0.07	2.11±0.18	0.16±0.02	1.11±0.12	333±13	300±35

[1]Universal Transverse Mercator coordinates are all in zone 11S.

[2]Field moisture (complete sample saturation). Ages were calculated using 50 percent of saturation values.

[3]Cosmic doses and attenuation with depth were calculated following Prescott and Hutton (1994). See the text in the section "Luminescence Dating Methods" for details.

[4]Dose rate and equivalent doses for fine silt (4–11 millimeters) polymineral IRSL.

Luminescence Dating Methods

Both optically stimulated luminescence (OSL) from quartz and post-infrared infrared-stimulated luminescence (post-IR IRSL) from feldspar were used to determine the ages of GWD deposits that are older than the practical limit of ^{14}C dating (approximately 40 ka) and to establish the age of the deposits where materials suitable for ^{14}C dating were absent (see fig. 3 for spatial coverage and table 2 for specific sampling locations). Samples for luminescence dating were taken from homogeneous, massive, fine-grained sediments using 4-centimeter (cm) diameter by 15-cm long, light-tight, metal tubes that were inserted horizontally into freshly excavated vertical surfaces. In the laboratory, subsamples for equivalent dose measurements were obtained from the center of the tubes, whereas sediment near the ends was analyzed for water content and radioelement (potassium, rubidium, uranium, and thorium) concentrations.

The systematics of OSL and IRSL dating are well established (Auclair and others, 2003; Preusser, 2003; Steffen and others, 2009). Luminescence samples were prepared for dating at the U.S. Geological Survey Luminescence Geochronology Laboratory in Denver, Colorado, using standard protocols (Mahan and others, 2015; Nelson and others, 2015). Briefly, under subdued orange-light conditions, sediments were treated with 4-molar HCl and 30 percent H_2O_2 to remove carbonates and organic material, respectively, and wet sieved to isolate grains with diameters between 63 and 250 micrometers (μm). After drying, heavy minerals were separated from lighter silicates with a Frantz magnetic separator using a high (1.5 ampere) current. Heavy liquids with a density of 2.56 grams per cubic centimeter were then used to separate feldspars from quartz. Feldspar grains were retained for ISRL analysis, whereas the isolated quartz grains were etched with 48 percent hydrofluoric acid (HF) to dissolve rinds affected by alpha particles and to remove any remaining feldspars; the isolate quartz grains were also treated with 8-molar HCl to remove any precipitated fluorides. The resulting quartz grains were retained for OSL analysis.

Steel target discs were dabbed with silica spray, and a single layer of 50–150 grains was added to each disc. The discs were then loaded into the luminescence reader for analysis. For each sample, as many as 30 aliquots of either quartz or feldspar were measured to allow for reliable statistical analysis (Rodnight, 2008).

The single aliquot regenerative dose protocol (Wintle and Murray, 2006) was used to determine the equivalent dose for each aliquot of quartz, whereas the 230 °C post-IR IRSL protocol (Kars and others, 2012) was used to determine the equivalent dose for feldspar. There was a small but persistent fade correction required for the post-IR IRSL data, which was on the order of 2.5–3.5 percent per decade (Huntley and Lamothe, 2001). We note that this is significantly less than fading ranges determined previously for wetland deposits elsewhere in the southwestern United States (Pigati and others, 2009, 2011).

Dose rates were determined based on concentrations of potassium, rubidium, uranium, and thorium measured by inductively coupled plasma mass spectrometry following Taggart (2002). The cosmic-ray dose rate was estimated for each sample as a function of depth, elevation, and geomagnetic latitude, and was added to the total dose rate (Prescott and Hutton, 1994). The total dose rate was then corrected using 50 percent of the measured saturated moisture content to simulate average annual moisture conditions.

Finally, although we report both OSL (app. 3) and IRSL (table 2) ages, only the latter is used for age control because, based on results from paleowetland deposits elsewhere in the deserts of the southwestern United States (Pigati and others, 2009, 2011), post-IR IRSL ages derived from feldspars appear to be more reliable than OSL ages on quartz. Similar to the calibrated ^{14}C results, all luminescence ages are presented in kilo-annum, and uncertainties are given at the 95 percent (2σ) confidence level.

Results and Discussion

This study reevaluates the Las Vegas Formation and its long-standing informal units with full descriptions and characterization of the entire lithostratigraphic sequence and its age relations. These fine-grained, vertebrate and invertebrate fossil-bearing sediments are a discontinuous and complex succession of GWD deposits that were deposited in an expansive desert wetland ecosystem that existed episodically from at least the middle Pleistocene to the early Holocene. Modern spring-discharge analogs and facies changes related to the highest groundwater established in the Las Vegas Valley during the last full-glacial are recognized and represent a paleohydrologic system that responded dynamically to abrupt changes in climate throughout the late Quaternary.

Paleohydrologic Environments of the Las Vegas Formation

The Las Vegas Formation is interpreted to be a lithostratigraphic sequence of GWD deposits; all subsequent descriptions of lithologies, microfauna, and positions on the landscape are viewed in this context. In addition to recognizing the deposits as products of groundwater-related processes, we recognize that the specific hydrologic regimes represented by the deposits (rheocrene, limnocrene, and helocrene discharge) are comparable to modern spring ecosystems (flowing streams, spring pools, and marshes/wet meadows, respectively) (fig. 4; Springer and Stevens, 2009). The specific types of spring discharge and their spatial distribution throughout the upper Las Vegas Wash are directly related to subsurface structures (faults), aquifer complexity, and local water table levels (Springer and others, 2015). Each of these spring-discharge regimes contains a unique combination of sedimentary features and microfauna that can be used to reconstruct and constrain past environmental and hydrologic conditions within the larger paleowetland system.

We also recognize sedimentary facies changes in the last full-glacial deposits as proposed by Quade and colleagues (Quade, 1986; Quade and Pratt, 1989, Quade and others, 1995), in which sediments related to helocrene discharge in the valley bottom grade from marshes and wet meadows in the valley axis to phreatophyte flats and xeric landscapes in more marginal, upland areas. The discussion presented in the next section references both the specific hydrologic environments and the facies changes as part of the description of the Las Vegas Formation sediments.

The Las Vegas Formation

The Las Vegas Formation was designated a formal lithostratigraphic unit by Longwell and others (1965). Our nomenclature retains the informal alphanumeric notation of Haynes (1967) for units within the formation and includes additional units that were not recognized previously. We also eliminate a previously named unit (unit C). Fine-grained sediments of units (now members) X, A, B, D, and E make up the Las Vegas Formation, represent GWD depositional regimes, and contain vertebrate and (or) invertebrate fossils. In contrast, the largely coarse-grained sediments of units F and G of Haynes (1967) are inset into the sediments of the Las Vegas Formation, were deposited under dry conditions during the middle and late Holocene, and do not contain fossils. This report does not discuss units F and G further.

The entire formation cannot be examined in one location; therefore, the composite stratigraphy presented in figure 5 is derived from 52 stratigraphic sections located throughout the upper Las Vegas Wash, as described later. The spatial relations of the various informal units can be extremely complex. Simple layered stratigraphy with a complete sequence of oldest to youngest units is rare in the formation. Instead, we more commonly observe cut-and-fill structures with inset relations, laterally discontinuous strata, buttressed unconformities, and differently aged units juxtaposed as the result of successive periods of dissection, deflation, and deposition (fig. 6). An important implication of this complexity is that units depicted in plan view on a two-dimensional geologic map (for example, Bell and others, 1998, 1999; Page and others, 2005; Ramelli and others, 2011, 2012) do not necessarily provide diagnostic information about the stratigraphy in the third dimension, regardless of the map scale. It is therefore critical that researchers work out the stratigraphic relations between units at a given site when trying to ascertain contextual information for paleoclimatic, paleontologic, or archaeologic studies.

Rheocrene discharge (flowing streams)

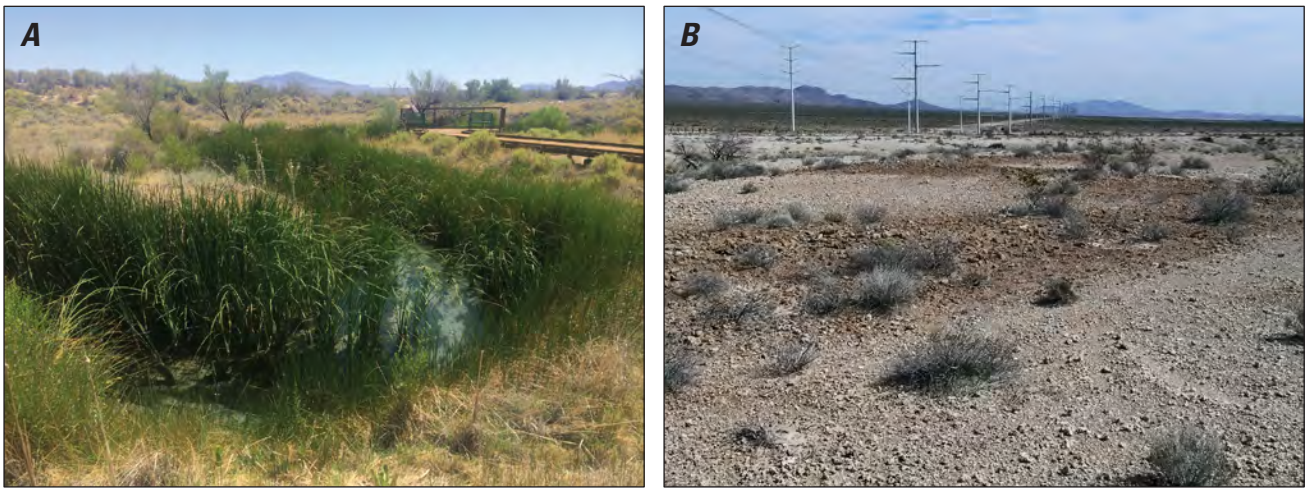

Limnocrene discharge (spring pools)

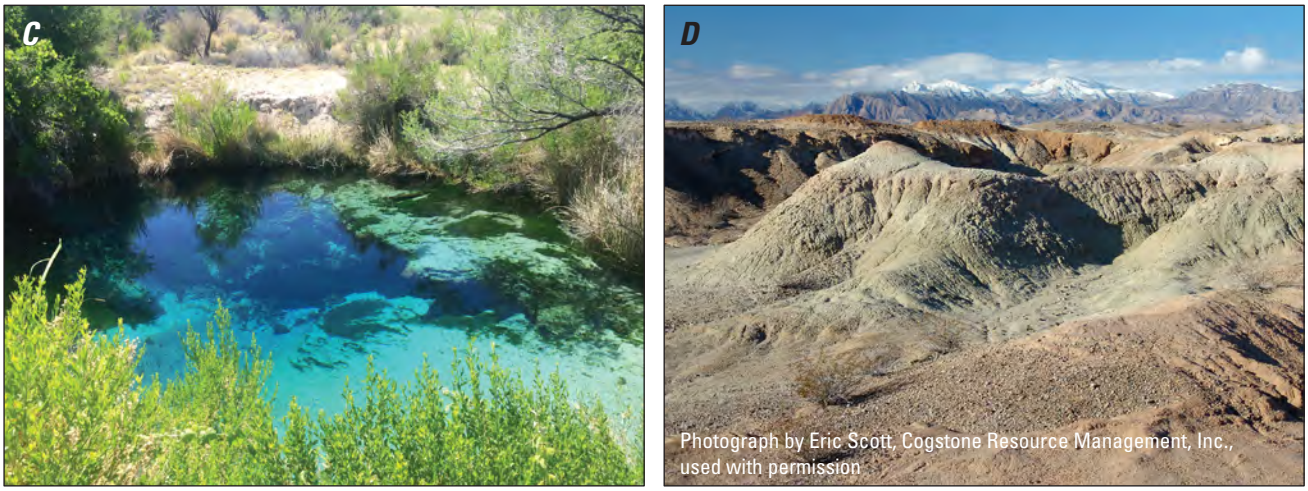

Helocrene discharge (marshes and wet meadows)

Figure 4. Examples of groundwater discharge regimes in extant wetlands (panels *A*, *C*, *E*) and their counterparts observed in sediments of the Las Vegas Formation (panels *B*, *D*, *F*). Rheocrene discharge is characterized by spring-fed streams and outflow channels (*A*) and is represented in the fossil record by dark-colored, sinuous channels composed of tufa lag (*B*). Limnocrene discharge is characterized by discrete spring-fed pools and ponds (*C*) and is represented by green-colored silts and sands in cauldron-shaped bedforms (*D*). Helocrene discharge is characterized by marshes and wet meadows (*E*) and is represented by extensive, light-colored, carbonate-rich marls, benches, and caps (*F*).

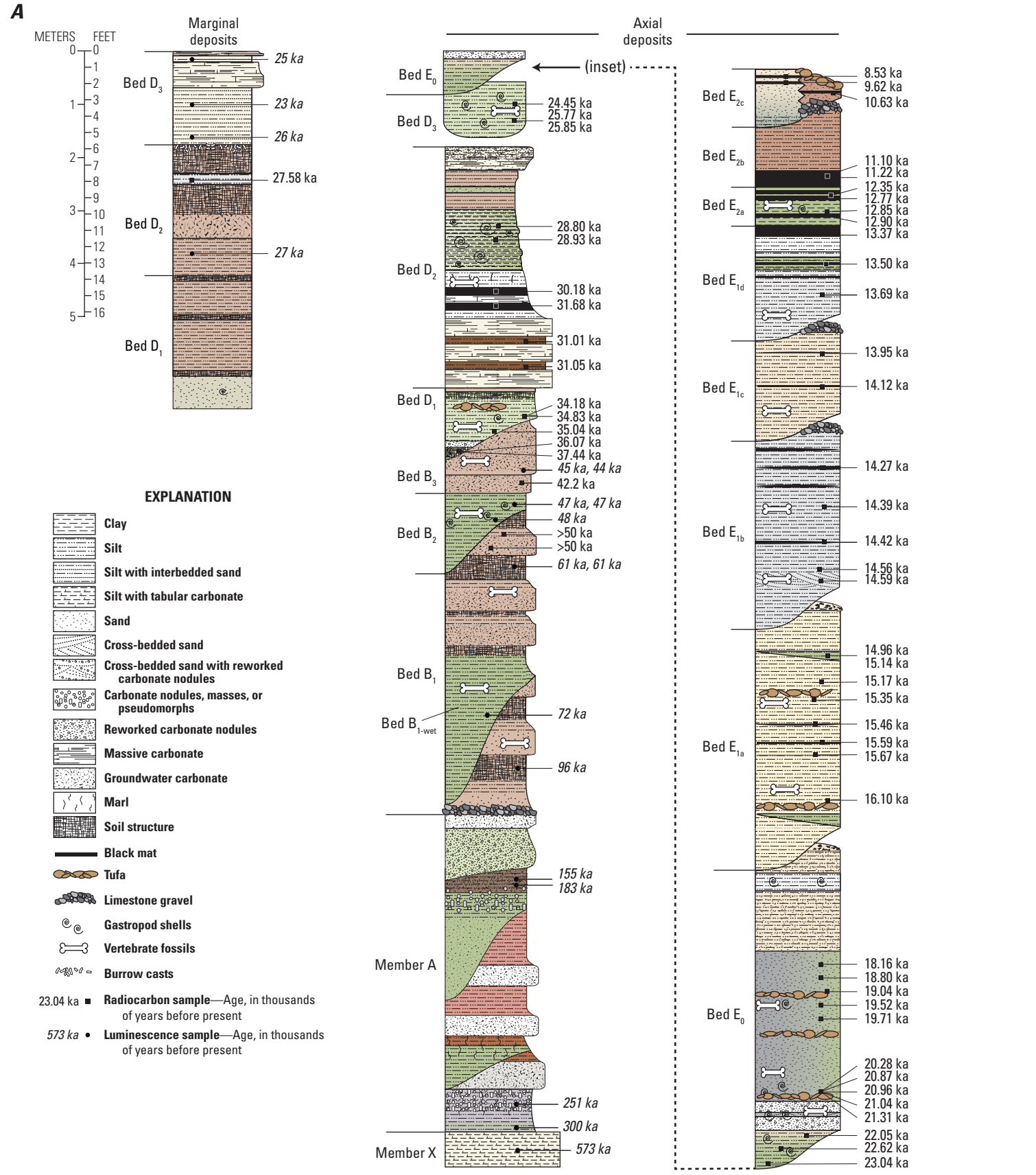

Figure 5. (this and facing page) Stratigraphy and chronology of the Las Vegas Formation. *A*, Composite stratigraphy and ages for sediments of the Las Vegas Formation based on 52 different stratigraphic sections located throughout the upper Las Vegas Wash. Note that colors shown in the composite profile are intentionally intensified to differentiate between members and (or) beds. Age control for the various

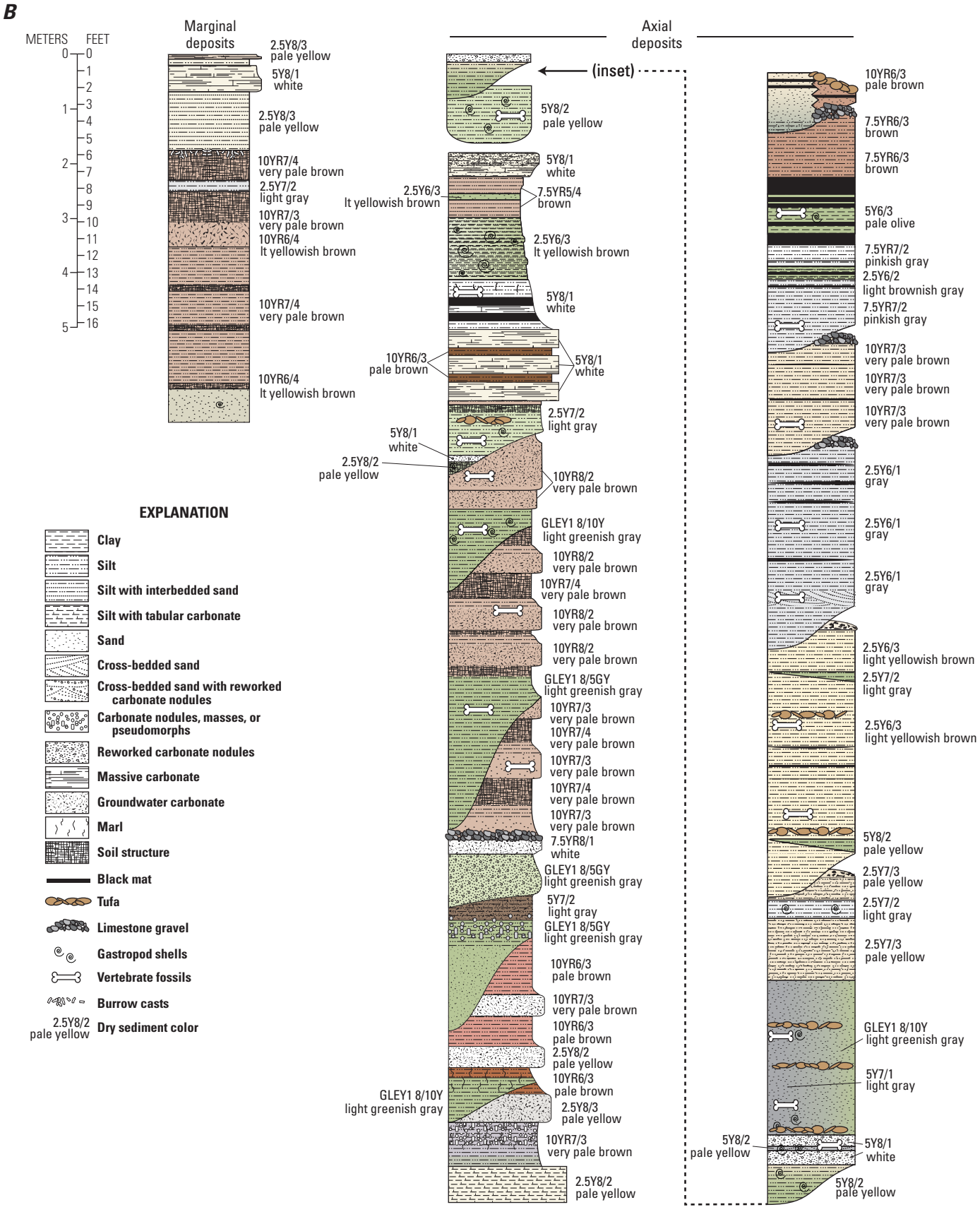

units is based on a combination of radiocarbon and infrared-stimulated luminescence dating (see tables 1 and 2). Calibrated radiocarbon ages (filled squares) are given in regular font and infrared-stimulated luminescence ages (filled circles) are italicized. *B*, Composite stratigraphy and dry colors (Munsell Color [Firm], 2010) for the Las Vegas Formation sediments. (ka, kilo-annum [thousands of years before present]; >, greater than).

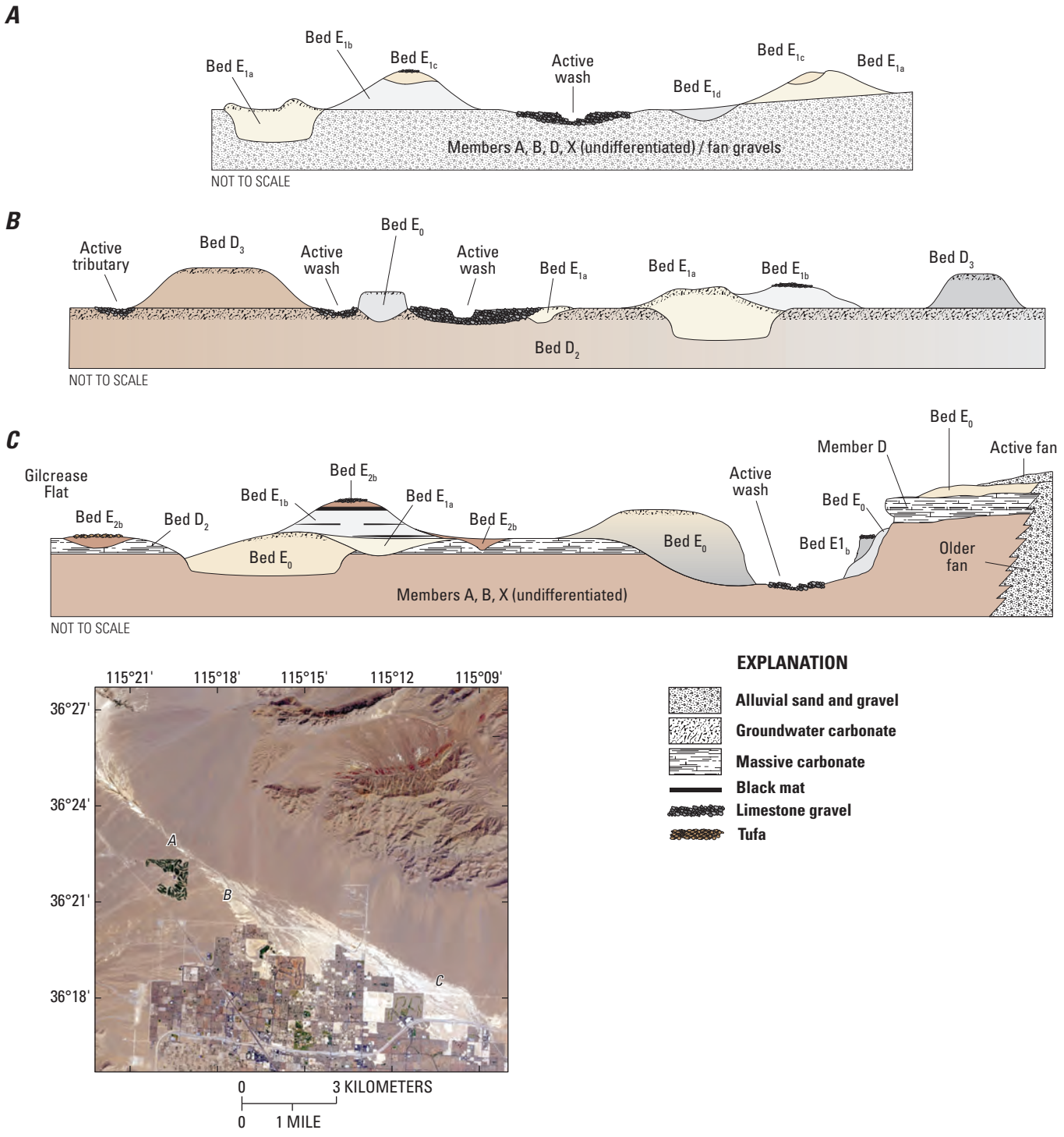

Figure 6. Index map and idealized cross sections of various members and beds attributed to the Las Vegas Formation in the (*A*) northern, (*B*) central, and (*C*) southern parts of the upper Las Vegas Wash. The vertical scale for each is on the order of 5–10 meters, whereas the horizontal scale is on the order of hundreds of meters. The spatial relations between different units within the formation can be extremely complex and include various combinations of cut-and-fill sequences, inset deposits, buttressed unconformities, and juxtaposition of differently aged units. Soil colors of beds are defined in figure 5*B*.

Finally, we note that the original chronologic framework of units within the Las Vegas Formation was established in conjunction with the first large-scale application of the ^{14}C dating method during the Tule Springs Expedition (Haynes, 1967). Subsequent to that work, beta-counting techniques, which require large sample sizes, have been largely replaced by accelerator mass spectrometry dating, which can provide more precise ages from smaller samples. In this study, we revise the previous chronology based on accelerator mass spectrometry ^{14}C dating of charcoal and small terrestrial gastropod shells, as well as luminescence dating when required. The fortuitous presence of charcoal and shells in the deposits, and our methodology of dating only these materials, has resulted in an unusually clear chronologic framework that is presented in the composite stratigraphy in figure 5, the individual stratigraphic sections and annotated photographs in figures 7–19, and the age information presented in table 1. Bulk organic matter, humic acids, and aquatic gastropod shells are common in Las Vegas Formation deposits and could also have been used for dating, but doing so would have resulted in a less robust chronology because ages obtained from these materials are known to be affected by carbon mobility and transport, contamination, and hard-water effects (Trumbore, 2000; Jull and Burr, 2015). This rigorous approach has allowed us to differentiate ages at submillenial scales for individual beds within members D and E.

In the following sections, we describe the primary physical characteristics, age ranges, depositional environments, and hydrologic and climatic interpretations for each member and bed within the Las Vegas Formation (figs. 7–20; tables 1 and 2; apps. 1–3).

Member X

Longwell and others (1965) attributed the light-colored, fine-grained deposits in the Las Vegas Valley to the Las Vegas Formation without differentiating sediments within the sequence. In contrast, Haynes (1967) recognized and described multiple units, including what he designated as "pre-unit A alluvium" south of the original Tule Springs site, also referring to them as "unit X" (map unit Qx). Haynes noted that unit X was older than the other fine-grained sediments in the Tule Springs area based on the presence of strongly developed paleosols, redder hues throughout the unit, and noticeable dips (unlike the flat-lying Tule Springs deposits). The degree of induration and weathering characteristics of unit X deposits, along with their deep dissection and conspicuous post-depositional tilting, led Haynes to infer that they were much older than (and not necessarily related to) the sediments at Tule Springs. Regardless, he noted that these deposits "have been mapped by Longwell and are a part of his Las Vegas formation (Longwell et al., in press, and personal communication)" (Haynes, 1967, p. 58).

Bingler (1977), Matti and Bachhuber (1985), Matti and others (1987, 1993), Bell and others (1998, 1999), Lundstrom and others (1998), Page and others (2005), and Ramelli and others (2011) mapped these older fine-grained deposits throughout the Las Vegas Valley in various ways, with some recognizing their genetic affinity with past groundwater discharge. Mapped units—such as QTs, QTss, and QTcs (Pliocene–Pleistocene silty sand [Bingler, 1977]); QTs (consolidated sediments [Matti and Bachhuber, 1985; Matti and others, 1987, 1993]); QTs (older fine-grained sediments, undivided [Bell and others, 1998, 1999]); QTs (undivided fine-grained sediments of the Las Vegas Valley, Quaternary and Tertiary? [Page and others, 2005]); Qs (fine-grained spring deposits, Pleistocene [Lundstrom and others, 1998]); Qso (old fine-grained spring deposits, middle Pleistocene [Page and others, 2005; Ramelli and others, 2011]); and Qfw (fine-grained deposits of Whitney Mesa, middle Pleistocene [Page and others, 2005])—all exhibit lithologies consistent with spring discharge. Today, these units are rarely exposed because of urbanization and generally lack age control. Based on limited exposures, Ramelli and others (2011) estimated that these older deposits are at least 5 meters (m) thick but noted that the base of the unit was not exposed in outcrop. Well-log data indicate they are actually more than 250 m thick in some areas (Plume, 1984; Donovan, 1996).

We refer to the stratigraphically lowest member of the Las Vegas Formation as member X (fig. 7, sections A-1 through A-5; fig. 8*A*). In the upper Las Vegas Wash, exposures of member X are rare, but where they occur, the deposits are highly indurated and consist of tan and gray silt and sand with abundant and strongly cemented, tabular to bedded carbonate horizons. Paleosols consisting of reddish-brown, gypsum-rich silt and silty clay exhibiting blocky structures are also common in the sequence. Member X deposits are typically capped by a well-developed carbonate horizon that is greater than (>) 1 m thick.

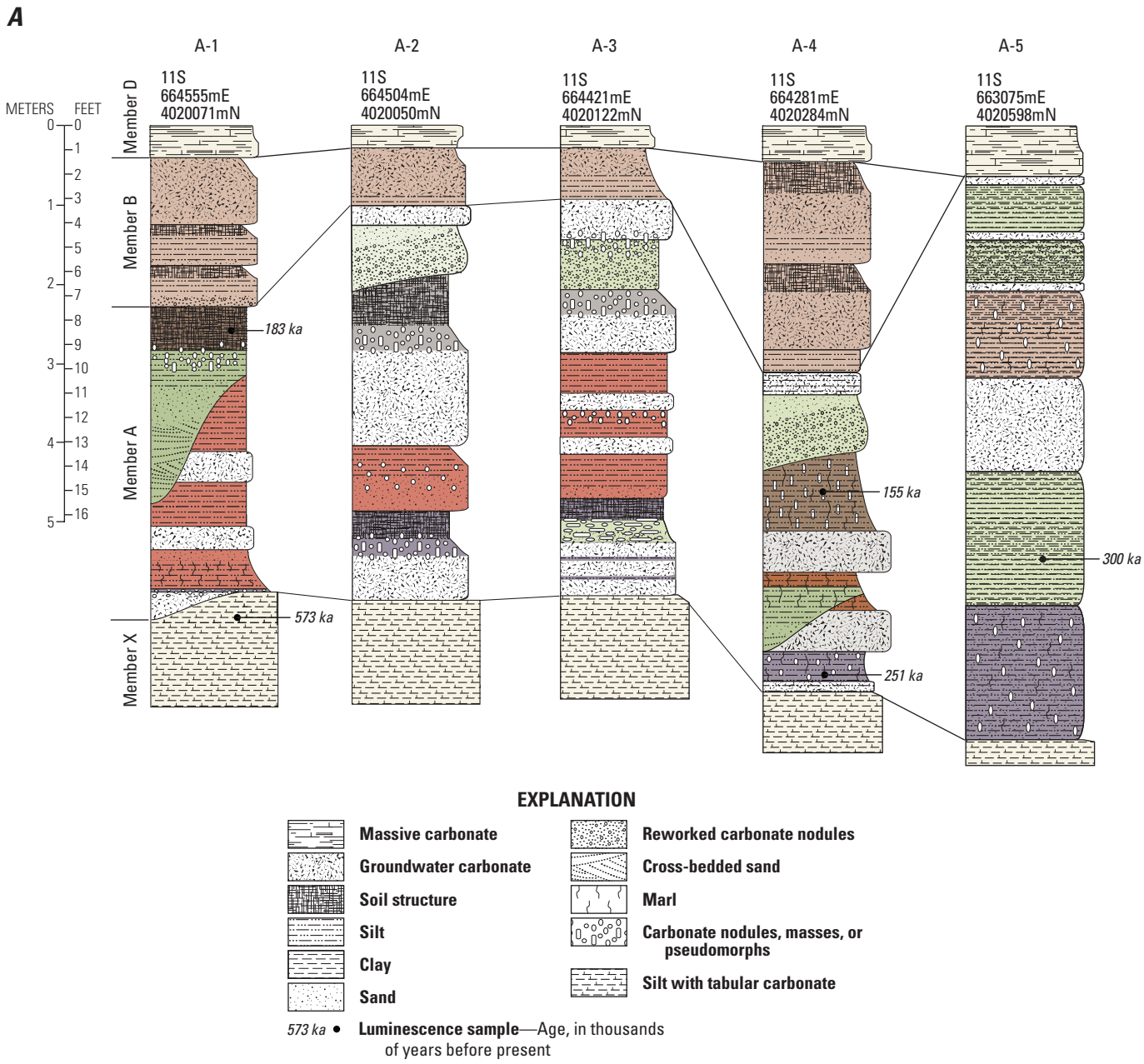

Figure 7. (this and facing page) Stratigraphic sections, ages, and colors featuring member A sediments. *A*, Stratigraphic profiles featuring member A deposits in context of bounding members, and associated infrared-stimulated luminescence ages (see table 2). Universal Transverse Mercator coordinates are in zone 11S. Overall, member A dates to between approximately

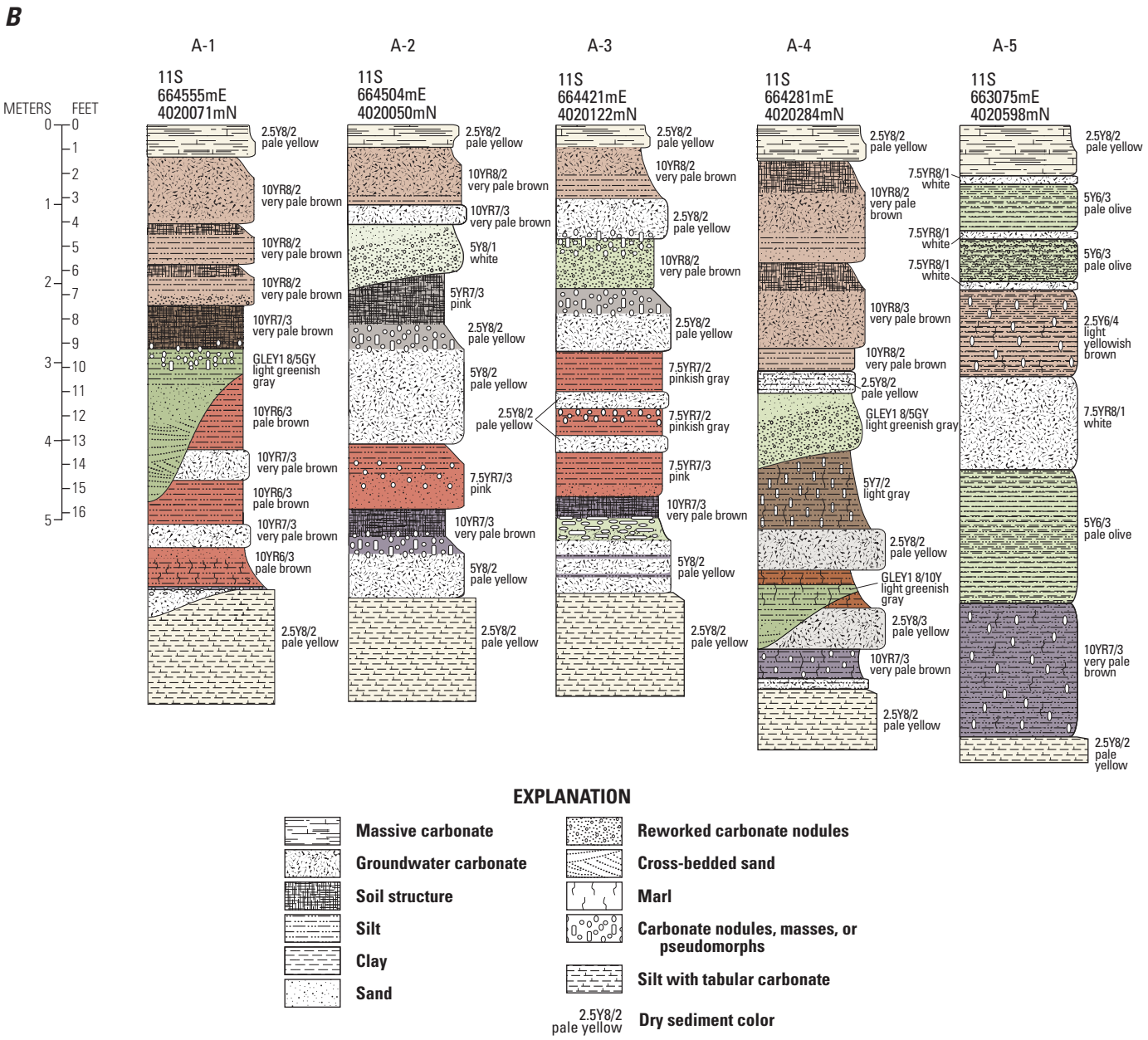

300 and 155 kilo-annum (ka [thousands of years before present]) and represents a complex and long-lived desert wetland ecosystem that spanned multiple glacial and interglacial cycles (marine isotope stages 8–6). *B*, Stratigraphy and dry colors (Munsell Color [Firm], 2010) of member A sediments. (m, meter; E, easting; N, northing)

Figure 8. Photographs featuring member A deposits (see fig. 7). Universal Transverse Mercator coordinates are in zone 11S. *A*, Deposit equivalent to section A-1; 664555 meters (m) easting (E), 4020071 m northing (N). View to the south. Section is 7.5 m thick. *B*, Multiple carbonate benches and horizons typical of member A; 662309 m E, 4020841 m N. View to the south. Section is approximately 6 m thick. *C*, Deposit equivalent to section A-4; 664281 m E, 4020284 m N. View to the south. Section is 8.0 m thick. *D*, Member A as it appears laid back in an outcrop; 663152 m E, 4020563 m N. View to the southeast. Section is approximately 2 m thick. *E*, Additional exposure of member A in the upper Las Vegas Wash; 663252 m E, 4020542 m N. View to the northwest. Section is 8.0 m thick. *F*, Additional exposure of member A in the upper Las Vegas Wash; 664717 m E, 4020080 m N. View to the southeast. Section is 7.0 m thick.

Age Control of Member X

Both Lundstrom and others (1998) and Page and others (2005) reported a thermoluminescence (TL) age range of 399–226 ka for a sample taken from member X sediments in the northern part of the Las Vegas Valley (app. 2). Lundstrom and others (1998) mapped these sediments as "fine-grained spring deposits" (Qs), whereas Page and others (2005) mapped them as "old fine-grained spring deposits" (Qso). Page and others (2005) also report a TL age range of 379–232 ka for a sample of the "fine-grained deposits of Whitney Mesa" in the eastern part of the valley (app. 2). In the upper Las Vegas Wash, we obtained a single IRSL age of 573±52 ka for member X near the base of our section A-1 (fig. 7; table 2).

In this study, we considered all of the older fine-grained deposits in the Las Vegas Valley that are associated with past groundwater discharge, to be part of member X. Given the general lack of exposures and age control for this member, it is essential that additional lithostratigraphic descriptions and temporal controls be established to further define and characterize these deposits. Within the Las Vegas Valley, noticeable dips in member X sediments indicate that the unit has been subjected to post-depositional tectonic modification, so establishing the unit's age will have importance for evaluating seismicity in the valley, with implications for understanding and quantifying long-term earthquake hazards and risk assessment. Additional age control for member X will also assist in determining the hydrologic conditions that prevailed in the Las Vegas Valley during the middle Pleistocene.

Member A

Haynes (1967) was the first to recognize and define unit A (his map unit Qa) in the area in and around the Tule Springs site (fig. 3). He found unit A to be the least exposed unit of the sediments that make up the Las Vegas Formation, cropping out at only a few places along the upper Las Vegas Wash, and interpreted it to be predominantly fluvial in nature with a thick, pedogenic carbonate at the top of the sequence. Although he lacked chronologic control for the unit, Haynes inferred that it was older than the upper limits of ^{14}C dating (>40 ka) based on its physical characteristics and stratigraphic relations with other units attributed to the formation. Published lithologic descriptions of this unit are sparse (Haynes, 1967; Bell and others, 1998, 1999; Page and others, 2005; Ramelli and others, 2011) and vary tremendously because multiple beds are present within the member that exhibit lateral facies changes orthogonal to the valley axis of the upper Las Vegas Wash.

Our studies indicate that member A is more common than Haynes recognized, but it is certainly not as widely exposed as the other members of the Las Vegas Formation. Member A crops out along the length of the upper Las Vegas Wash, most prominently between the Tule Springs site, where it is as much as 4–8 m thick and in some areas accounts for approximately 80 percent of the total bluff height (figs. 7 and 8), as well as the area in and around the Eglington fault scarp (fig. 3). Additional minor exposures of member A can be found in undeveloped lots scattered throughout the Las Vegas metropolitan area.

Member A contains at least four potential beds, but because of the limited number and discontinuous nature of the exposures, as well as the considerable lateral facies variation perpendicular to the valley axis, it is unlikely that all beds within this member have been identified. Therefore, we have chosen not to parse out subunits within member A at this time and instead simply describe them in stratigraphic order, from oldest to youngest.

The basal part of member A is exposed in the southern part of the upper Las Vegas Wash and sits unconformably on top of the uneven topography of member X (figs. 7 and 8*A*). It is generally about 1 m thick and consists of greenish-gray silts and sands in cauldron-shaped bedforms. These sediments transition laterally (away from the valley axis) into grayish-brown to gray clays and silts with abundant root traces that are filled or lined with iron and manganese oxides. Carbonate in the lower part of member A ranges from sparse to abundant and also varies laterally. Where present, carbonate horizons or benches are as much as 30 cm thick; see, for example, sections A-2 and A-3 (fig. 7).

Above this basal part are greenish-gray silts and sands in cauldron-shaped bedforms and outflow channels that transition laterally to reddish-tan silts and sands with numerous carbonate stringers (fig. 7, section A-1; fig. 8*A*). Locally, this part of member A also contains abundant root traces that are filled or lined with iron and manganese oxides. In this part of member A, carbonate ranges from sparse to abundant, forms horizons and benches that are up to 10–20 cm thick, and coalesces in places to form a single bench that is up to about 1 m thick.

Farther up the section, greenish-gray silts and cross-bedded sands in cauldron-shaped bedforms transition laterally into grayish-brown to brown clays and silts, with locally preserved angular blocky soil structures and root traces filled or lined with iron and manganese oxides (fig. 7, sections A-1 and A-4; figs. 8*A* and 8*C*). Here again, carbonate ranges from sparse to abundant, and some horizons coalesce locally to form benches that are approximately 30 cm thick (fig. 7, section A-3).

The uppermost part of member A consists of light greenish-gray silts and sands with reworked carbonate nodules that were deposited as clast-supported, channel bed load up to 25 cm thick (fig. 7, sections A-2 and A-3). Groundwater carbonate cements the uppermost 50–60 cm of this bed, forming a thick, extensive, resistant cap similar to the extensive carbonate benches of member D (see discussion in the section "Member D"). The younger, stratigraphically higher members of the Las Vegas Formation unconformably rest upon the dissected sediments of member A throughout the upper Las Vegas Wash.

Several features differentiate member A from other members and beds, including a high degree of induration, strong soil development, abundant secondary carbonate, and highly contrasting mottled color patterns interpreted as

redoxymorphic features. Evidence of oxidation in these soils include iron and manganese oxide linings of macropores (root voids) and ped faces, whereas reduction is expressed as gleyed horizons, macropore halos, and to a lesser extent, small areas of green and gray hues. Finally, carbonate benches and horizons that are resistant to erosion are common within member A and act as important marker beds, with a prominent carbonate cap marking the top of the deposits (fig. 7).

Age Control of Member A

Chronologic control of member A was absent prior to Page and others (2005), who obtained a single TL age range of 225–131 ka near the Haynes type section (1967) at the Tule Springs site. We collected additional samples for luminescence dating at stratigraphic sections that contained well-preserved, traceable lithologies (fig. 7). Altogether, we obtained four IRSL ages for member A that range from approximately 300 to 155 ka. IRSL ages at section A-4 are 251±18 ka at the base of the section and 155±12 ka at approximately 2.5 m upsection (figs. 7 and 8*C*; table 2). Additional IRSL ages of 300±35 ka and 183±15 ka were obtained for member A at sections A-5 and A-1, respectively (figs. 7 and 8; table 2).

The uppermost part of member A has not been dated directly, so the upper limiting age of this member is unknown. Based on the stratigraphy and thickness of sediments between the uppermost luminescence age in section A-1 and the top of the member A deposits, we postulate that deposition continued long after the 155 ka upper limiting age, possibly until the end of marine isotope stage (MIS) 6 at approximately 130 ka (Martinson and others, 1987; Lisiecki and Raymo, 2005).

Depositional Environments, Paleohydrology, and Paleoclimatic Interpretations of Member A

Member A is characterized by a number of wetland soils, which are indicative of high water tables, and carbonate caps and benches, which represent drier conditions. Redoxymorphic features are also abundant in member A, an indication that fluctuating water table levels were common during its formation. Member A often exhibits considerable lateral variations that represent different facies of wetland development. Along the valley axis, greenish to light-gray silts and sands present in cauldron-shaped bedforms represent limnocrene ponding, and similarly colored deposits present in channel bedforms represent rheocrene discharge, or outflow streams, emanating from the ponds. In contrast, away from the valley axis, sediments within member A transition to reddish-brown, brown, and gray clays and silts that were deposited in more marginal (drier) settings.

Although exposures are limited, sedimentary evidence suggests that the base of member A consists of sediments deposited in both alluvial and wetland settings. Alluvial gravels and sands representing drier conditions accompanied by overland flow are present, as are wetland silts and clays representing limnocrene discharge that created localized ponding within depressions and helocrene discharge that supported wet meadows and phreatophyte flats. A period of surface stability resulting from a hiatus in groundwater discharge followed, allowing soil development to occur.

In the middle of the member A sequence, well-exposed outcrops provide evidence for continued alternating alluvial and wetland sedimentation. Wetland facies in this part of the member include localized limnocrene discharge that formed spring pools and outflow streams and helocrene discharge associated with wet meadows and phreatophyte flats accompanied by fluctuating water table levels. This discharge episode was also followed by stable surface conditions as evidenced by extensive carbonate horizons and benches.

The upper part of member A was formed in broad, spring-fed fluvial channels (rheocrene discharge) and is topped by a thick, resistant carbonate cap. Nonpedogenic carbonate caps and benches are common features in GWD deposits (Pigati and others, 2014; Springer and others, 2015) and are formed at the ground surface or very shallow subsurface by the upward capillary migration of groundwater through the vadose zone. We attribute cap formation to a sequence that begins with groundwater discharge under relatively wet conditions during which carbonate-rich marls are formed, followed by abrupt warming that intensifies evaporative effects and depresses the water table leading to desiccation of the wetlands and case hardening of the carbonate-rich silts and clays. This per ascensum model of carbonate cap formation in desert wetland depositional settings is in contrast to the per descensum formation of calcretes, which have a pedogenic origin and are driven by different processes altogether[1] (Carlisle, 1980; Arakel and McDonchie, 1982; Carlisle, 1983; Goudie and Pye, 1983; Mack and others, 1993, 2000; Birkeland, 1999).

Invertebrate microfossils have been identified in member A; they consist mostly of ostracodes (small, bivalved crustaceans that live in aquatic environments) at section A-4 (fig. 7). Vertebrate fossils have yet to be discovered in member A in the Las Vegas Valley (Scott and others, 2017), but based on the lithologic characteristics of this member and the presence of fossils in other geographic locations where the Las Vegas Formation crops out, the potential for finding them in these older deposits in the future is high.

Overall, member A is a thick and complex sedimentary sequence resulting from alluvial, groundwater discharge, and pedogenic processes that spanned multiple glacial-interglacial cycles. Member A exhibits evidence of a wide range of spring discharge regimes, stable surfaces, and fluctuating water tables and represents a long-lived and diverse desert wetland ecosystem. Well-developed carbonate horizons and benches in member A represent periods of surface stability that punctuated alluvial and wetland deposition that occurred during MIS 8–6. Based on the IRSL ages, the upper part of member A correlates in time with MIS 6 and the capping carbonate may correlate to the MIS 6/5 transition. Significant erosion occurred after formation of the cap but prior to deposition of member B, possibly during MIS 5e.

[1]Note that nonpedogenic carbonate caps, benches, and horizons were referred to as “Aridisols” in Springer and others (2015, 2017a, b).

Member B

Haynes (1967) first recognized and defined unit B (his map unit Qb) in the area in and around the Tule Springs site. The unit includes Paleozoic limestone gravels and tan silts and sands (units B_1 and B_3) that are interpreted as being largely fluvial in nature, representing both stream channel deposits and broad flood-plain sediments. Haynes (1967) recorded a soil at the top of unit B_1 and documented pale green mudstones in the middle of unit B that he called unit B_2. He interpreted unit B_2 as forming in shallow spring pools, which are often associated with feeder conduits filled with vertebrate fossils. Based on a number of infinite ^{14}C ages (app. 1), Haynes concluded that the unit B sequence was beyond the limits of the ^{14}C dating technique (>40 ka).

We document and interpret member B as exhibiting a complex stratigraphy, with at least four subunits consisting of alluvial cut-and-fill sequences, flood-plain sediments, and discrete GWD deposits. We designate these subunits (from oldest to youngest) as beds B_1, $B_{1\text{-wet}}$, B_2, and B_3. Additionally, we attribute some of the sediments that Haynes (1967) called unit C to bed B_3; see the discussion in the section "Dissolution of Unit C."

Beds B_1 and $B_{1\text{-wet}}$

The basal part of bed B_1 often exhibits a thick (>1 m) sequence of subangular to subrounded Paleozoic limestone cobbles and gravels in a series of channels at the erosional contact with underlying member A deposits. Overlying these limestone clasts, bed B_1 is as much as 5–6 m thick and is characterized by an iterative sequence of well-sorted, massive to bedded (thin to medium) tan to reddish-brown silts and sands, intercalated with dark-colored, prismatic clays and thin carbonate-rich horizons (figs. 9 and 10). In a few places along the upper Las Vegas Wash, laterally discontinuous, cauldron-shaped bedforms composed of pale green to gray clay, silt, and sand punctuate the rhythmic tan sediments of bed B_1 (fig. 9, section B-2). This inset subunit, which is referred to as bed $B_{1\text{-wet}}$, contains abundant vertebrate and invertebrate fossils (Scott and others, 2017).

Age Control of Beds B_1 and $B_{1\text{-wet}}$

Page and others (2005) obtained a single TL age range of 144–89 ka for unit B near the Tule Springs site. We obtained four IRSL ages for bed B_1 that range between approximately 100 and 55 ka, including a single age of 72±8 ka for bed $B_{1\text{-wet}}$ (fig. 9, sections B-2, B-3, B-4, and B-5; table 2).

Depositional Environments, Paleohydrology, and Paleoclimatic Interpretations of Beds B_1 and $B_{1\text{-wet}}$

Bed B_1 lithologies reflect a broad range of depositional environments and highly variable hydrologic conditions. Repeated flood events and through-going fluvial flow were punctuated by groundwater discharge and relatively short-lived, high water-table stands. The fluvial system has been previously interpreted as the ancestral "Las Vegas River," which at one time made a substantial contribution to the Colorado River (Hubbs and Miller, 1948; Haynes, 1967). We interpret the pervasive tan alluvial silt and sand, wetland soils, and carbonate horizons of bed B_1 as representing multiple flood events followed by periods of surface stability and widespread drying. Periodically, increased precipitation resulted in episodes of high water-table conditions that supported spatially restricted, ephemeral marshes (helocrene discharge) with significant groundwater carbonate accumulation. Subsequent lowering of the water table triggered desiccation of the wetlands, case hardening of the carbonate-rich sediments, and formation of carbonate benches and horizons. The cauldron-shaped deposits of bed $B_{1\text{-wet}}$ that are inset into the tan silt/sand alluvium of bed B_1 represent a brief period of groundwater discharge characterized by limnocrene flow.

The age of bed B_1 (approximately 100–55 ka) corresponds temporally to the middle of MIS 5c through the early part of MIS 3. Notably, bed $B_{1\text{-wet}}$ was apparently deposited as climate conditions were transitioning from the globally warmer MIS 5a to the colder glacial time of MIS 4. Overall, the lithologies of bed B_1 are the result of rapid oscillation between fluvial processes, wetland development, surface stability, and erosion. Based on the strong temporal correlation between abrupt warming events known as Dansgaard-Oeschger (D-O) events recorded in the Greenland ice cores (Dansgaard and others, 1993; Svensson and others, 2008) and wetland contraction in the Las Vegas Valley in the younger, more highly resolved part of the Las Vegas Formation sedimentary sequence (Springer and others, 2015), we speculate that the unstable climate conditions recorded in the bed B_1 deposits may be related to D-O events 22 through 16.

Bed B_2

Haynes (1967) described unit B_2 as the "green-pond unit" and recognized lithologies that are consistent with that interpretation. Similar to Haynes, our studies show that bed B_2 consists of 1–3 m of massive, greenish-gray silt, sand, and clay in laterally discontinuous, cauldron-shaped, lenticular beds (figs. 9 and 10*B–F*). Bed B_2 often contains organic material in the form of charcoal and carbonized wood fragments, as well as Paleozoic limestone gravels at the base of the bed. Vertebrate fossils and aquatic mollusk shells of *Helisoma* sp., *Pisidium* sp., *Physa* sp., Hydrobiidae, and *Gyraulus* sp. are common to abundant in bed B_2.

Age Control of Bed B_2

Haynes (1967) attempted to date both carbonized wood and gastropod shells from unit B_2, but the results revealed that the material was beyond the limit of ^{14}C dating (>40 ka). We obtained three IRSL ages for bed B_2 that indicate it was deposited between approximately 55 and 45 ka (table 2). We also obtained uncalibrated ^{14}C ages of 47.3±2.8 ^{14}C ka (fig. 9, section B-6) and 47.5±2.5 ka (fig. 9, section B-8) from charcoal in B_2 spring deposits, which are beyond the current limits of calibration. We report these ages as >50 ka (figs. 9 and 10*C*; table 1).

A

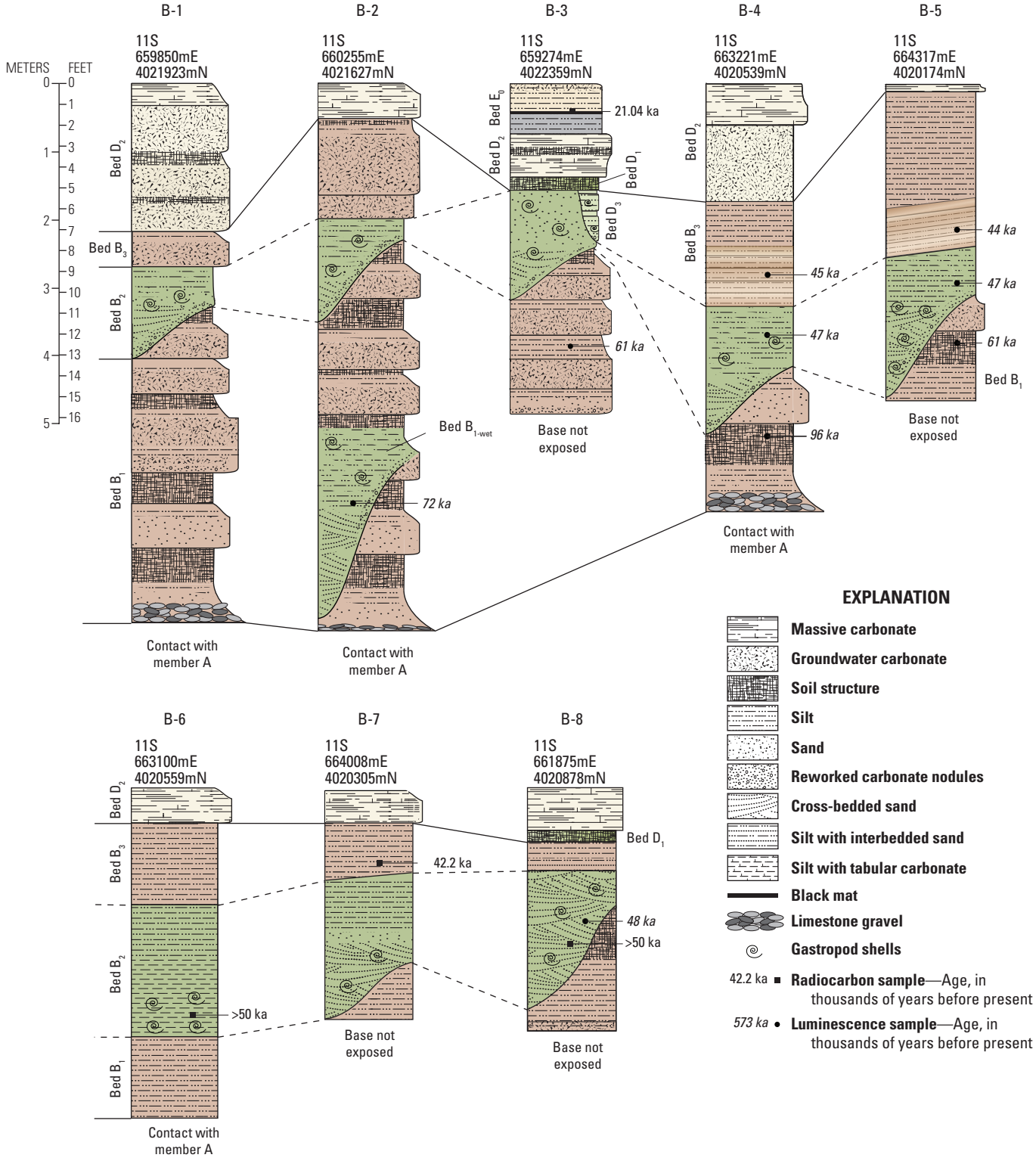

Figure 9. (this and facing page) Stratigraphic sections, ages, and colors featuring member B sediments. *A*, Stratigraphic profiles featuring member B deposits in context of bounding members, and associated radiocarbon and infrared-stimulated luminescence ages (see tables 1 and 2). Universal Transverse Mercator coordinates are in zone 11S. Overall, member B dates to between approximately 100 and 40 kilo-annum (ka [thousands of years before present]) and represents periods of discrete groundwater discharge,

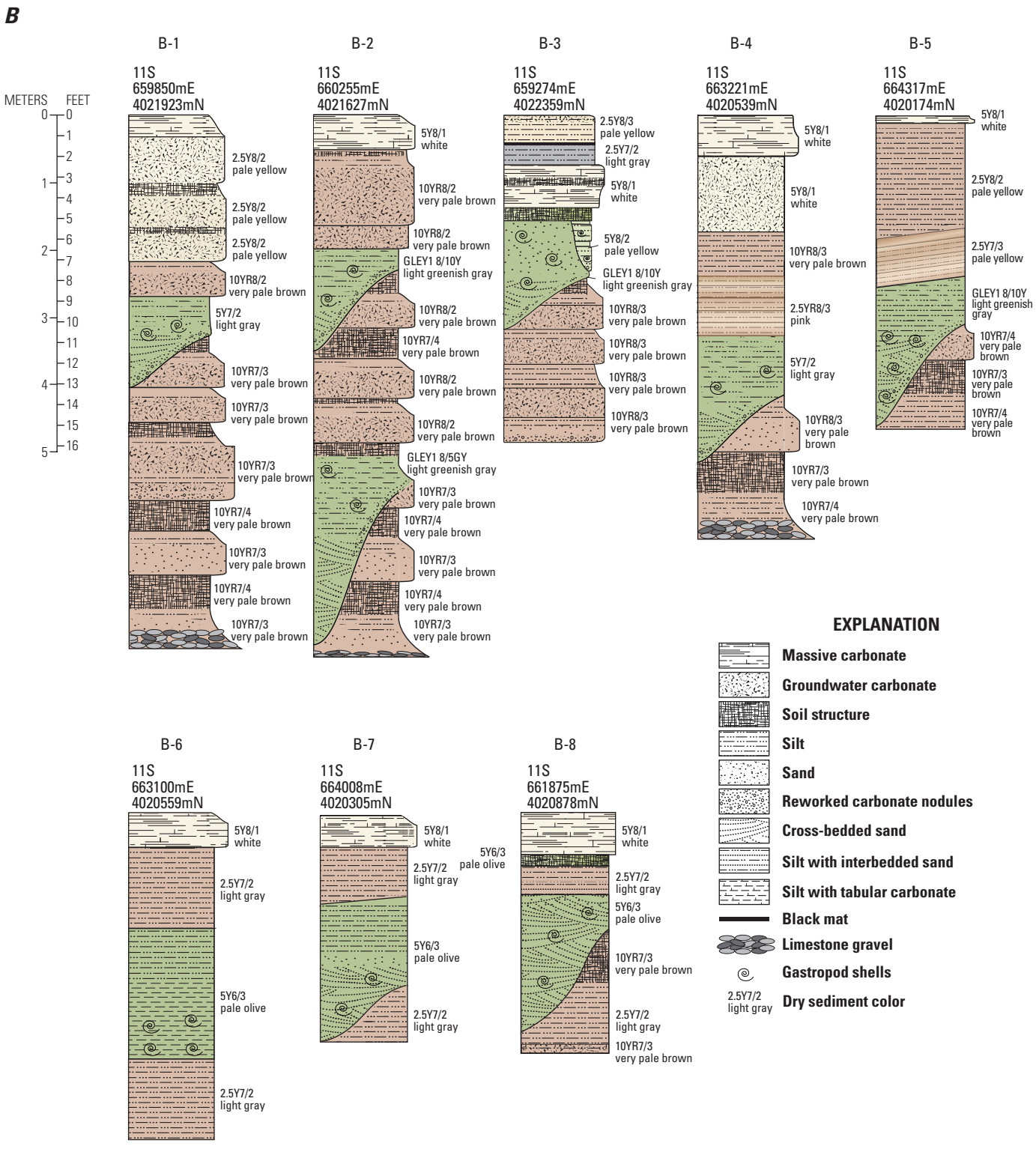

alluvial cut-and-fill processes, and flood-plain deposition. Calibrated radiocarbon ages (filled squares) are given in regular font and infrared-stimulated luminescence ages (filled circles) are italicized. *B*, Stratigraphy and dry colors (Munsell Color [Firm], 2010) of member B sediments. (m, meter; E, easting; N, northing; >, greater than)

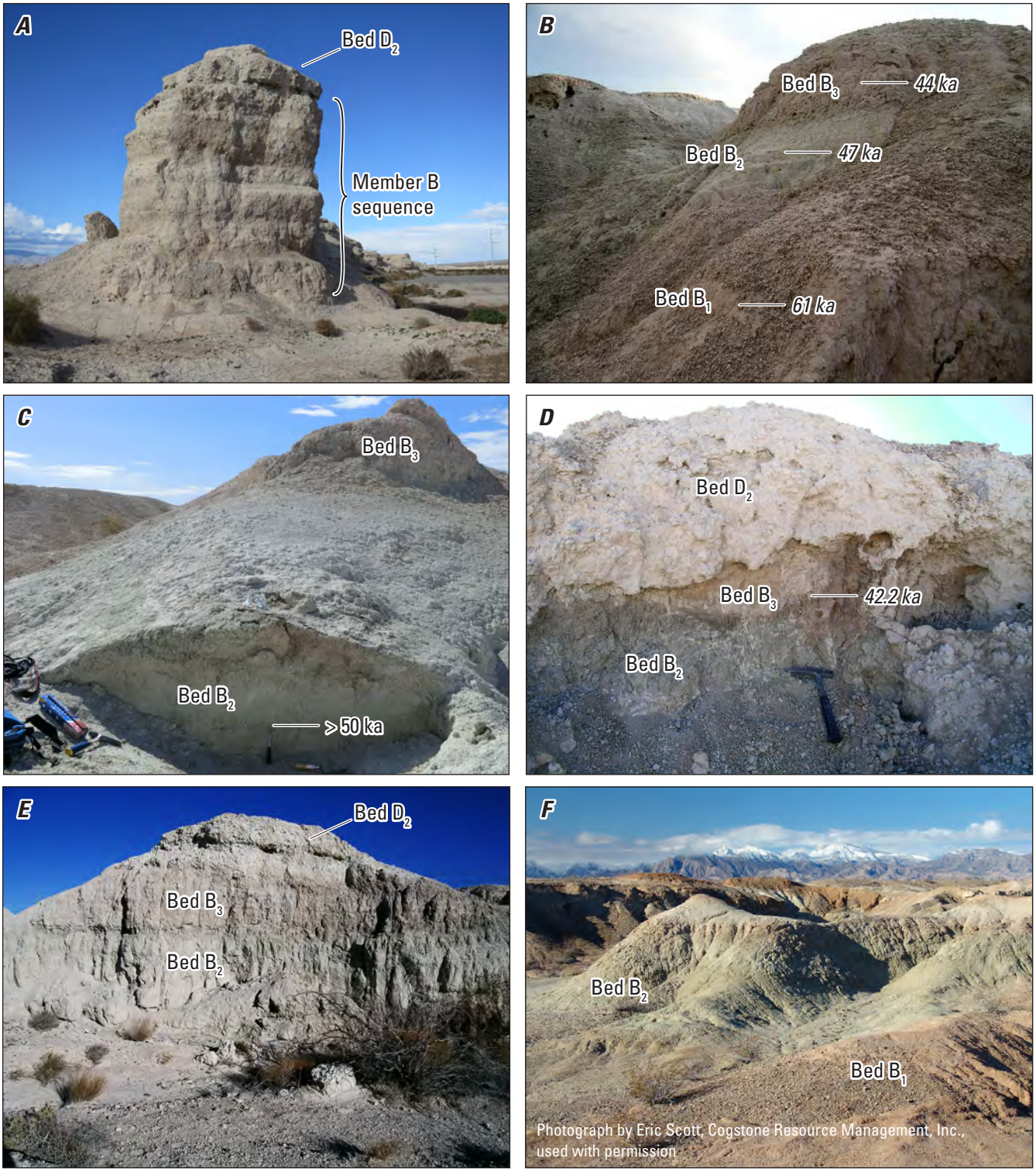

Figure 10. Photographs featuring member B deposits (see fig. 9). Universal Transverse Mercator coordinates are in zone 11S. *A*, Distinctive rhythmic sediments that are typical of member B, representing rapid oscillation between fluvial processes, wetland development, stable surfaces, and erosion; 659850 meters (m) easting (E), 4021923 m northing (N). View to the nothwest. Section is 8.0 m thick. Deposit equivalent to section B-1. *B*, Deposit equivalent to section B-5; 664317 m E, 4020174 m N. View to the south. Section is 5.5 m thick. *C*, Deposit equivalent to section B-6; 663100 m E, 4020559 m N. View to the southeast. Section is 5.0 m thick. *D*, Deposit equivalent to section B-7; 664008 m E, 4020305 m N. View to the southwest. Section is 4.5 m thick. *E*, Distinct contact between beds B_2 and B_3; 663235 m E, 4020522 m N. View to the north. Section is approximately 6.5 m thick. *F*, Dramatic limnocrene ponding that is characteristic of bed B_2 with green silt and clay deposits in cauldron-shaped bedforms inset into the older brown, alluvial sediments of bed B_1; 662820 m E, 4020675 m N. View to the southwest. Section is approximately 2 m thick. Calibrated radiocarbon ages are given in regular font and infrared-stimulated luminescence ages are italicized.

Depositional Environments, Paleohydrology, and Paleoclimatic Interpretations of Bed B_2

Similar to the earlier groundwater discharge episode of bed $B_{1\text{-wet}}$, bed B_2 represents a discharge interval characterized by a series of interconnected spring pools and outflow streams. The laterally discontinuous, cauldron-shaped bedforms of bed B_2 are characteristic of limnocrene spring discharge and were fed by feeder conduits associated with faults in the valley. Some of these conduits were unearthed in the original trenches of the Tule Springs Expedition, and Haynes (1967) documented the presence of well-sorted, fine-grained sands and abundant vertebrate fossils within them.

Bed B_2 stands in stark contrast to the tan alluvium stratigraphically above and below (beds B_1 and B_3) and marks an increase in groundwater availability related to increased effective precipitation. The timing of the deposition of bed B_2 falls within early MIS 3 and represents a period of groundwater discharge with prevalent limnocrene ponding. Water-table levels were high at this time, and groundwater traveled upward through the subsurface, through fault traces, with enough hydraulic head to scour out the spring pools.

The different hydrologic environments can be differentiated based on the sedimentology, as well as on mollusk assemblages. The presence of the aquatic gastropod *Helisoma* sp. in bed B_2, for example, is indicative of limnocrene ponding (Shanahan and others, 2005). Overflow of some of the ponds created outflow streams associated with bed B_2, as evidenced by the presence of abundant Hydrobiidae shells. Vertebrate fossils are also prolific in bed B_2, with a diverse assemblage of taxa recovered from multiple locations throughout the upper Las Vegas Wash (Scott and others, 2017).

Bed B_3

Bed B_3 is typically 1–2 m thick and exhibits a suite of lithologies that are similar to the deposits of bed B_1, including massive, tan-colored silt, cross-bedded sands and localized clay, and thin carbonate horizons (figs. 9 and 10).

Age Control of Bed B_3

One calibrated ^{14}C age (42.2±5.3 ka; table 1) on charcoal and two IRSL ages (44±6 ka and 45±7 ka; table 2) indicate bed B_3 was deposited between approximately 45 and 40 ka.

Depositional Environments, Paleohydrology, and Paleoclimatic Interpretations of Bed B_3

The sediments of bed B_3 represent fluvial channel and overbank deposits. The pervasive tan alluvium of bed B_3 follows the same depositional pattern as bed B_1, with episodic flood events followed by periods of surface stability and soil formation. The carbonate horizons reflect the presence of groundwater at or near the surface during short-lived wet phases that were followed by brief periods of relatively dry conditions. Overall, bed B_3 records highly variable environmental conditions resulting from climate fluctuations that were prevalent during early MIS 3 (Dansgaard and others, 1993; Svensson and others, 2008).

Member D

Unit D is the most widespread and best exposed of all the Haynes subdivisions (1967) of the Las Vegas Formation sedimentary sequence. This unit is characterized by pale-green calcareous silts and clays in the valley axis that grade to tan siltstones in more marginal areas. The presence of extensive green axial mudstones in the valley was the primary line of evidence used to support the idea of a large pluvial lake during full-glacial time (Hubbs and Miller, 1948; Maxey and Jamesson, 1948; Snyder and others, 1964; Longwell and others, 1965; Haynes, 1967); however, these deposits have since been shown to represent extensive marshes (Quade, 1986; Quade and Pratt, 1989). Notably, this unit has produced prolific Pleistocene megafaunal and microfaunal assemblages (Haynes, 1967; Mawby, 1967; Quade, 1986; Quade and Pratt, 1989; Quade and others, 1995, 2003; Scott and others, 2017).

Member D (figs. 11–13) represents the highest groundwater levels attained in the Las Vegas Valley during the late Quaternary. Pervasive spring discharge during this time supported widespread marshes and wet meadows that are preserved as distinct and spatially extensive carbonate caps and benches. Within member D, we recognize three beds—D_1, D_2, and D_3—that contain multiple black mats (organic-rich sediments that accumulate in poorly drained environments), carbonate benches and caps, and lithologies that vary laterally from the valley axis (wetter) into more marginal facies (drier) upslope. Within member D, discharge episodes represented by the three beds are separated by periods of surface stability and (or) erosion. As above, we attribute some of the sediments that Haynes (1967) called unit C to bed D_2; see the discussion in the section "Dissolution of Unit C."

Bed D_1

The lowest bed of member D, called bed D_1, was first recognized and characterized by Ramelli and others (2011) in the axial part of the valley (fig. 11, section D-7; fig. 12*F*). This bed is exposed in both the valley axis and the margins of the upper Las Vegas Wash and overlies the older deposits of members A and B. The basal part of bed D_1 in the valley axis consists of green clays with blocky structures and approximately 1 m of green silts and clays (figs. 11 and 12), all of which contain abundant mollusk shells, including both terrestrial (Succineidae, *Fossaria* sp., *Physa* sp.) and aquatic (*Helisoma* sp., *Gyraulus* sp., *Pisidium* sp.) taxa. Upsection, multiple channels of reworked subangular to subrounded carbonate nodules form gravel bed loads that are up to 15 cm thick. The middle part of bed D_1 exhibits olive-green silts and clays present in discrete cauldron-shaped bedforms that are 1–3 m thick, similar to beds $B_{1\text{-wet}}$ and B_2. Aquatic gastropods (*Helisoma* sp.) and bivalves (*Pisidium* sp.) are abundant in these sediments, which also contain disseminated charcoal that was utilized for ^{14}C dating. Vertebrate fossils are abundant in the bed D_1 cauldrons, similar to beds $B_{1\text{-wet}}$ and B_2 (Scott and others, 2017). Unlike these older deposits, however, the middle part of bed D_1 also contains tufa (calcium carbonate) precipitated

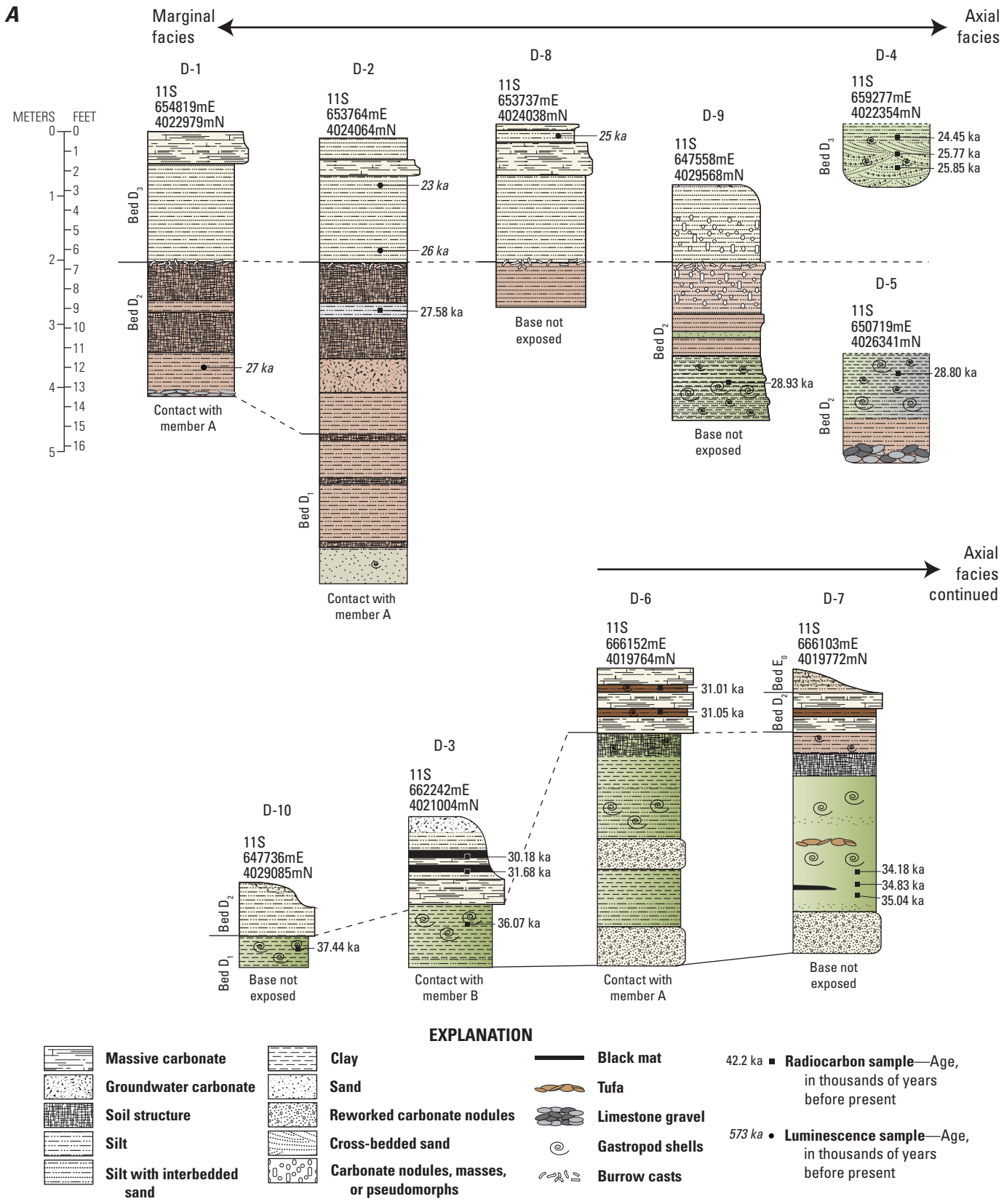

Figure 11. (this and facing page) Stratigraphic sections, ages, and colors featuring member D sediments. *A*, Stratigraphic profiles featuring member D deposits in context of bounding members, and associated radiocarbon and infrared-stimulated luminescence ages (see tables 1 and 2). Universal Transverse Mercator coordinates are in zone 11S. Overall, member D dates to between 37.44 and

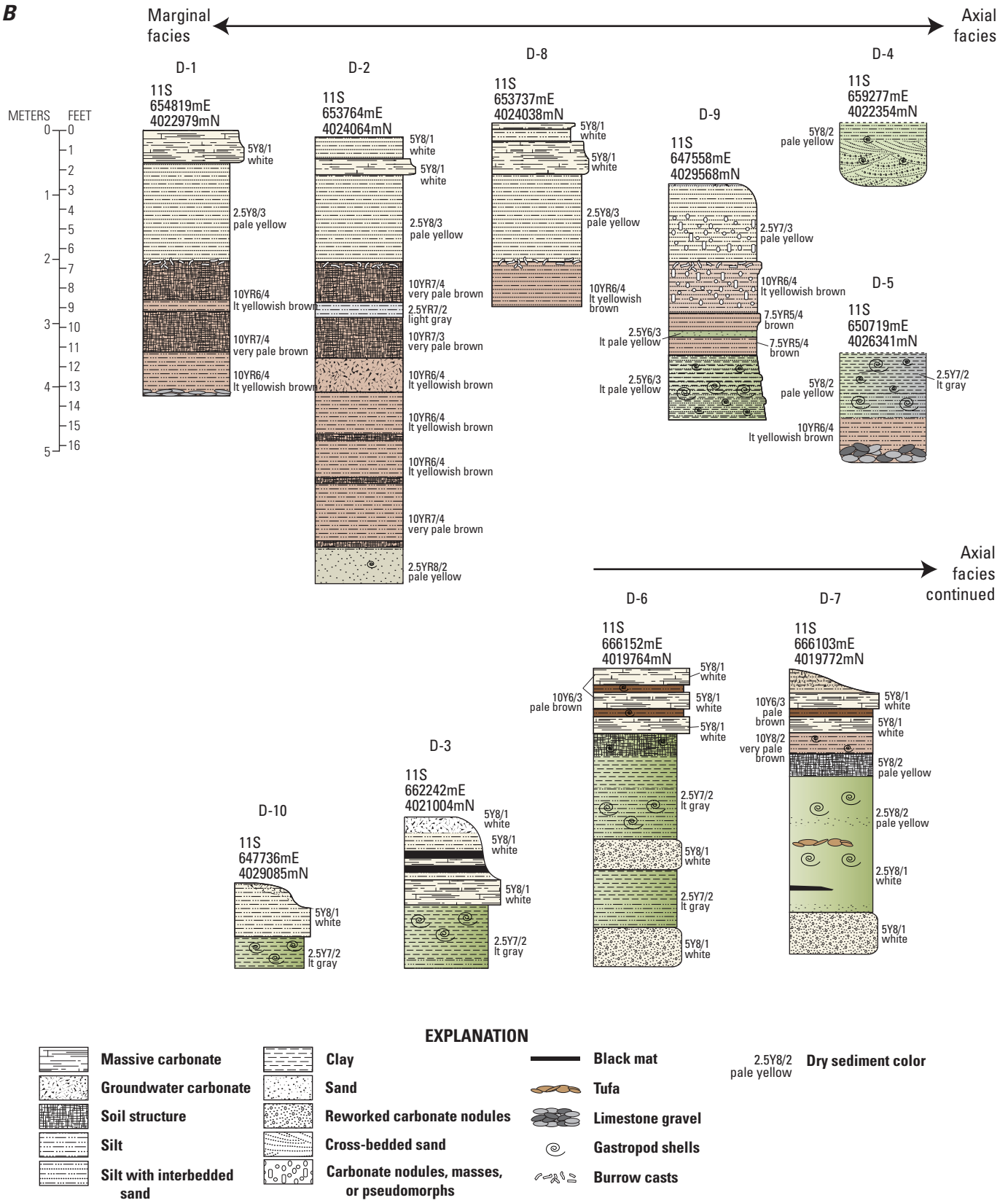

24.45 kilo-annum (ka [thousands of years before present]) and represents the highest groundwater levels achieved in the Las Vegas Valley during the late Quaternary. Calibrated radiocarbon ages (filled squares) are given in regular font and infrared-stimulated luminescence ages (filled circles) are italicized. *B*, Stratigraphy and dry colors (Munsell Color [Firm], 2010) of member D sediments. (m, meter; E, easting; N, northing)

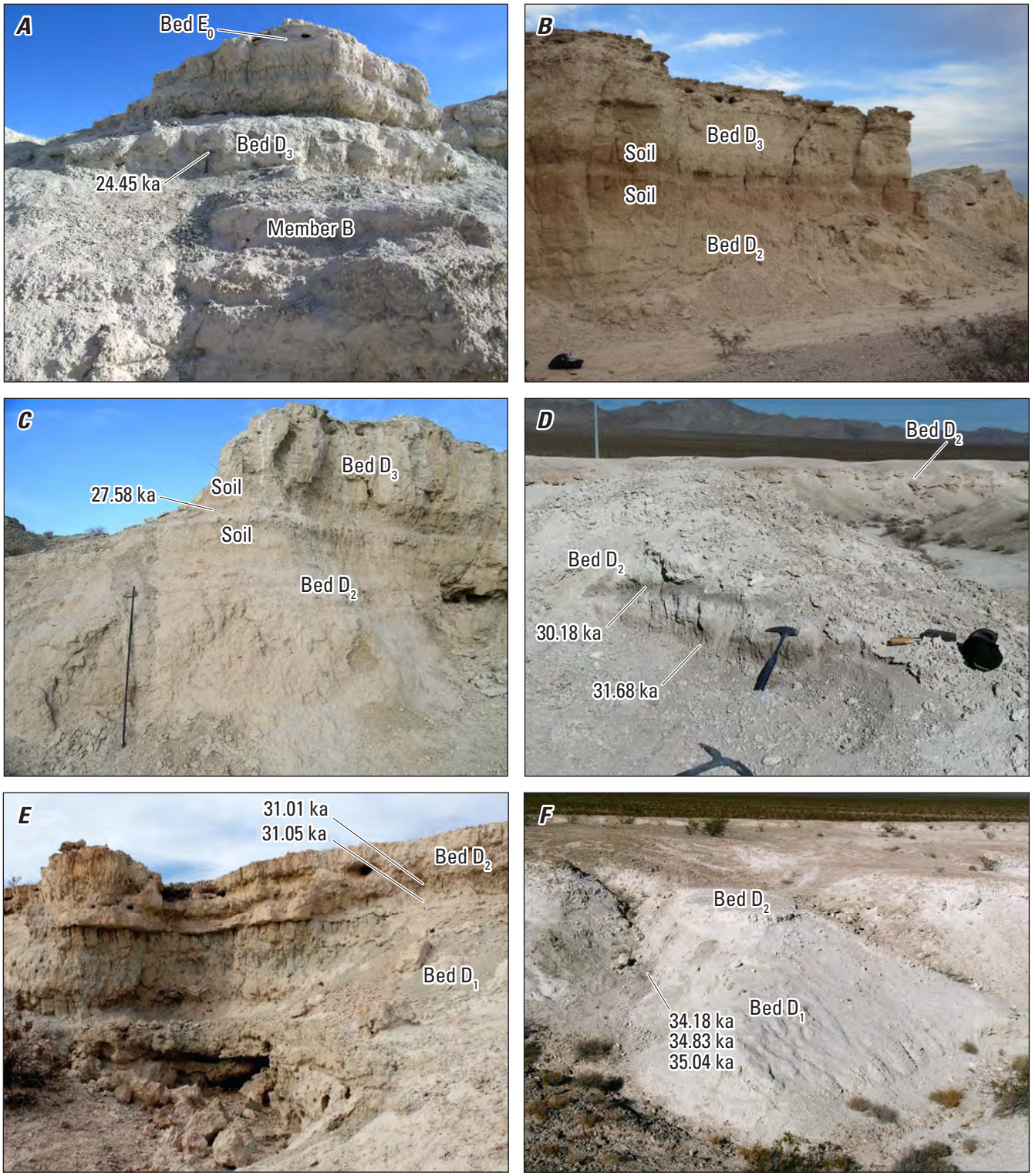

Figure 12. Photographs featuring member D deposits (see fig. 11). Universal Transverse Mercator coordinates are in zone 11S. *A*, Deposit equivalent to sections D-4 and B-3 (see fig. 9); 659277 meters (m) easting (E), 4022354 m northing (N). View to northeast. Section is 5.0 m thick. *B*, Characteristic tan marginal facies deposits of the bed D_2/D_3 sequence with two distinct, reddish soils at the top of bed D_2; 653648 m E, 4024002 m N. View to the southwest. Section is 7.0 m thick. *C*, Deposit equivalent to section D-2; 653764 m E, 4024064 m N. View to the east. Section is 8.0 m thick. *D*, Deposit equivalent to section D-3; 662242 m E, 4021004 m N. View to the west. Section is 2.2 m thick. *E*, Deposit equivalent to section D-6; 666152 m E, 4019764 m N. View to the north. Section is 4.0 m thick. *F*, Deposit equivalent to section D-7; 666103 m E, 4019772 m N. View to the north. Section is 4.5 m thick.

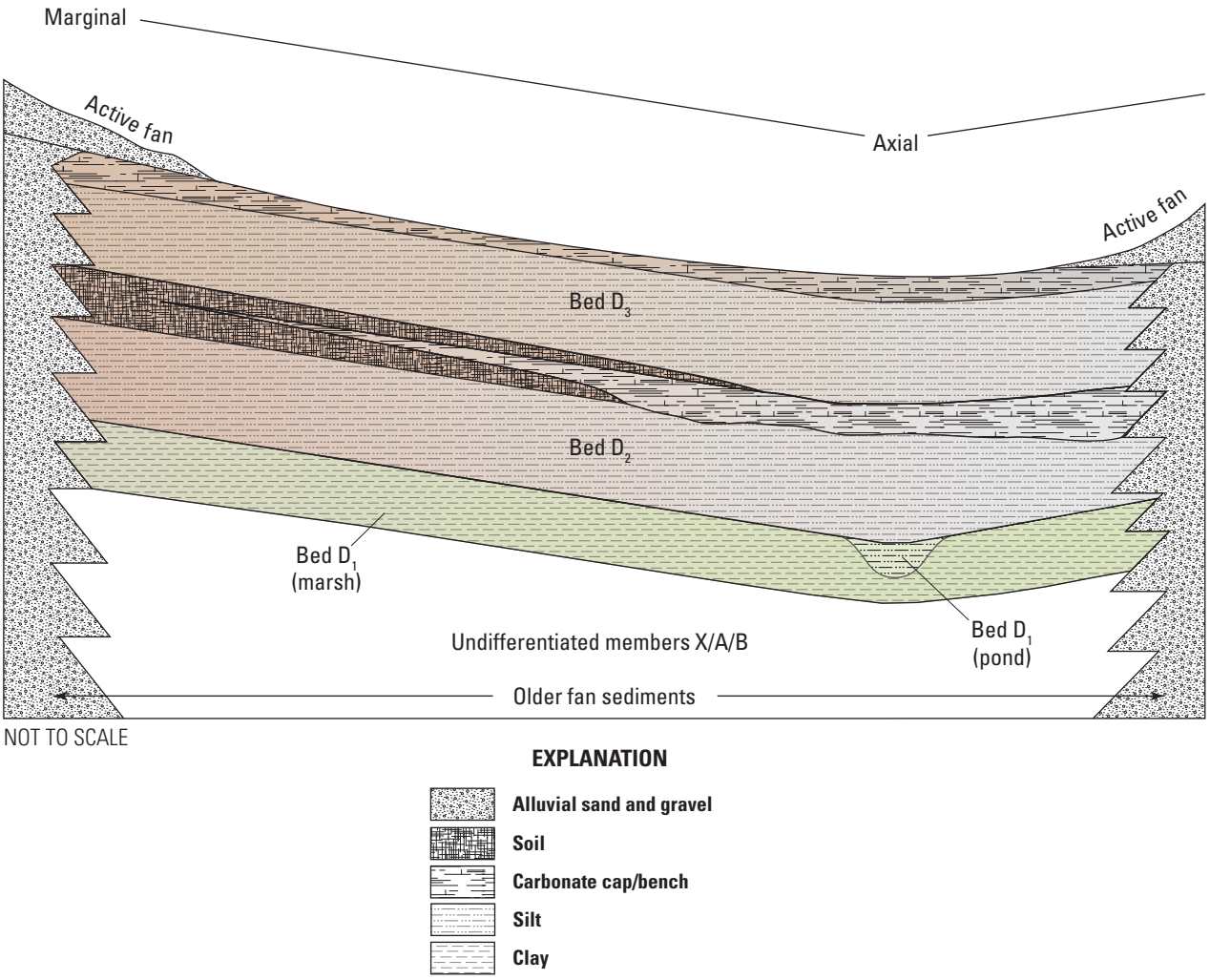

Figure 13. Schematic diagram showing the sedimentary facies changes in member D first described by Quade and colleagues (Quade and Pratt, 1989; Quade and others, 1995) that occur between the axial and marginal portions of the Las Vegas Valley. Member D sediments, which date to the last full-glacial period (marine isotope stage 2), are characterized by green clays and white to gray marls deposited in marshes and wet meadows in the axial part of the valley that grade into tan silts and sands deposited in phreatophyte flat settings in more marginal areas. Similar lateral facies changes are also seen in member A sediments, which were also deposited (in part) under full-glacial conditions (marine isotope stage 6).

by physicochemical processes. Approximately 1–2 m of green clays with prismatic structure containing abundant Succineidae shells, an incipient carbonate horizon, and strongly oxidized silts occur in the upper part of bed D_1 and are positioned stratigraphically above the cauldrons (fig. 11, sections D-6 and D-7). The marginal facies of bed D_1 consists of approximately 2 m of massive, grayish-green to brown silts with a mottled appearance, rare terrestrial mollusk shells, and less carbonate than in the axial deposits (fig. 11, section D-2).

Age Control of Bed D_1

Haynes (1967) reported an age of 31.3±2.1 ^{14}C ka (corresponding to a calibrated age of approximately 35 ka; app. 1) for unit D from his type section in Trench K at the original Tule Springs site. This age was obtained from deposits that are lithologically and stratigraphically similar to those from which we obtained a calibrated age of 36.07±0.47 ka from a Succineidae shell (fig. 11, section D-3; table 1). Overall, we obtained five ^{14}C ages for bed D_1 that range between 37.44 and 34.18 ka, including three stacked ages at section D-7 that maintain stratigraphic order and range from 35.04 to 34.18 ka (figs. 11 and 12*F*; table 1).

Depositional Environments, Paleohydrology, and Paleoclimatic Interpretations of Bed D_1

Initial deposition of bed D_1 began at approximately 38 ka when groundwater levels were relatively low. In the valley axis, sedimentation was characterized by streams that deposited bed loads composed of reworked carbonate gravels derived from units exposed at the surface from previous discharge intervals, including the pervasive cap at the top of member A. At approximately 37 ka, the water table rose and silt- and clay-rich deposits containing aquatic and terrestrial gastropod shells were deposited in ponds and marshes. Shortly thereafter, at around 35.5 ka, another drop in the water table occurred, which was once again accompanied by vigorous fluvial activity. The reworked carbonate nodules present in this part of bed D_1 make up the bed load of at least three major channels that coursed through the upper Las Vegas Wash. The intervals of low groundwater levels and high fluvial activity in bed D_1 correlate temporally with D-O 8 and 7, respectively (fig. 20).

Subsequently, at approximately 35 ka, the water table rose and the high-energy fluvial environment gave way to limnocrene ponding as represented by the olive-green silts and clays with abundant aquatic mollusks (*Helisoma* sp. and *Pisidium* sp.) in cauldron-shaped spring pools. Precipitation of tufa at this time likely occurred at the edges of these ponds, which were fed by carbonate-laden water flowing out of spring orifices. Additionally, the presence of terrestrial snails (Succineidae) in this part of the bed indicates that water tables rose and water spread away from the spring pools into a broader marsh. Between 34.2 and 31.7 ka, spring discharge ceased and arid conditions prevailed as evidenced by the groundwater carbonate horizon and strongly oxidized lithologies that are present at the top of the bed. These breaks in discharge reflect widespread drying events that correspond in time to D-O 6 and 5, respectively (fig. 20; Springer and others, 2015).

Bed D_2

Bed D_2 rests on the older discharge units of the Las Vegas Formation (members A and B and occasionally bed D_1) and is the most geographically extensive unit within the formation. Sedimentary facies changes between the valley axis and margins have resulted in a high degree of lithologic variation within this bed (fig. 13). In the valley axis, for example, bed D_2 consists of 1–2 m of white to gray silts with interbedded black mats and abundant secondary carbonate overlain by greenish-gray silts and clays. In more marginal areas, bed D_2 typically consists of pale-brown to tan silts and sands and is capped by two distinctive reddish soils (fig. 11, sections D-1 and D-2; fig. 12*B*). In addition, thousands of burrow casts (possibly from cicada nymphs [Quade, 1986]) can be observed weathering out of the D_2–D_3 contact in the marginal areas (fig. 11, sections D-1, D-2, and D-8), a phenomenon that occurs throughout the northern reaches of the upper Las Vegas Wash.

In both axial and marginal areas, the bed D_2 sedimentary sequence is completed by a thick (approximately 1 m), spatially extensive groundwater carbonate cap (fig. 11, sections D-3, D-6, and D-7; fig. 12*D*).

Age Control of Bed D_2

Haynes (1967) acquired very few ages from unit D that he considered to be reliable, but he estimated the age range of the unit to be between approximately 30 and 16 ^{14}C ka (corresponding to approximately 34 and 19 ka; app. 1). McVicker and Spaulding (1993) obtained two ^{14}C ages, 31.9±1.3 ka and 30.8±1.5 ka, for unit D sediments. We obtained seven additional ^{14}C ages for bed D_2 that range between 31.68 and 27.58 ka. A single IRSL age of 27±2 ka obtained from the marginal deposits at section D-1 (fig. 11, section D-1; table 2) further augments the chronology of this bed.

Depositional Environments, Paleohydrology, and Paleoclimatic Interpretations of Bed D_2

Groundwater levels were extremely high during the deposition of bed D_2 and the marked lithologic variation documented in this report (figs. 6 and 11) is the result of hydrologic differences between the valley axis and more marginal areas that occurred during full-glacial times. The axial greenish-gray clays and silts represent extensive marshes characteristic of helocrene discharge, and axial whitish-gray silts with interbedded black mats and secondary carbonates represent associated wet meadows. Away from the valley axis, these sediments grade into tan silts and sands that represent topographically higher and drier phreatophyte flats, consistent with the facies model of Quade and Pratt (1989) and Quade and others (1995).

The extensive groundwater carbonate cap and benches at the top of bed D_2 represent the familiar sequence of wet conditions, during which carbonate-rich silts and clays were deposited in marshes and wet meadows, followed by warm, dry conditions associated with D-O 4 and 3. This abrupt warming led to the rapid depression of the water table, which in turn led to desiccation of

the wetlands and commensurate intensified evaporative effects and case hardening. As in the discussion of the carbonate cap and benches in member A, carbonate in member D is formed at or below the water-table capillary fringe and is derived from groundwater, again in contrast to typical pedogenic calcretes that form from soil waters percolating downward through the vadose zone.

The marginal wetland deposits of bed D_2 provide particularly good illustrations of the effects of lateral expansion and contraction of the full-glacial wetlands in response to climate fluctuations. Specifically, two soils at the top of bed D_2 (fig. 11, sections D-1 and D-2; fig. 12*B*-*C*) represent dry conditions and wetland contraction that also correlate in time to D-O 4 and 3, respectively, and are separated by a brief discharge event in bed D_2 dating to 27.58±0.23 ka (fig. 20; table 1; Springer and others, 2015). In addition, the presence of the burrow casts at the top of the bed D_2 sequence marks a stable surface that was followed by renewed wetland deposition during D_3 time.

Bed D_3

Bed D_3 exhibits a variety of lithologies and occupies a position on the landscape similar to that of bed D_2. The axial facies of bed D_3 includes 1–2 m of massive, yellowish-gray silts and sands with interbedded black mats, abundant carbonate, and fossil mollusks. Exposures of this bed are extremely limited as it has been largely stripped from the axial part of the valley. Similar to bed D_2, the marginal facies of bed D_3 is extensive and consists of 1–3 m of massive, pale brown to tan silts and sands (fig. 11, section D-4; fig. 12). The top of bed D_3 also exhibits a massive groundwater carbonate cap that marks the highest groundwater levels achieved in the Las Vegas Valley.

Age Control of Bed D_3

We obtained three ^{14}C ages (table 1) and three IRSL ages (table 2) for bed D_3 that constrain its age to between 25.83 and 24.45 ka.

Depositional Environments, Paleohydrology, and Paleoclimatic Interpretations of Bed D_3

The marginal wetland deposits of bed D_3 provide another vivid illustration of expansion and contraction of wetlands in the Las Vegas Valley in response to climate fluctuations. After desiccation of the marshes following bed D_2 time, water tables rose and again reached the highest levels observed in the Las Vegas Valley, supporting widespread helocrene flow and deposition of bed D_3. This deposition was followed by a significant warming event coincident with D-O 2 that led to desiccation of the vast full-glacial wetland system in the valley and formation of the D_3 carbonate cap (fig. 20; Springer and others, 2015).

Member E

Member E contains three primary units—beds E_0, E_1, and E_2—the latter two of which are divided into seven secondary subunits—beds E_{1a}, E_{1b}, E_{1c}, E_{1d}, E_{2a}, E_{2b}, and E_{2c}. Each of these beds is temporally and stratigraphically distinct and mappable at the outcrop scale. The spatial relations and relative ages of member E deposits can be determined by observing cross-cutting relations and their position on the landscape relative to one another.

Overall, the multiple cycles of deposition, erosion, and surface stability recorded in member E reflect the extreme hydrologic variability that characterized the Las Vegas Valley following desiccation of the valley-wide wetland ecosystem after the Last Glacial Maximum. Member E also marks the appearance of an exclusively rheocrene flow regime, characterized by numerous fluvial channels that often contain ambient-temperature, microbially mediated tufa, as well as some physicochemical tufa.

Bed E_0

Geologic mapping and detailed stratigraphic studies in the upper Las Vegas Wash have led to the discovery and documentation of a previously unrecognized lithologic unit that postdates member D and predates beds E_1 and E_2 (Ramelli and others, 2011; Springer and others, 2015). Sediments of this new unit, called bed E_0 (figs. 14 and 15), were initially designated as either "unit D" or "unit E" (Haynes, 1967; Bell and others, 1998, 1999; Page and others, 2005) and later were subsumed into map unit Qtse (Ramelli and others, 2011).

The basal part of bed E_0 exhibits cauldron-shaped bedforms that are 1–2 m thick and contain massive, pale olive-green silts and sands with abundant aquatic and terrestrial mollusks, including *Helisoma* sp., *Fossaria* sp., *Physa* sp., *Gyraulus* sp., *Pisidium* sp., and Succineidae. Upsection, this bed contains two thin (10–30 cm) layers of rounded carbonate gravels derived from the underlying carbonate cap of bed D_2 (and possibly bed D_3) mixed with rounded Paleozoic limestone gravels, as well as the earliest known appearance of microbially mediated tufa in the Las Vegas Formation. These gravel layers are often separated by 10–20 cm of gray to olive-green sands containing abundant aquatic mollusk shells (*Pisidium* sp., *Physa* sp.). Overlying these layers are 1–2 m of massive, light-green or gray sands and silts that contain abundant vertebrate fossils (Scott and others, 2017) and exhibit iron-oxide staining and numerous spring-feeder conduits filled with well-sorted fine sands. In turn, these sediments are overlain by as much as 2 m of buff-colored fine sands and silts with carbonate and are capped by 10–30 cm of platy carbonate and (or) carbonate rubble.

Age Control of Bed E_0

Bell and others (1999) obtained a single ^{14}C age of 14.29±0.44 ^{14}C ka (which correlates to a calibrated age of 17.3±1.1 ka) in bed E_0 deposits that they mapped as unit D (app. 1). We obtained a calibrated ^{14}C age of 18.16±0.19 ka on charcoal at the same locality (table 1), as well as 12 other ^{14}C ages for bed E_0 from sites throughout the upper Las Vegas Wash. In all, calibrated ^{14}C ages for this bed range between 23.04 and 18.16 ka (table 1).

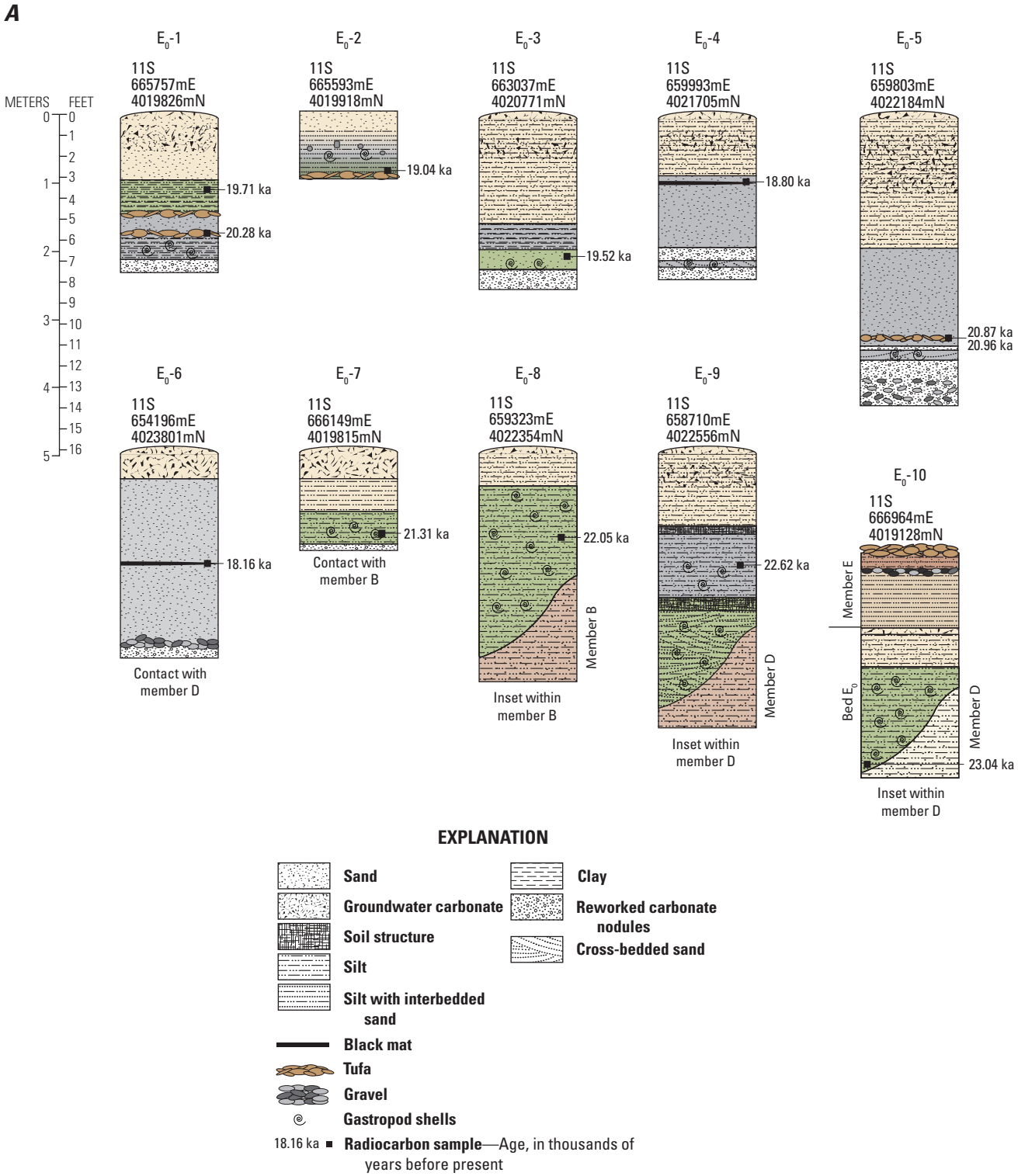

Figure 14. (this and facing page) Stratigraphic sections, ages, and colors featuring bed E_0 sediments. *A*, Stratigraphic profiles featuring bed E_0 deposits in context of lower bounding members, and associated radiocarbon ages (see table 1). Universal Transverse Mercator coordinates are in zone 11S. Overall, bed E_0 dates to between 23.04 and 18.16 kilo-annum (ka [thousands of years before

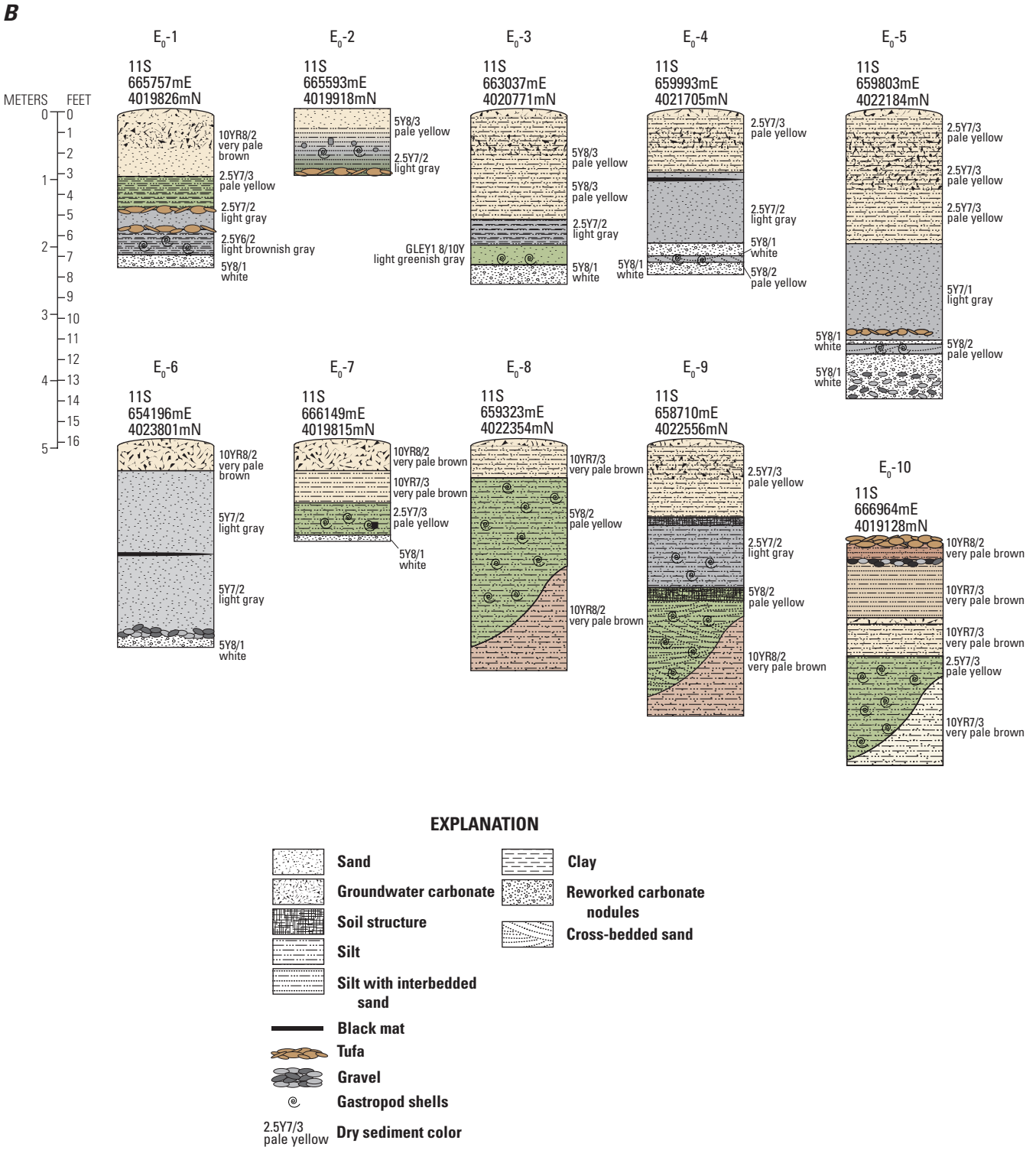

present]) and represents a series of spring pools, outflow streams, and flood plains. *B*, Stratigraphy and dry colors (Munsell Color [Firm], 2010) of bed E_0 sediments. (m, meter; E, easting; N, northing)

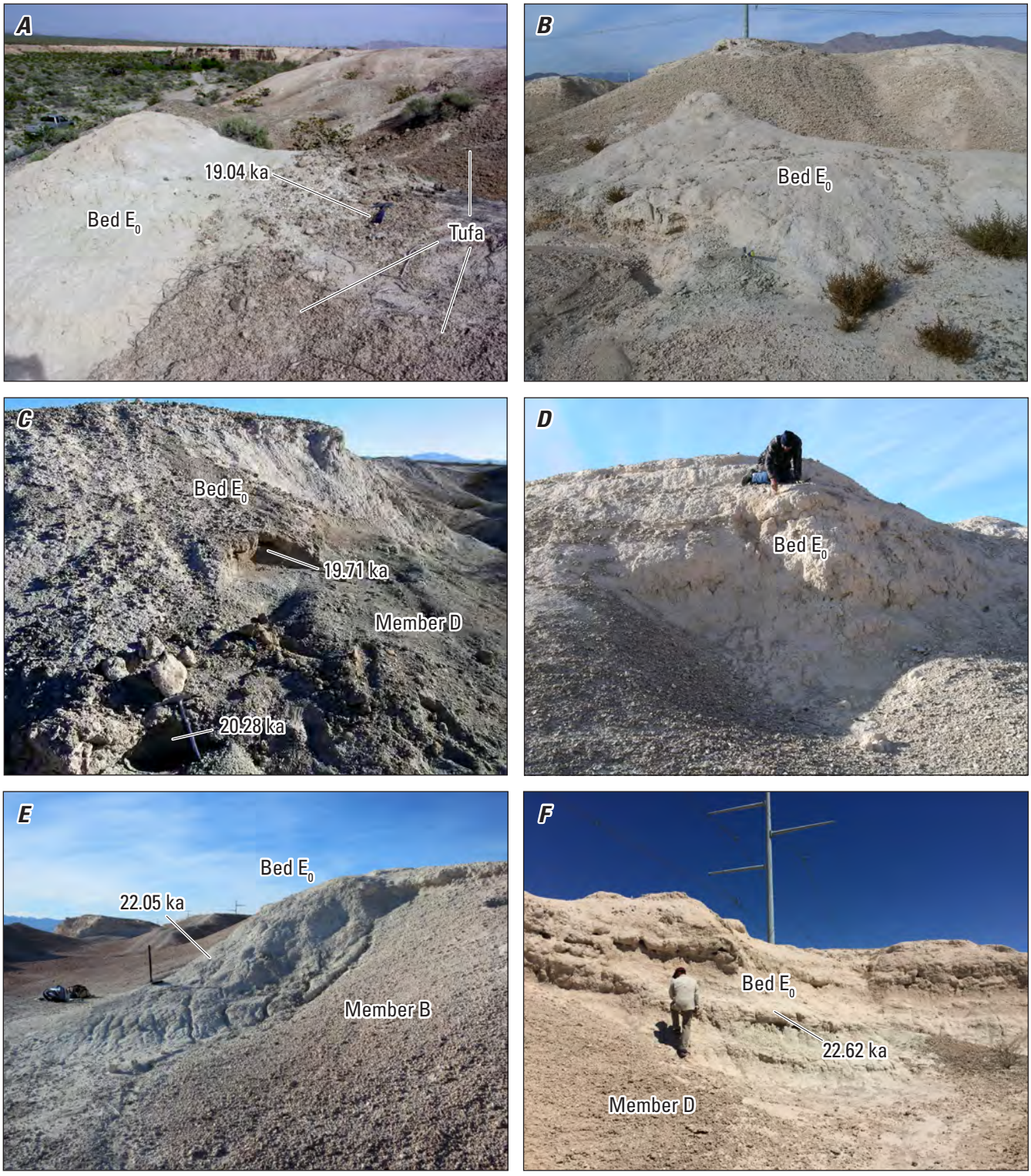

Figure 15. Photographs featuring bed E_0 deposits (see fig. 14). Universal Transverse Mercator coordinates are in zone 11S. *A*, Deposit equivalent to section E_0-2; 665593 meters (m) easting (E), 4019918 m northing (N). View to the east. Section is 1.0 m thick. *B*, Characteristic buff-colored silts and sands in the upper part of the E_0 sequence; 659803 m E, 4022184 m N. View to north. Section is 4.0 m thick. Deposit equivalent to section E_0-5. *C*, Deposit equivalent to section E_0-1; 665757 m E, 4019826 m N. View to east. Section is 2.3 m thick. *D*, Weathered surface of the upper part of the E_0 sequence; 659289 m E, 4022347 m N. View to the south. Section is approximately 1 m thick. Deposit equivalent to the top of section B-3 (see fig. 9). *E*, Deposit equivalent to section E_0-8; 659323 m E, 4022354 m N. View to the northwest. Section is 3.0 m thick. *F*, Deposit equivalent to section E_0-9; 658710 m E, 4022556 m N. View to the east. Section is 3.0 m thick.

Depositional Environments, Paleohydrology, and Paleoclimatic Interpretations of Bed E_0

A depositional hiatus followed the desiccation of the extensive, full-glacial wetland ecosystem associated with member D. Quade and others (2003) placed the timing of the hiatus between the end of unit D at approximately 24.5 ka and the beginning of unit E_1, then dated to approximately 16 ka, which indicates a hiatus of approximately 8,500 years. With the discovery and improved age control of bed E_0, data now show that wetland development was actually reestablished by 23 ka, meaning the hiatus was only approximately 1,500 years in duration.

In contrast to the extensive full-glacial marshes and wet meadows that dominated the landscape during the deposition of member D, the deposits of bed E_0 are the result of point-source limnocrene ponding and rheocrene discharge with multiple outflow streams. Thus, bed E_0 marks a dramatic change in the type of discharge that prevailed through the rest of the late glacial period.

At the base of bed E_0, cauldron-shaped bedforms dating to approximately 23 ka represent limnocrene discharge and are analogous to the spring pools in beds $B_{1\text{-wet}}$, B_2, and D_1. Overlying these deposits, the massive light-green sands and silts that exhibit iron-oxide staining and numerous feeder conduits are indicative of vigorous spring activity. Ambient-temperature, microbially and physicochemically mediated tufa first occurs in bed E_0 at approximately 21 ka and is associated with rheocrene flow. Colder temperatures inhibit the formation of microbially mediated tufa (Pedley, 1990, 2000; Ford and Pedley, 1996; Capezzuoli and others, 2014). Because microbially mediated tufa is strikingly absent from the older deposits of members X, A, B, and D, its appearance in bed E_0 suggests that rising temperatures crossed an unspecified threshold at this time. (Note that modern tufa forms in water when temperatures are above approximately 20 °C [Capezzuoli and others, 2014].)

The distinct lithologic change between the light-green, reduced sands and silts and the overlying buff-colored, oxidized sands, silts, and carbonate in bed E_0 is pervasive throughout the Las Vegas Valley and dates to between approximately 18 and 16 ka based on calibrated ^{14}C ages in bed E_0 and the overlying bed E_{1a} (see fig. 5). Importantly, the oxidized silts and sands are indicative of a drier environment followed by intense erosion that together correlate temporally with the "Big Dry" of Broecker and others (2009), a dry period that is thought to have affected much of the Great Basin, including the Las Vegas Valley (fig. 20; Springer and others, 2015). The platy carbonate and rubble at the top of bed E_0 is thinner and darker in color than the caps of member D and marks the cessation of this discharge interval.

Bed E_1

Haynes (1967) recognized multiple spring-fed channels on top of, and inset within, unit D. He attributed these deposits collectively to unit E_1 but did not further differentiate them. We show that bed E_1 actually consists of several discrete subunits (E_{1a}, E_{1b}, E_{1c}, and E_{1d}) that each exhibit their own unique lithologies and represent distinct discharge episodes (figs. 16 and 17). These subunits are inset within and cross-cut the dissected topography of beds D_2, D_3, and E_0, as well as each other.

Bed E_{1a}.—Bed E_{1a} is prevalent throughout the northern reaches of the upper Las Vegas Wash and is often inset into the eroded topography of bed D_2 (fig. 17*B*). It consists of 1–4 m of rhythmically bedded (10–30 cm), well-sorted, buff-colored, carbonate-rich silts and sands and exhibits a hummocky and honeycombed weathering pattern in outcrop. A typical outcrop of bed E_{1a} is shown in figure 17*A* and the range of lithologies is depicted in sections E_1-1, E_1-4, E_1-5, E_1-7, E_1-8, E_1-11, and E_1-13 of figure 16. Bed E_{1a} deposits are capped by 20–40 cm of carbonate rubble that is platy in some places (fig. 16, section E_1-4). Bed E_{1a} often contains charcoal and incipient black mats at the base of exposures, as well as lenses of rounded Paleozoic limestone gravels. Tufa also occurs locally within the bed E_{1a} deposits, appearing as bed load crusts, phytoclasts, and oncoids. Vertebrate fossils are common in this bed and include the only confirmed specimen of *Smilodon fatalis* (saber-toothed cat) from the Las Vegas Formation (Scott and Springer, 2016).

Bed E_{1b}.—Bed E_{1b} consists of 1–2 m of whitish to light-gray, massive or cross-bedded silts and sands that often contain black mats, feeder conduits, and thin carbonate horizons (figs. 16 and 17*C–E*). Shells of the semiaquatic snail *Physa* sp. are common within bed E_{1b} sediments. Notably, bed E_{1b} is mantled by Paleozoic limestone gravels as opposed to groundwater carbonate. The juxtaposition of these dark-colored gravels on the nearly white-colored silts and sands contributes to its distinct appearance on the landscape. Throughout the upper Las Vegas Wash, bed E_{1b} contains vertebrate fossils, including the first definitive record of *Canis dirus* (dire wolf) from the State of Nevada (Scott and Springer, 2016). Additionally, a single site in the northern part of the upper Las Vegas Wash that yielded more than 500 vertebrate fossils, including a mammoth skull and jaw, numerous mammoth tusks, bison, horse, and other large vertebrates (fig. 17*D*), was dated to 14.59±0.50 ka (table 1), establishing it firmly within E_{1b} time (Scott and others, 2017).

Bed E_{1c}.—Bed E_{1c} typically overlies or is inset within the earlier discharge intervals of beds E_{1a} and E_{1b}. It consists of 1–2 m of massive, yellowish to light-gray silts and sands that exhibit a honeycombed weathering pattern and are often mantled by Paleozoic limestone gravels, similar to bed E_{1b} (fig. 16, sections E_1-7, E_1-8, and E_1-10; fig. 17*E*). This bed also contains shells of the aquatic bivalve *Pisidium* sp. and rare vertebrate fossils (Scott and others, 2017). Where it is not mantled in its characteristic limestone gravel clasts, bed E_{1c} can be difficult to distinguish from bed E_{1a}. However, stratigraphic relations and chronologic control have established that they are, in fact, separate units.

Bed E_{1d}.—Bed E_{1d} is not as spatially extensive as the other subunits of bed E_1, but where it is present in The Narrows of the upper Las Vegas Wash (fig. 3) it consists of approximately 1 m of massive, light-greenish-gray silt and cross-bedded sand with reworked carbonate clasts, abundant aquatic mollusks (*Pisidium* sp., *Physa* sp.), interbedded black mats, and localized inclined bedding associated with spring orifices (fig. 16, sections E_1-8, E_1-9; fig. 17). Bed E_{1d} deposits in this area also contain vertebrate fossils, including the only Pleistocene horse distinguishable to species (*Equus scotti*) within the Tule Springs local fauna (Scott and others, 2017). Elsewhere, within the warp of Eglington fault scarp (fig. 3), E_{1d} sediments consist of approximately 2 m of white, carbonate-rich silt interbedded with black mats that contain rare Succineidae shells (fig. 16, section E_1-12; fig. 17).

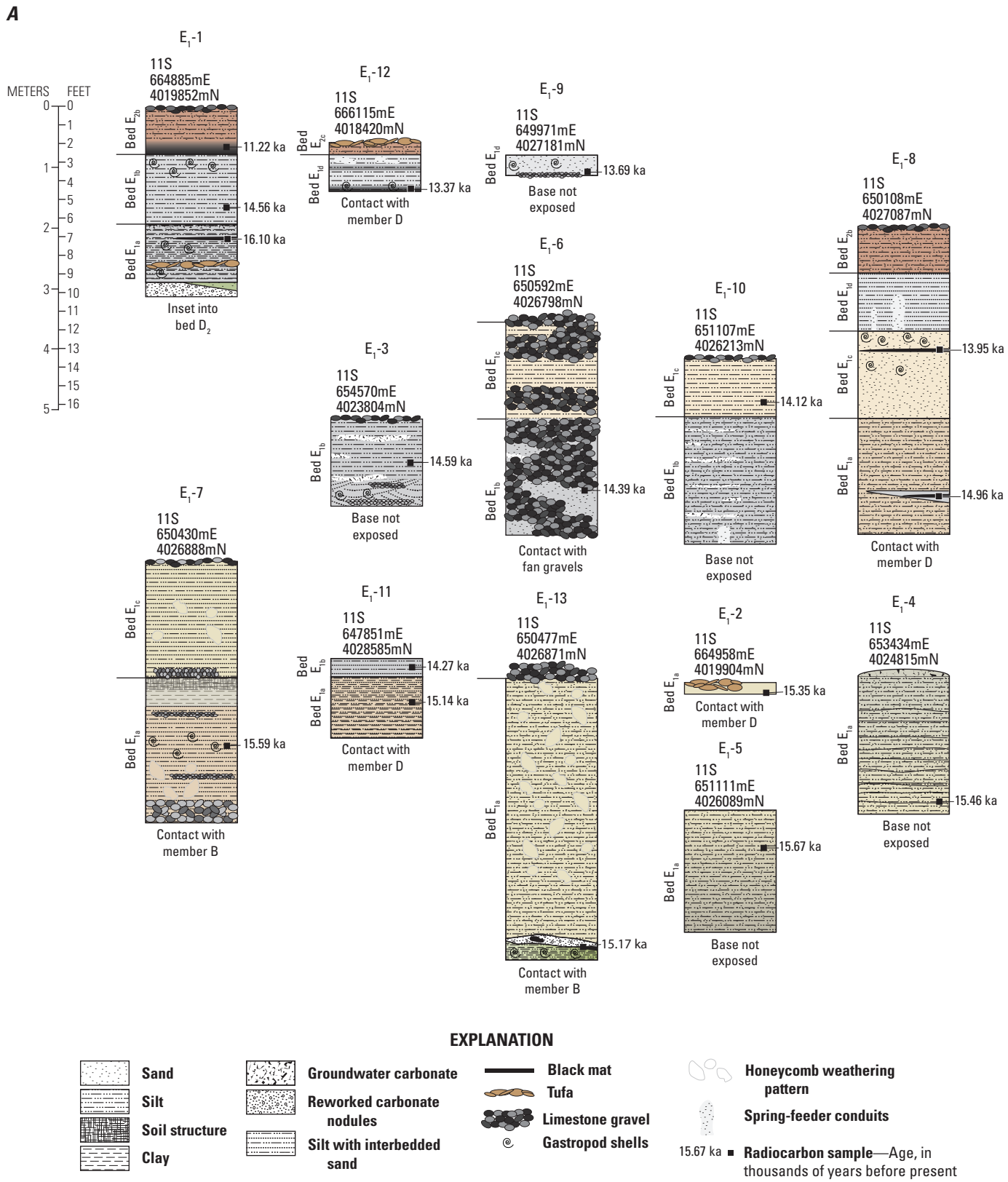

Figure 16. (this and facing page) Stratigraphic sections, ages, and colors featuring bed E_1 sediments. *A*, Stratigraphic profiles featuring bed E_1 deposits in context of bounding members and beds, and associated radiocarbon ages (see table 1). Universal Transverse Mercator coordinates are in zone 11S. Overall, bed E_1 dates to between 16.10 and 13.37 kilo-annum (ka [thousands of years before present]) and consists of four distinct subunits (beds $E_{1a–1d}$) that each exhibit a unique appearance and represent distinct episodes of rheocrene flow.

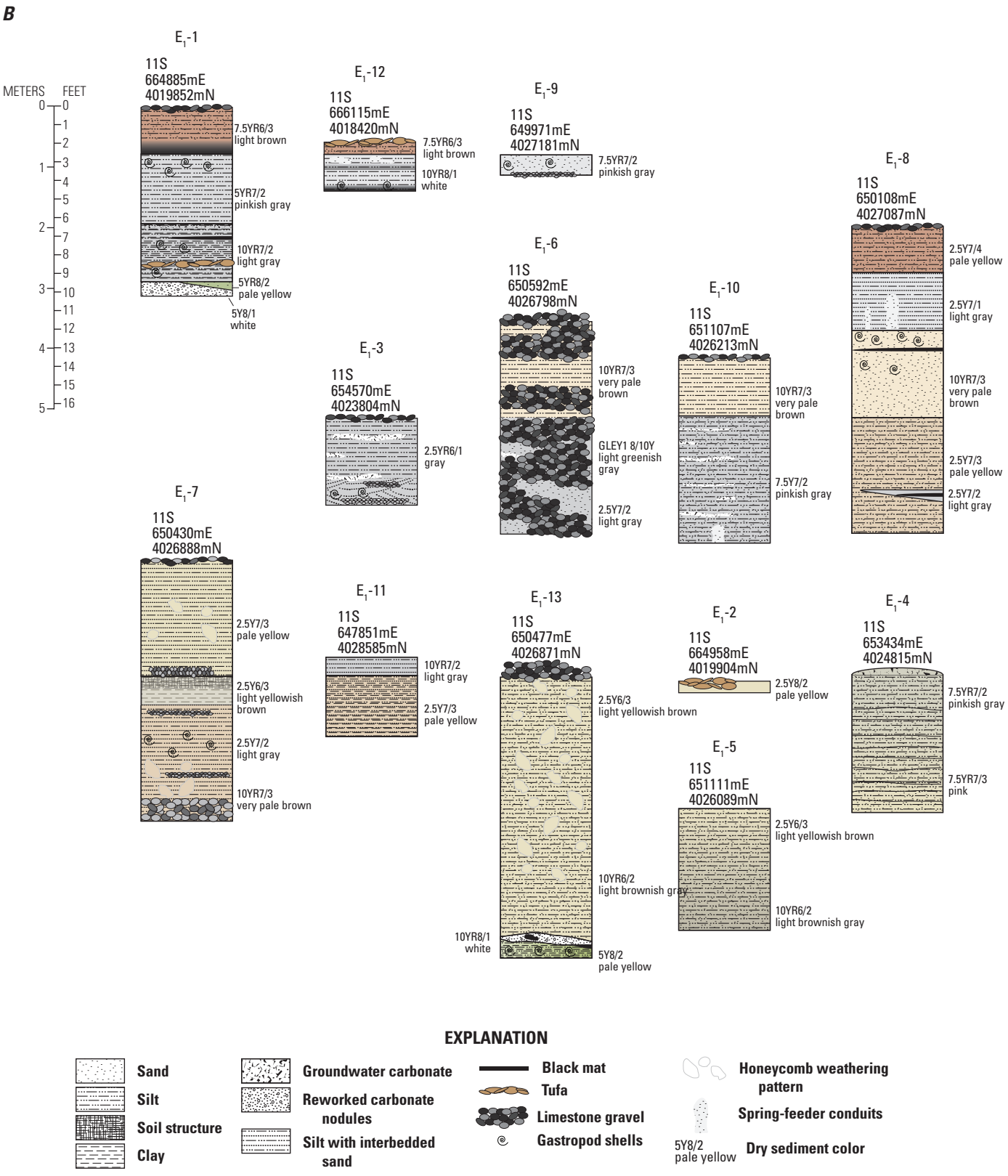

Note the honeycomb weathering patterns (voids shown as rounded and subrounded shapes) in beds E_{1a} and E_{1c} at section E_1-7 and bed E_{1a} at E_1-13, discontinuous carbonate horizons in bed E_{1b} at sections E_1-3 and E_1-10, and spring-feeder conduits filled with well-sorted sand in bed E_{1d} at section E_1-8 and in bed E_{1b} at section E_1-10. *B*, Stratigraphy and dry colors (Munsell Color [Firm], 2010) of bed E_1 sediments. (m, meter; E, easting; N, northing)

Figure 17. Photographs featuring member E_1 deposits (see fig. 16). Universal Transverse Mercator coordinates are in zone 11S. *A*, Deposit equivalent to section E_1-4; 653434 meters (m) easting (E), 4024815 m northing (N). View to the northeast. Section is 2.5 m thick. *B*, Fluvial channel of bed E_{1a} inset into the eroded topography of bed D_2; 653785 m E, 4024604 m N. View to the south. *C*, Light-colored sediments of bed E_{1b} with its capping layer of Paleozoic limestone gravel as lag in the foreground; 664885 m E, 4019852 m N. View to the west. Section is 3.0 m thick. Deposit equivalent to section E_1-1 and E_2-1 (see fig. 18). *D*, Deposit equivalent to section E_1-3; 654570 m E, 4023804 m N. View to the northwest. Section is 1.5 m thick. *E*, Deposit equivalent to section E_1-10; 651107 m E, 4026213 m N. View to the southeast. Section is 3.0 m thick. *F*, Deposit equivalent to section E_1-9; 649971 m E, 4027181 m N. View to the northwest. Section is 0.5 m thick.

Age Control of Bed E_1

Bed E_{1a}.—We obtained eight ^{14}C ages on charcoal from black mats and sediments of bed E_{1a}; ages range from 16.10 to 14.96 ka (table 1).

Bed E_{1b}.—We obtained five calibrated ^{14}C ages on charcoal from bed E_{1b}; ages range from 14.59 to 14.27 ka (table 1).

Bed E_{1c}.—We obtained two calibrated ^{14}C ages on charcoal from bed E_{1c}; ages are 14.12 and 13.95 ka (table 1).

Bed E_{1d}.—We obtained three calibrated ^{14}C ages on charcoal from bed E_{1d}; ages range from 13.69 to 13.37 ka (table 1).

Depositional Environments, Paleohydrology, and Paleoclimatic Interpretations of Bed E_1

Bed E_{1a}.—Bed E_{1a} is spatially extensive and is interpreted to represent a period of significant groundwater discharge that corresponds temporally to the "Big Wet" of Broecker and others (2009), a widespread, high-precipitation event that also corresponds temporally to the Oldest Dryas (fig. 20). Deposition of bed E_{1a} began at 16.10 ka with point-source rheocrene discharge resulting in numerous spring-fed streams with localized tufa formation, and continued for approximately 1,000 years. Deposition ended abruptly at 14.96 ka, followed by intense erosion of the E_{1a} deposits in response to a drop in the water table during the Bølling warm period (D-O 1) (fig. 20; Springer and others, 2015).

Bed E_{1b}.—Following erosion that coincided with the abrupt warming of the Bølling warm period (D-O 1), the deposition of bed E_{1b} represents rheocrene discharge that occurred for approximately 300 years as temperatures fell (fig. 20; Springer and others, 2015). The lithologies, microfauna, and position on the landscape of this bed indicate it was deposited in streams, flood plains, and wet meadows set within a series of swales and undulating topography. The Paleozoic limestone gravels that overlie the fine-grained sediments of bed E_{1b} capped by limestone gravels were deposited in high-energy stream channels that were likely similar to those found throughout the valley today.

Bed E_{1c}.—Bed E_{1c} represents another groundwater discharge interval exhibiting rheocrene flow associated with spring-fed outflow streams. Channelized bedforms and the presence of shells of the aquatic bivalve *Pisidium* sp. further support the interpretation of its deposition in shallow flowing water. The sharp lithologic transition from the conspicuously white deposits of bed E_{1b} capped by limestone gravels to the tan sediments of E_{1c} coincides with the timing of Older Dryas cooling, yet another example of how wetland ecosystems in the Las Vegas Valley responded dynamically to abrupt climate change in the recent geologic past (fig. 20; Springer and others, 2015).

Bed E_{1d}.—Exposures of bed E_{1d} represent a discrete discharge interval characterized by outflow streams, minor ponding, and wetland development. The presence of aquatic and terrestrial mollusk shells (*Pisidium* sp., *Physa* sp., Succineidae) provides additional evidence of shallow flowing water and moist ground conditions during E_{1d} time.

Bed E_2

Haynes (1967) recognized multiple spring-fed channels on top of, and inset within, unit D in the Tule Springs area that were younger than his unit E_1. He attributed these deposits collectively to unit E_2 but did not differentiate the sediments further. Our results show that bed E_2 of member E actually consists of three distinct subunits, beds E_{2a}, E_{2b}, and E_{2c}, that are the stratigraphically highest units within the Las Vegas Formation (figs. 18 and 19). Collectively, bed E_2 represents the final phase of wetland development in the Las Vegas Valley.

Bed E_{2a}.—Deposits of bed E_{2a} are exposed only rarely in the upper Las Vegas Wash, likely because the lack of a resistant capping material (either carbonate or gravel) left it particularly vulnerable to erosion. Where present, it consists of 1–2 m of massive, olive-green silts and sands that contain terrestrial gastropod shells (Succineidae, *Fossaria* sp.) (fig. 18, sections E_2-4, E_2-5, and E_2-6; fig. 19*A*). Vertebrate fossils known from this bed (Scott and others, 2017) represent the last vestiges of the Pleistocene megafauna in the Las Vegas Valley prior to the terminal Pleistocene extinction.

Bed E_{2b}.—Bed E_{2b} consists of 1–2 m of massive, reddish-brown to buff-colored sands and silts armored by gravelly limestone alluvium (fig. 18, sections E_2-1, E_2-2, E_2-4, and E_2-6). Where covered by gravels, bed E_{2b} exhibits characteristic sinuous inverted topography. This bed also contains numerous black mats (fig. 19*B*) from which the ^{14}C ages were obtained.

Bed E_{2c}.—Bed E_{2c} lithologies consist of 1–2 m of massive, gray to olive-green silty clay and light tan silts and sands that contain multiple black mats and mollusk shells (*Physa* sp., *Pisidium* sp., and Hydrobiidae) (fig. 18, sections E_2-3 and E_2–7; fig.19*C*). Bed E_{2c} also contains abundant tufa deposits that exhibit various morphologies, including phytoclasts, oncoids, and stromatolites. The tufa is preserved both as surficial lag deposits and as in situ deposits within the sandy host sediments of bed E_{2c}.

A

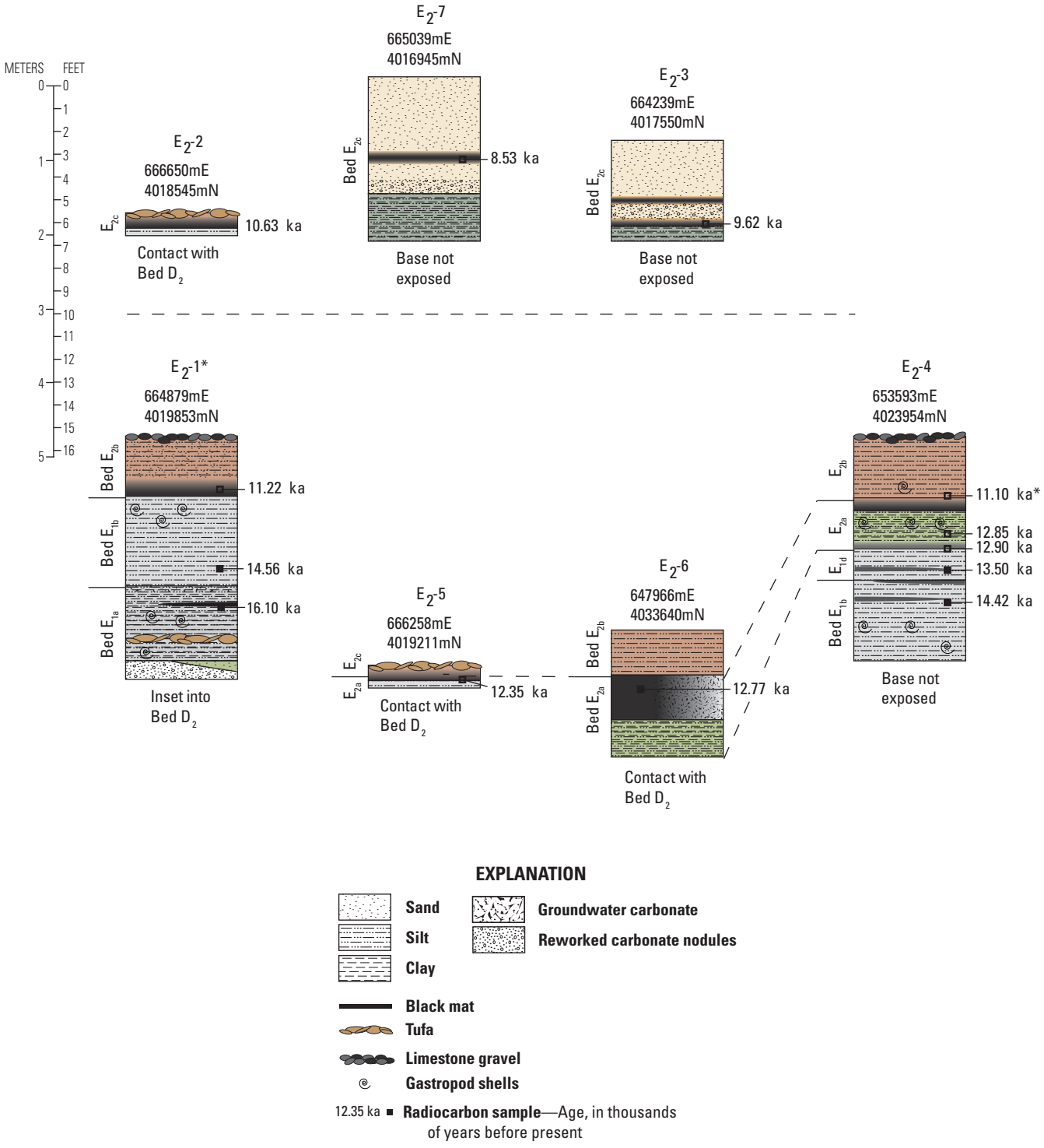

Figure 18. (this and facing page) Stratigraphic sections, ages, and colors featuring bed E_2 sediments. *A*, Stratigraphic profiles featuring bed E_2 deposits in context of lower bounding beds, and associated radiocarbon ages (see table 1). Universal Transverse Mercator coordinates are in zone 11S. Overall, bed E_2 dates to between 12.90 and 8.53 kilo-annum (ka, thousands of years before present) and consists of three distinct subunits (beds E_{2a} through E_{2c}). Each subunit exhibits a unique appearance and contains

B

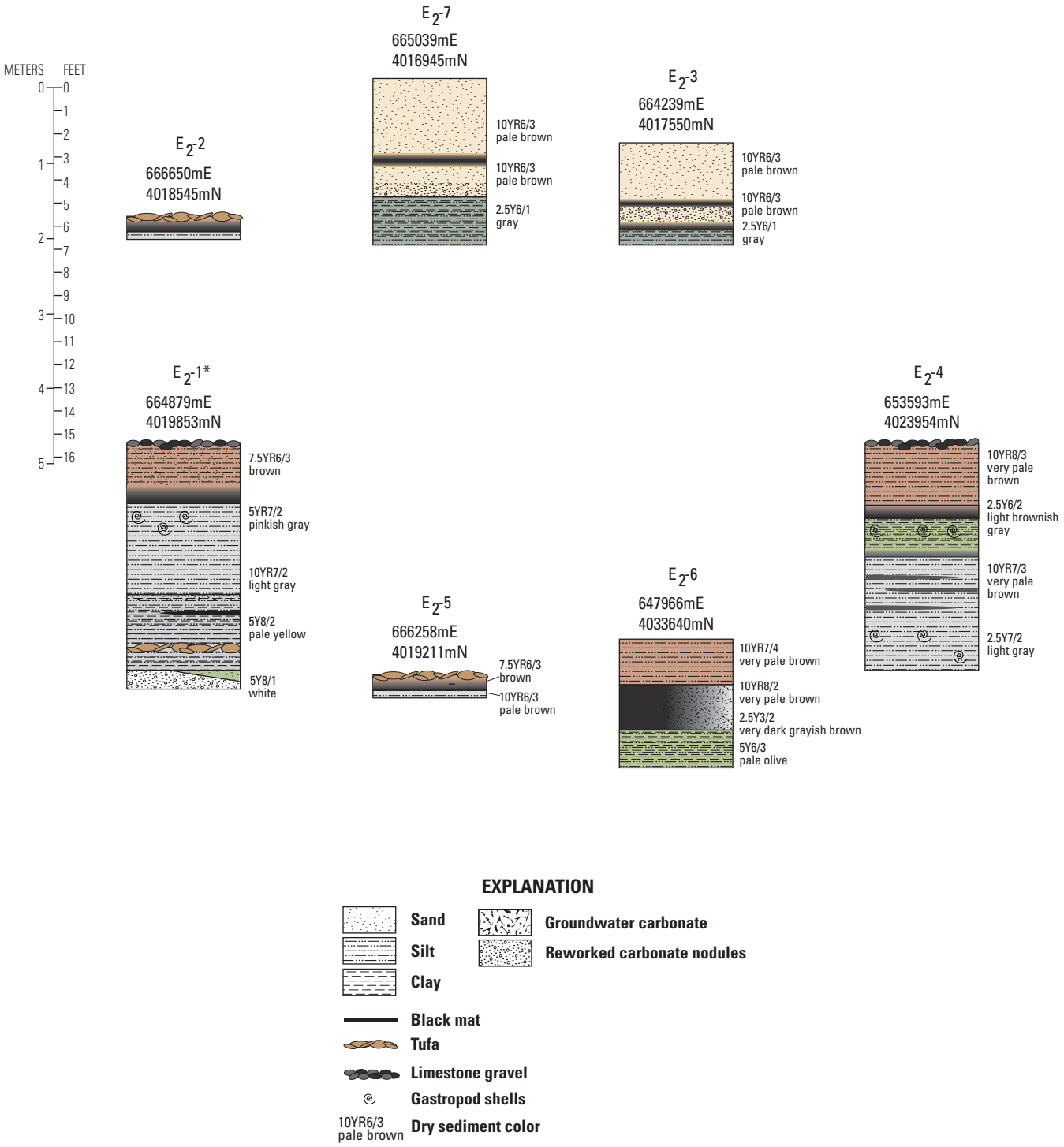

numerous black mats; bed E_{2c} also contains an extensive braided fluvial tufa system that is unique in North America. Section E_2-1 is the same as section E_1-1 in figure 16. Also, note that the asterisk for the uppermost age in section E_2-4 signifies that it is a weighted mean age because calibration resulted in two possible age ranges (see table 1).*B*, Stratigraphy and dry colors (Munsell Color [Firm], 2010) of bed E_2 sediments. (m, meter; E, easting; N, northing)

Figure 19. Photographs featuring member E_2 deposits (see fig. 18). Universal Transverse Mercator coordinates are in zone 11S. *A*, Deposit equivalent to section E_2-4; 653593 meters (m) easting (E), 4023954 m northing (N). Asterisk denotes a weighted mean age derived from multiple calibrated age ranges (see table 1). View to the southeast. Section is 3.0 m thick. *B*, Deposit equivalent to section E_2-1; 664879 m E, 4019853 m N. View to west. Section is 3.0 m thick. *C*, Deposit equivalent to section E_2-7; 665039 m E, 4016945 m N. View to the north. Section is 1.5 m thick, but is currently covered by development. *D*, Remnant of the typical inverted topography characteristic of bed E_{2b}; 663579 m E, 4019838 m N. View to the east. Section is approximately 2 m thick. *E*, Braided fluvial channels filled with tufa that are common in bed E_{2c}; 665985 m E, 4019351 m N. View to the east. *F*, Spectacular phytoclast tufa from bed E_{2c} channel; 666964 m E, 4019128 m N. View to the east. Rock hammer is 32.5 centimeters in length.

Age Control of Bed E_2

Bed E_{2a}.—We obtained four calibrated ^{14}C ages from charcoal, organic sediment, and Succineidae shells from bed E_{2a}; ages range from 12.90 to 12.35 ka (table 1).

Bed E_{2b}.—We obtained two ^{14}C ages on charcoal and organic sediment from black mats for bed E_{2b}; ages are 11.22 and 11.10 ka (table 1).

Bed E_{2c}.—We obtained three calibrated ^{14}C ages on charcoal from black mats in bed E_{2c}; ages range from 10.63 to 8.53 ka (table 1).

Depositional Environments, Paleohydrology, and Paleoclimatic Interpretations of Bed E_2

Bed E_{2a}.—We interpret the massive, olive-green silts and sands of bed E_{2a} as being deposited in marshes supported by the wetter climate that prevailed in the Las Vegas Valley during the Younger Dryas cold event (fig. 20; Springer and others, 2015).

Bed E_{2b}.—The oxidized, tan to brown silts of bed E_{2b} represent intermittent rheocrene discharge that occurred under relatively dry conditions during the pre-Boreal climate oscillations (fig. 20). Similar to deposition of bed E_{1b}, the Paleozoic alluvial gravels that overlie the E_{2b} silts were deposited in stream channels under dry conditions that were probably similar to those that exist today. In both cases, erosion of the surrounding fine-grained sediments was greater than that of sediments capped by the gravelly alluvium, resulting in the inverted topography shown in figure 19*D*.

Bed E_{2c}.—Bed E_{2c} represents intermittent groundwater discharge that occurred in the Las Vegas Valley during the early Holocene. The aquatic mollusks present in these deposits are indicative of flowing water and represent localized limnocrene ponding or marshy conditions. Also during bed E_{2c} time, flowing streams emanating from numerous point sources created an extensive, anastomosing braided fluvial network consisting of largely microbially mediated, but also physico-chemically precipitated, ambient-temperature tufas (fig. 19*E*). Although fluvial tufas predominate, paludal and lacustrine tufas associated with pooling water are also noted. Barrage tufa (Springer and Stevens, 2009) with phytoclasts encasing branches, logs, and other stream-edge plants is spectacularly exposed in bed E_{2c} (fig. 19*F*). Following this discharge event, episodes of widespread erosion, dune formation, and alluvial deposition indicate that arid conditions prevailed in the Las Vegas Valley for the remainder of the Holocene.

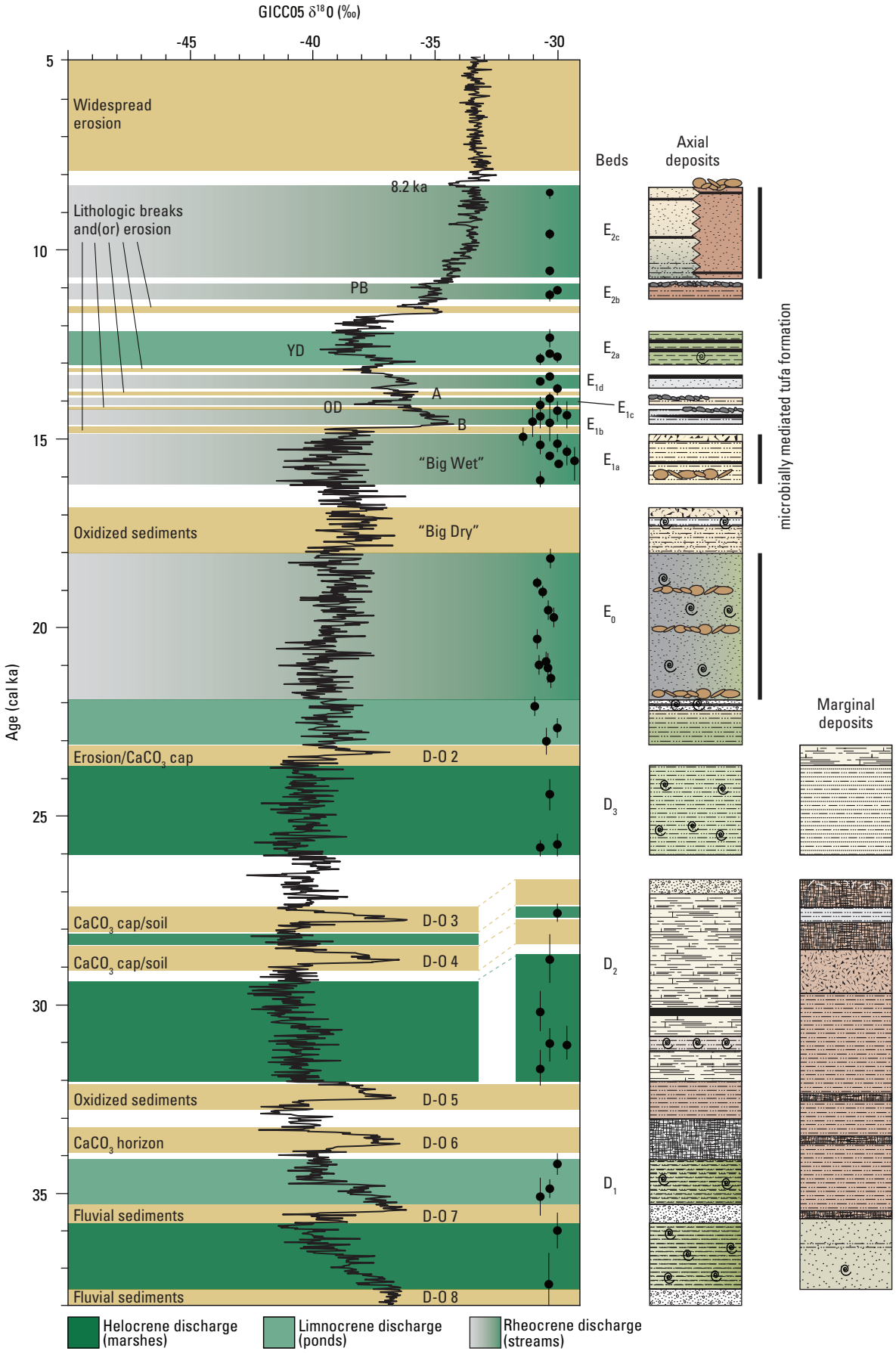
GICC05 δ18O (‰)
-45
-40
-35
-30
5
10
15
20
25
30
35
Age (cal ka)
Widespread erosion
8.2 ka
Lithologic breaks and(or) erosion
PB
YD
A
OD
B
"Big Wet"
Oxidized sediments
"Big Dry"
Erosion/CaCO3 cap
D-O 2
CaCO3 cap/soil
D-O 3
CaCO3 cap/soil
D-O 4
Oxidized sediments
D-O 5
CaCO3 horizon
D-O 6
Fluvial sediments
D-O 7
Fluvial sediments
D-O 8
Beds
Axial deposits
E2c
E2b
E2a
E1d
E1c
E1b
E1a
E0
D3
D2
D1
microbially mediated tufa formation
Marginal deposits
Helocrene discharge (marshes)
Limnocrene discharge (ponds)
Rheocrene discharge (streams)

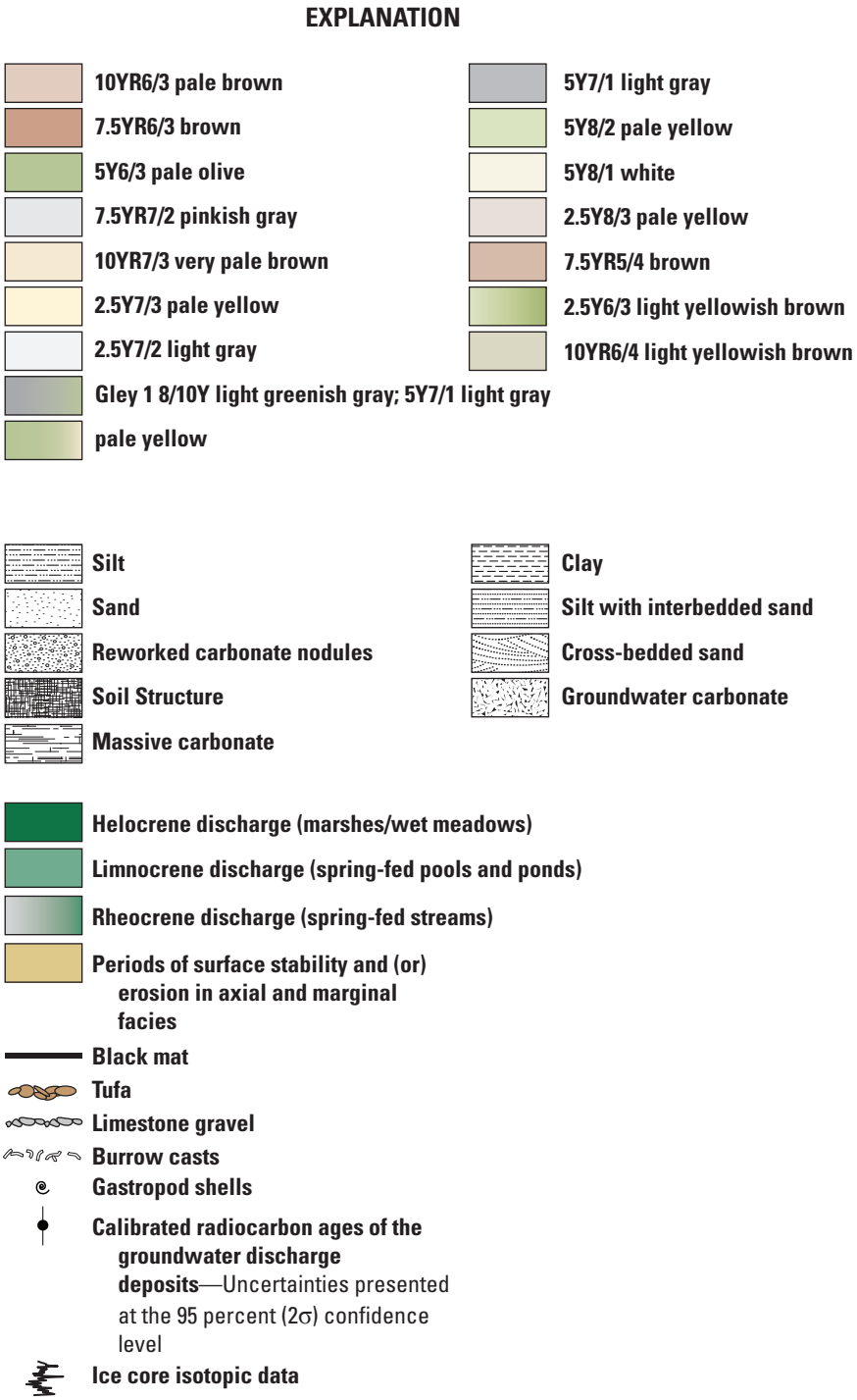

Figure 20. (this page and facing page) Stratigraphic and chronologic records of groundwater discharge deposits of members D and E in the Las Vegas Valley of southern Nevada (after Springer and others, 2015, 2017a,b) compared to the timing of changes in oxygen isotope ($\delta^{18}O$) data from Greenland ice core records using the Greenland Ice Core Chronology 2005 (Svensson and others, 2008). Dark filled circles are calibrated radiocarbon ages of the groundwater discharge deposits with uncertainties presented at the 95 percent (2σ) confidence level. Wetland discharge (by type) is shown in graduated shades of green. Tan horizontal bars indicate periods of surface stability and (or) erosion in axial and marginal facies. Event names "Big Wet" and "Big Dry" are after Broecker and others (2009); the "Big Wet" is equivalent to the Oldest Dryas. The isotopic spike at 8.2 kilo-annum (ka, thousands of years before present) is the 8.2-ka cold event (Alley and others, 1997). (PB, pre-boreal transitional phase; YD, Younger Dryas stadial; OD, Older Dyras stadial; A, Allerød oscillation; B, Bølling oscillation, or D-O 1; D-O, Dansgaard-Oeschger event; $CaCO_3$, calcium carbonate)

Dissolution of Unit C

The type section for Haynes' unit C is located in Trench K of the original Tule Springs site (Haynes, 1967). Haynes' lithologic description of this unit indicates that it consists of gravel and very pale brown calcareous silt formed in a broad flood plain, a depositional environment similar to that of units B_1 and B_3 (Haynes, 1967). He reported that these sediments were overlain by unit D, conformably in some places and uncomformably in others. Subsequent stratigraphic analyses, along with new ^{14}C and luminescence ages, have revealed that "unit C" in the Trench K area is actually composed of the tan silts of bed B_3 (fig. 9, section B-8; tables 1 and 2; Page and others, 2005; Ramelli and others, 2011).

Other deposits attributed to unit C in subsequent topical studies and geologic mapping efforts (for example, Quade, 1986; Quade and Pratt, 1989; Bell and others, 1998, 1999; Page and others, 2005; Ramelli and others, 2011, 2012) include the prominent cliff-forming outcrops of tan silts and sands on the west side of the upper Las Vegas Wash (fig. 11, sections D-1 and D-2). These sediments were initially interpreted as representing a dry phase that occurred between deposition of units B and D (fig. 2), with Bell and others (1999) noting that the tan cliff-forming deposits grade into gray-colored, fine-grained deposits toward the valley axis. Results of our field investigations have since confirmed that this is indeed the case.

Both Bell and others (1999) and Ramelli and others (2011, 2012) obtained ^{14}C ages from these deposits and suggested that unit C was likely interbedded with unit D. In addition, Page and others (2005) dated a sample taken at the same locality used by Bell and others (1999) for ^{14}C dating; they obtained a TL age range of 36–24 ka (app. 2) and concluded the deposits were unit C.

We tested these chronologic results using ^{14}C dating of charcoal and luminescence dating of the tan, cliff-forming deposits. Specifically, we targeted ^{14}C analysis to the short-lived wet phase between the two reddish soils near the top of the deposits (fig. 11, section D-2) to provide an upper age limit, which yielded a calibrated ^{14}C age of 27.58±0.23 ka on charcoal (table 1). We also obtained an IRSL age of 27±2 ka from the same unit exposed in a nearby outcrop (fig. 11, section D-1; table 2).

Our field observations, stratigraphic analysis, and new age control show unequivocally that these deposits, which were previously referred to as unit C, do not represent a distinct stratigraphic unit but instead represent a marginal wetland facies of the middle bed of member D, specifically bed D_2. The lateral lithologic variation of bed D_2 is part of the sedimentologic and hydrologic facies differentiation from the valley axis to the margins of the upper Las Vegas Wash that records the expansion and contraction of wetland facies during bed D_2 time (fig. 13). In light of these observations and our new chronologic data for sediments in this area and Trench K, we no longer recognize unit C as a distinct lithologic unit.

Conclusions

The Las Vegas Formation was established to designate light-colored, fine-grained, fossil-bearing sedimentary deposits exposed in and around the Las Vegas Valley. This study provides a comprehensive reevaluation of the lithostratigraphic sequence attributed to the Las Vegas Formation, building upon previously established informal stratigraphic and chronologic frameworks. We now recognize an informal hierarchy of 17 distinct geologic units, including stratigraphically ascending members X, A, B, D, and E with attendant beds in members B, D, and E. Moreover, we have established a robust and clear chronologic framework for the deposits by using targeted radiocarbon dating of charcoal and, to a lesser extent, terrestrial gastropod shells, as well as luminescence techniques when necessary. The age of the Las Vegas Formation spans at least the middle Pleistocene to early Holocene (approximately 573–8.53 kilo-annum [thousands of years before present]) and is related to past groundwater discharge. Continued use of this informal nomenclature will stabilize scientific communication with regard to these deposits, which will have great utility in future studies of paleowetland deposits elsewhere in the southwestern United States.

Desert wetland ecosystems and their resultant deposits in the Las Vegas Valley exhibit evidence of dramatic hydrologic responses to episodes of abrupt climate change that occurred during the late Quaternary. Each of the informal units described in this report represents a discrete "bin of time" in a highly resolved chronologic framework; this structure allows the sequence to be queried and examined to quantify changes in vertebrate and invertebrate faunal assemblages through time. The framework also allows the response of past ecosystems and environments to abrupt climatic oscillations to be reconstructed on millennial and submillennial timescales. The continued development of desert wetland deposits as a paleoclimate proxy will facilitate the evaluation of landscape-scale behavior of these systems throughout the American Southwest, with the deposits that compose the Las Vegas Formation serving as the linchpin.

References

Alley, R.B., Mayewski, P.A., Sowers, T., Stuiver, M., Taylor, K.C., and Clark, P.U., 1997, Holocene climatic instability—A prominent, widespread event 8200 yr ago: Geology, v. 25, no. 6, p. 483–486.

Amoroso, L., and Miller, D.M., 2012, Surficial geologic map of the Cuddeback Lake 30'×60' quadrangle, San Bernardino and Kern Counties, California: U.S. Geological Survey Scientific Investigations Map 3107, 1 sheet, scale 1:100,000, 31-p. pamphlet. [Also available at https://pubs.usgs.gov/sim/3107.]

Arakel, A.V., and McDonchie, D., 1982, Classification and genesis of calcrete and gypsite lithofacies in paleodrainage systems of inland Australia and their relationship to carnotite mineralization: Journal of Sedimentary Petrology, v. 52, p. 1149–1170.

Auclair, M., LaMothe, M., and Huot, S., 2003, Measurement of anomalous fading for feldspar IRSL using SAR: Radiation Measurements, v. 37, no. 4–5, p. 487–492.

Bedford, D.R., Miller, D.M., and Phelps, G.A., 2010, Surficial geologic map of the Amboy 30'×60' quadrangle, San Bernardino County, California: U.S. Geological Survey Scientific Investigations Map 3109, 1 sheet, scale 1:100,000, 30-p. pamphlet. [Also available at https://pubs.usgs.gov/sim/3109/.]

Bell, J.W., Ramelli, A.R., and Caskey, S.J., 1998, Geologic map of the Tule Springs Park quadrangle, Nevada: Nevada Bureau of Mines and Geology Map 113, 1 sheet, scale 1:24,000.

Bell, J.W., Ramelli, A.R., dePolo, C.M., Maldonado, F., and Schmidt, D.L., 1999, Geologic map of the Corn Creek Springs quadrangle, Nevada: Nevada Bureau of Mines and Geology Map 121, 1 sheet, scale 1:24,000.

Bequaert, J.C., and Miller, W.B., 1973, The mollusks of the arid Southwest, with an Arizona check list: Tucson, Ariz., University of Arizona Press, 271 p.

Bingler, E.C., 1977. Geologic map of the Las Vegas SE quadrangle, Clark County, Nevada: Nevada Bureau of Mines and Geology Map 3Ag, 1 sheet, scale 1:24,000.

Birkeland, P.W., 1999, Soils and geomorphology: New York, Oxford University Press, 430 p.

Broecker, W.S., McGee, D., Adams, K.D., Cheng, H., Edwards, R.L., Oviatt, C.G., and Quade, J., 2009, A Great Basin-wide dry episode during the first half of the Mystery Interval?: Quaternary Science Reviews, v. 28, no. 25–26, p. 2557–2563.

Capezzuoli, E., Gandin, A., and Pedley, M., 2014, Decoding tufa and travertine (fresh water carbonates) in the sedimentary record—The state of the art: Sedimentology, v. 61, no. 1, p. 1–21.

Carlisle, D., 1980, Possible variations on the calcrete-gypcrete uranium model: U.S. Department of Energy, Office of Scientific and Technical Information, GJBX-53(80), 38 p.

Carlisle, D., 1983, Concentration of uranium and vanadium in calcretes and gypcretes, *in* Wilson, R.C.L., ed., Residual deposits—Surface related weathering processes and materials: London, Blackwell Scientific Publications, Geological Society of London Special Publication No. 11, p. 185–195.

Dansgaard, W., Johnsen, S.J., Clausen, H.B., Dahl-Jensen, D., Gundestrup, N.S., Hammer, C.U., Hvidberg, C.S., Steffensen, J.P., Sveinbjörnsdottir, A.E., Jouzel, J., and Bond, G., 1993, Evidence for general instability of past climate from a 250-kyr ice-core record: Nature, v. 364, p. 218–220.

Donovan, D.J., 1996, Hydrostratigraphy and allostratigraphy of the Cenozoic alluvium in the northwestern part of Las Vegas Valley, Clark County, Nevada: Las Vegas, Nev., University of Nevada Las Vegas, M.S. Thesis, 199 p.

DuBarton, A.E., Spaulding, W.G., Kelly, M.S., and Cleland, J.H., 1991, City of Las Vegas land transfer final report on archaeological and paleoenvironmental testing of three sites along the Eglington Escarpment: Las Vegas, Nev., prepared by Dames & Moore for the City of Las Vegas.

Ford, T.D., and Pedley, H.M., 1996, A review of tufa and travertine deposits of the world: Earth-Science Reviews, v. 41, no. 3–4, p. 117–175.

Forester, R.M., 1991, Ostracode assemblages from springs in the western United States—Implications for paleohydrology: The Memoirs of the Entomological Society of Canada, v. 123, no. S155, p. 181–201.

Goudie, A.S., and Pye, K., 1983, Chemical sediments and geomorphology—Precipitates and residua in the near-surface environment: London, Academic Press Inc., 439 p.

Harrington, M.R., 1955, A new Tule Springs expedition: The Masterkey, v. 29, p. 112–114.

Harrington, M.R., and Simpson, R.D., 1961, Tule Springs, Nevada, with other evidences of Pleistocene man in North America: [Los Angeles] Southwest Museum Papers no. 18, 146 p.

Hay, R.L., Pexton, R.E., Teague, T.T., and Kyser, T.K., 1986, Spring-related carbonate rocks, Mg clays, and associated minerals in Pliocene deposits of the Amargosa Desert, Nevada and California: Geological Society of America Bulletin, v. 97, no. 12, p. 1488–1503.

Haynes, C.V., Jr., 1967, Quaternary geology of the Tule Springs area, Clark County, Nevada, in Wormington, H.M., and Ellis, D., eds., Pleistocene studies in southern Nevada: [Carson City] Nevada State Museum Anthropological Papers no. 13, p. 15–104.

Hubbs, C.L., and Miller, R.R., 1948, The Great Basin—II. The zoological evidence: University of Utah Bulletin, v. 38, p. 17–166.

Huntley, D.J., and Lamothe, M., 2001, Ubiquity of anomalous fading in K-feldspars and the measurement and correction for it in optical dating: Canadian Journal of Earth Sciences, v. 38, no. 7, p. 1093–1106.

Jull, A.J.T., and Burr, G.S., 2015, Radiocarbon dating, in Rink, W.J., Thompson, J.W., Heaman, L.M., Jull, A.J.T., and Paces, J.B., eds., Encyclopedia of scientific dating methods: New York, Springer Publishing, p. 669–676.

Kars, R.H., Busschers, F.S., and Wallinga, J., 2012, Validating post IR-IRSL dating on K-feldspars through comparison with quartz OSL ages: Quaternary Geochronology, v. 12, p. 74–86.

Lisiecki, L.E., and Raymo, M.E., 2005, A Pliocene-Pleistocene stack of 57 globally distributed benthic $\delta^{18}O$ records: Paleoceanography, v. 20, no. 1, PA1003, 17 p.

Longwell, C.R., 1946, How old is the Colorado River?: American Journal of Science, v. 244, no. 12, p. 817–835.

Longwell, C.R., 1963, Reconnaissance geology between Lake Mead and Davis Dam, Arizona-Nevada: U.S. Geological Survey Professional Paper 374-E, 51 p.

Longwell, C.R., Pampeyan, E.H., Bowyer, B., and Roberts, R.J., 1965, Geology and mineral deposits of Clark County, Nevada: Nevada Bureau of Mines and Geology Bulletin 62, 218 p.

Lundstrom, S.C., Page, W.R., Langenheim, V.E., Young, O.D., Mahan, S.A., and Dixon, G.L., 1998, Preliminary geologic map of the Valley quadrangle, Clark County, Nevada: U.S. Geological Survey Open-File Report 98–508, 1 sheet, scale 1:24,000, 19-p. pamphlet. [Also available at https://pubs.er.usgs.gov/publication/ofr98508.]

Mack, G.H., Cole, D.R., and Trevino, L., 2000, The distribution and discrimination of shallow, authigenic carbonate in the Pliocene-Pleistocene Palomas Basin, southern Rio Grande rift: Geological Society of America Bulletin, v. 112, no. 5, p. 643–656.

Mack, G.H., James, W.C., and Monger, H.C., 1993, Classification of paleosols: Geological Society of America Bulletin, v. 105, no. 2, p. 129–136.

Mahan, S.A., Martin, F.W., and Taylor, C., 2015, Construction ages of the Upton Stone Chamber—Preliminary findings and suggestions for future luminescence research: Quaternary Geochronology, v. 30B, p. 422–430.

Martinson, D.G., Pisias, N.G., Hays, J.D., Imbrie, J., Moore, T.C., Jr., and Shackleton, N.J., 1987, Age dating and the orbital theory of the ice ages—Development of a high-resolution 0 to 300,000-year chronostratigraphy: Quaternary Research, v. 27, no. 1, p. 1–29.

Matti, J.C., and Bachhuber, F.W., 1985, Las Vegas SW quadrangle—Geologic map: Nevada Bureau of Mines and Geology Urban Map 3Bg, 1 sheet, scale 1:24,000.

Matti, J.C., Bachhuber, F.W., Morton, D.M., and Bell, J.W., 1987, Las Vegas NW quadrangle—Geologic map: Nevada Bureau of Mines and Geology Urban Map 3Dg, 1 sheet, scale 1:24,000.

Matti, J.C., Castor, S.B., Bell, J.W., and Rowland, S.M., 1993, Las Vegas NE quadrangle—Geologic map: Nevada Bureau of Mines and Geology Urban Map 3Cg, 1 sheet, scale 1:24,000.

Mawby, J.E., 1967, Fossil vertebrates of the Tule Springs site, Nevada, in Wormington, H.M., and Ellis, D., eds., Pleistocene studies in southern Nevada: [Carson City] Nevada State Museum Anthropological Papers no. 13, p. 105–129.

Maxey, G.B., and Jamesson, C.H., 1948, Geology and water resources of Las Vegas, Pahrump, and Indian Springs Valleys, Clark and Nye Counties, Nevada: State of Nevada, Office of the State Engineer, Water Resources Bulletin No. 5, 128 p.

McVicker, J.L., and Spaulding, W.G., 1993, Monitoring and mitigation of paleontologic resources—Final draft technical report, Upper Las Vegas Wash Flood Control Facility, Clark County, Nevada: Las Vegas, Nev., prepared by Dames and Moore for the U.S. Bureau of Land Management and the Clark County Regional Flood Control District, 37 p.

Mifflin, M.D., and Wheat, M.M., 1979, Pluvial lakes and estimated pluvial climates of Nevada: Nevada Bureau of Mines and Geology Bulletin 94, 57 p.

Munsell Color (Firm), 2010, Munsell soil color charts, with genuine Munsell color chips: Grand Rapids, Mich., Munsell Color (Firm).

Nelson, M.S., Gray, H.J., Johnson, J.A., Rittenour, T.M., Feathers, J.K., and Mahan, S.A., 2015, User guide for luminescence sampling in archaeological and geological contexts: Advances in Archaeological Practice, v. 3, no. 2, p. 166–177.

North American Commission on Stratigraphic Nomenclature, 2005, North American Stratigraphic Code: The American Association of Petroleum Geologists Bulletin, v. 89, no. 11, p. 1547–1591.

Page, W.R., Lundstrom, S.C., Harris, A.G., Langenheim, V.E., Workman, J.B., Mahan, S.A., Paces, J.B., Dixon, G.L., Rowley, P.D., Burchfiel, B.C., Bell, J.W., and Smith, E.I., 2005, Geologic and geophysical maps of the Las Vegas 30'×60' quadrangle, Clark and Nye Counties, Nevada, and Inyo County, California: U.S. Geological Survey Scientific Investigations Map 2814, 1 sheet, scale 1:100,000, 58-p. pamphlet. [Also available at https://pubs.usgs.gov/sim/2005/2814/.]

Pedley, H.M., 1990, Classification and environmental models of cool freshwater tufas: Sedimentary Geology, v. 68, no. 1–2, p. 143–154.

Pedley, M., 2000, Ambient temperature freshwater microbial tufas, in Riding, R.E., and Awramik, S.M., eds., Microbial sediments: New York, Springer-Verlag, p. 179–186.

Pigati, J.S., Bright, J.E., Shanahan, T.M., and Mahan, S.A., 2009, Late Pleistocene paleohydrology near the boundary of the Sonoran and Chihuahuan Deserts, southeastern Arizona, USA: Quaternary Science Reviews, v. 28, no. 3–4, p. 286–300.

Pigati, J.S., McGeehin, J.P., Muhs, D.R., and Bettis, E.A., III, 2013, Radiocarbon dating late Quaternary loess deposits using small terrestrial gastropod shells: Quaternary Science Reviews, v. 76, p. 114–128.

Pigati, J.S., Miller, D.M., Bright, J.E., Mahan, S.A., Nekola, J.C., and Paces, J.B., 2011, Chronology, sedimentology, and microfauna of groundwater discharge deposits in the central Mojave Desert, Valley Wells, California: Geological Society of America Bulletin, v. 123, no. 11–12, p. 2224–2239.

Pigati, J.S., Rech, J.A., and Nekola, J.C., 2010, Radiocarbon dating of small terrestrial gastropod shells in North America: Quaternary Geochronology, v. 5, no. 5, p. 519–532.

Pigati, J.S., Rech, J.A., Quade, J., and Bright, J., 2014, Desert wetlands in the geologic record: Earth-Science Reviews, v. 132, p. 67–81.

Plume, R.W., 1984, Ground-water conditions in the Las Vegas Valley, Clark County, Nevada—Part 1—Hydrologic framework: U.S. Geological Survey Open-File Report 84–130, 40 p., 5 plates. [Also available at https://pubs.usgs.gov/wsp/2320a/report.pdf.]

Prescott, J.R., and Hutton, J.T., 1994, Cosmic ray contributions to dose rates for luminescence and ESR dating—Large depths and long-term time variations: Radiation Measurements, v. 23, no. 2–3, p. 497–500.

Preusser, F., 2003, IRSL dating of K-rich feldspars using the SAR protocol—Comparison with independent age control: Ancient TL, v. 21, p. 17–23.

Quade, J., 1986, Late Quaternary environmental changes in the upper Las Vegas Valley, Nevada: Quaternary Research, v. 26, no. 3, p. 340–357.

Quade, J., Forester, R.M., Pratt, W.L., and Carter, C., 1998, Black mats, spring-fed streams, and late-glacial-age recharge in the southern Great Basin: Quaternary Research, v. 49, no. 2, p. 129–148.

Quade, J., Forester, R.M., and Whelan, J.F., 2003, Late Quaternary paleohydrologic and paleotemperature change in southern Nevada, in Enzel, Y., Wells, S.G., and Lancaster, N., eds., Paleoenvironments and paleohydrology of the Mojave and southern Great Basin deserts: Geological Society of America Bulletin Special Paper 368, p. 165–188.

Quade, J., Mifflin, M.D., Pratt, W.L., McCoy, W.D., and Burckle, L., 1995, Fossil spring deposits in the southern Great Basin and their implications for changes in water-table levels near Yucca Mountain, Nevada, during Quaternary time: Geological Society of America Bulletin, v. 107, no. 2, p. 213–230.

Quade, J., and Pratt, W.L., 1989, Late Wisconsin groundwater discharge environments of the southwestern Indian Springs Valley, southern Nevada: Quaternary Research, v. 31, no. 3, p. 351–370.

Ramelli, A.R., Page, W.R., Manker, C.R., and Springer, K.B., 2011, Geologic map of the Gass Peak SW quadrangle, Clark County, Nevada: Nevada Bureau of Mines and Geology Map 175, 1 sheet, scale 1:24,000.

Ramelli, A.R., Page, W.R., Manker, C.R., and Springer, K.B., 2012, Preliminary geologic map of the Corn Creek Springs NW quadrangle, Clark County, Nevada: Nevada Bureau of Mines and Geology Open-File Report 12-7, 1 sheet, scale 1:24,000.

Reimer, P.J., Bard, E., Bayliss, A., Beck, J.W., Blackwell, P.G., Bronk Ramsey, C.B., Buck, C.E., Cheng, H., Edwards, R.L., Friedrich, M., Grootes, P.M., Guilderson, T.P., Haflidason, H., Hajdas, I., Hatte, C., Heaton, T.J., Hoffmann, D.L., Hogg, A.G., Hughen, K.A., Kaiser, K.F., Kromer, B., Manning, S.W., Niu, M., Reimer, R.W., Richards, D.A., Scott, E.M., Southon, J.R., Staff, R.A., Turney, C.S.M., and van der Plicht, J., 2013, IntCal13 and Marine13 radiocarbon age calibration curves 0–50,000 years cal BP: Radiocarbon, v. 55, no. 4, p. 1869–1887.

Rodnight, H., 2008, How many equivalent dose values are needed to obtain a reproducible distribution?: Ancient TL, v. 26, p. 3–10.

Rose, R.H., 1938, Pleistocene deposits in southern Nevada [abs.]: Proceedings of the Geological Society of America, 1937, p. 250–251.

Schmidt, K.M., and McMackin, M., 2006, Preliminary surficial geologic map of the Mesquite Lake 30'×60' quadrangle, California and Nevada: U.S. Geological Survey Open-File Report 2006–1035, 1 sheet, scale 1:100,000, 89-p. pamphlet. [Also available at https://pubs.usgs.gov/of/2006/1035/.]

Scott, E., and Springer, K.B., 2016, First records of *Canis dirus* and *Smilodon fatalis* from the late Pleistocene Tule Springs local fauna, upper Las Vegas Wash, Nevada: PeerJ, v. 4, e2151, 17 p., accessed April 11, 2018, at https://doi.org/10.7717/peerj.2151.

Scott, E., Springer, K.B., and Sagebiel, J.C., 2017, The Tule Springs local fauna—Rancholabrean vertebrates from the Las Vegas Formation, Nevada: Quaternary International, v. 443A, p. 105–121.

Shanahan, T.M., Pigati, J.S., Dettman, D.L., and Quade, J., 2005, Isotopic variability in the aragonite shells of freshwater gastropods living in springs with nearly constant temperature and isotopic composition: Geochimica et Cosmochimica Acta, v. 69, no. 16, p. 3949–3966.

Simpson, G.G., 1933, A Nevada fauna of Pleistocene type and its probable association with man: New York, The American Museum of Natural History, American Museum Novitates Number 667, 10 p.

Snyder, C.T., Hardman, G., and Zdenek, F.F., 1964, Pleistocene lakes in the Great Basin: Nevada Bureau of Mines and Geology Map I-416, 1 sheet, scale 1:1,000,000.

Springer, A.E., and Stevens, L.E., 2009, Spheres of discharge of springs: Hydrogeology Journal, v. 17, no. 1, p. 83–93.

Springer, K.B., Manker, C.R., and Pigati, J.S., 2015, Dynamic response of desert wetlands to abrupt climate change: Proceedings of the National Academy of Sciences of the United States of America, v. 112, no. 47, p. 14522–14526.

Springer, K.B., Pigati, J.S., and Scott, E., 2017a, Geology and vertebrate paleontology of Tule Springs Fossil Beds National Monument, Nevada, USA, in Kraatz, B., Lackey, J.S., and Fryxell, J.E., eds., Field excursions in southern California—Field guides to the 2016 GSA Cordilleran Section Meeting: Boulder, Colo., The Geological Society of America Field Guide 45, p. 1–30.

Springer, K.B., Pigati, J.S., and Scott, E., 2017b, Vertebrate paleontology, stratigraphy, and paleohydrology of Tule Springs Fossil Beds National Monument, Nevada (USA): Geology of the Intermountain West, v. 4, p. 55–98.

Steffen, D., Preusser, F., and Schlunegger, F., 2009, OSL quartz age underestimation due to unstable signal components: Quaternary Geochronology, v. 4, no. 5, p. 353–362.

Stuiver, M., and Reimer, P.J., 1993, Extended ^{14}C data base and revised CALIB 3.0 ^{14}C age calibration program: Radiocarbon, v. 35, no. 1, p. 215–230.

Svensson, A., Andersen, K.K., Bigler, M., Clausen, H.B., Dahl-Jensen, D., Davies, S.M., Johnsen, S.J., Muscheler, R., Parrenin, F., Rasmussen, S.O., Röthlisberger, R., Seierstad, I., Steffensen, J.P., and Vinther, B.M., 2008, A 60 000 year Greenland stratigraphic ice core chronology: Climate of the Past, v. 4, no. 1, p. 47–57.

Taggart, J.E., Jr., ed., 2002, Analytical methods for chemical analysis of geologic and other materials, U.S. Geological Survey: U.S. Geological Survey Open File Report 02–223, 20 p., accessed April 11, 2018, at https://pubs.usgs.gov/of/2002/ofr-02-0223/OFR-02-0223.pdf.

Trumbore, S.E., 2000, Radiocarbon geochronology, in Noller, J.S., Sowers, J.M., and Lettis, W.R., eds., Quaternary geochronology—Methods and applications: Washington, D.C., American Geophysical Union, p. 41–60.

U.S. Department of Agriculture, 1951, Soil survey manual: U.S. Department of Agriculture Handbook 18, 203 p.

Wintle, A.G., and Murray, A.S., 2006, A review of quartz optically stimulated luminescence characteristics and their relevance in single-aliquot regeneration dating protocols: Radiation Measurements, v. 41, no. 4, p. 369–391.

Wormington, H.M., and Ellis, D., 1967, Pleistocene studies in southern Nevada: Carson City, Nev., Nevada State Museum Anthropological Papers no. 13, 411 p.

Appendix 1. Summary of Radiocarbon Ages Obtained Previously for the Las Vegas Formation

Appendix 1. Summary of radiocarbon ages obtained previously for the Las Vegas Formation.

[Uncertainties for the calibrated ages are given at the 95 percent (2σ) confidence level. All other uncertainties are given at the 68 percent (1σ) confidence level. Map units: Qsc, unit C; Qsd, unit D; Qse, unit E. Analyzed fractions: A, humins (insoluble in base); B, humates or humic acids (soluble in base); C, carbonate. no., number; AMS, accelerator mass spectrometry; ^{14}C, radiocarbon; ka, kilo-annum (thousands of years before present); cal, calibrated; P, probability of the calibrated age falling within the reported range as calculated by CALIB v.7.1html; –, not applicable; >, greater than; m, meter; ~, approximately; quad., quadrangle]

Sample no.	AMS no.	Location	Section	Unit	Material dated	Fraction analyzed	^{14}C age (ka BP)	Age (cal ka BP)[1]	P	Original source	Sample notes[2]
—	UCLA-519	Tule Springs	—	E_2	Carbonized wood	—	7.48±0.12	8.25±0.23	0.99	Haynes, 1967	
—	A-463a	Tule Springs	—	E_2	Carbonized wood	—	8.54±0.34	9.47±0.84	0.99	Haynes, 1967	
—	UCLA-510	Tule Springs	—	E_2	Fine carbonized wood	—	9.0±1.0	10.3±2.4	1.00	Haynes, 1967	
—	I-991	Tule Springs	—	E_2	Carbonized wood	—	9.67±0.20	11.07±0.59	0.98	Haynes, 1967	
—	UCLA-505	Tule Springs	—	E_2	Carbonized wood	—	10.00±0.20	11.66±0.59	0.96	Haynes, 1967	
—	UCLA-508	Tule Springs	—	E_2	Carbonized wood	—	11.20±0.20	13.07±0.35	1.00	Haynes, 1967	Possibly mixed with material from unit E_1
—	UCLA-636	Tule Springs	—	E_1	Carbonized wood	—	11.50±0.50	13.7±1.3	1.00	Haynes, 1967	
—	UCLA-637	Tule Springs	—	E_1	Carbonized wood	—	11.90±0.25	13.92±0.71	1.00	Haynes, 1967	
—	UCLA-507	Tule Springs	—	E_1	Carbonized wood	—	12.27±0.20	14.41±0.66	1.00	Haynes, 1967	
—	UCLA-514	Tule Springs	—	E_1	Carbonized wood	—	12.30±0.35	14.5±1.0	1.00	Haynes, 1967	
—	UCLA-512	Tule Springs	—	E_1	Carbonized wood	—	12.40±0.35	14.6±1.0	1.00	Haynes, 1967	
—	UCLA-604	Tule Springs	—	E_1	Carbonized wood	—	12.40±0.20	14.55±0.64	0.99	Haynes, 1967	
—	UCLA-509	Tule Springs	—	E_1	Carbonized wood	—	12.45±0.23	14.57±0.75	1.00	Haynes, 1967	
—	UCLA-518	Tule Springs	—	E_1	Carbonized wood	—	12.65±0.20	14.89±0.73	1.00	Haynes, 1967	
—	UCLA-521	Tule Springs	—	E_1	Carbonized wood	—	12.92±0.22	15.37±0.77	1.00	Haynes, 1967	
—	UCLA-552	Tule Springs	—	E_1	Carbonized wood	—	13.00±0.20	15.56±0.62	1.00	Haynes, 1967	
—	UCLA-522	Tule Springs	—	E_1	Carbonized wood	—	13.10±0.20	15.69±0.56	1.00	Haynes, 1967	
—	UCLA-554	Tule Springs	—	E_1	Tufa organics	—	17.6±1.5	21.3±3.6	1.00	Haynes, 1967	Too old due to initial ^{14}C deficiency, organic fractionation, or both
—	UCLA-546	Tule Springs	—	E_1	Tufa organics	—	16.90±0.30	20.38±0.76	1.00	Haynes, 1967	Same sample as above
—	A-466	Tule Springs	—	E_1	Tufa organics	—	>28.0	>31.7	1.00	Haynes, 1967	Too old due to initial ^{14}C deficiency, organic fractionation, or both
—	UCLA-503	Tule Springs	—	E_1	Tufa carbonate	C	15.92±0.22	19.24±0.50	1.00	Haynes, 1967	
—	UCLA-543	Tule Springs	—	E_1	Mollusc shell	C	13.90±0.30	16.83±0.83	1.00	Haynes, 1967	Equivalent to UCLA 521; ~1,000 years too old due to “dead” carbon
—	I-887	Tule Springs	—	E_1	Carbonized wood	—	>40.0	>43.6	1.00	Haynes, 1967	
—	UCLA-536	Tule Springs	—	D	Mollusc shell	C	22.60±0.55	26.80±0.95	1.00	Haynes, 1967	
—	A-462	Tule Springs	—	D	Mollusc shell	C	31.3±2.5	35.8±5.1	1.00	Haynes, 1967	
—	UCLA-420	Tule Springs	—	D	Burned bone	—	>23.0	>27.3	1.00	Haynes, 1967	
—	UCLA-524	Tule Springs	—	D	Mollusc shell	C	>31.0	>34.9	1.00	Haynes, 1967	
—	UCLA-513	Tule Springs	—	D	Carbonized wood	—	>35.0	>40.0	1.00	Haynes, 1967	

Appendix 1. Summary of radiocarbon ages obtained previously for the Las Vegas Formation.—Continued

[Uncertainties for the calibrated ages are given at the 95 percent (2σ) confidence level. All other uncertainties are given at the 68 percent (1σ) confidence level. Map units: Qsc, unit C; Qsd, unit D; Qse, unit E. Analyzed fractions: A, humins (insoluble in base); B, humates or humic acids (soluble in base); C, carbonate. no., number; AMS, accelerator mass spectrometry; ^{14}C, radiocarbon; ka, kilo-annum (thousands of years before present); cal, calibrated; P, probability of the calibrated age falling within the reported range as calculated by CALIB v.7.1html; –, not applicable; >, greater than; m, meter; ~, approximately; quad., quadrangle]

Sample no.	AMS no.	Location	Section	Unit	Material dated	Fraction analyzed	^{14}C age (ka BP)	Age (cal ka BP)[1]	P	Original source	Sample notes[2]
—	UCLA-528	Tule Springs	—	B_3	Carbonized wood	—	>40.0	>34.6	1.00	Haynes, 1967	
—	UCLA-501	Tule Springs	—	B_2	Carbonized wood	—	26.0±1.0	29.8±1.9	1.00	Haynes, 1967	
—	UCLA-547	Tule Springs	—	B_2	Mollusc shell	C	>30.0	>34.1	1.00	Haynes, 1967	
—	UCLA-502	Tule Springs	—	B_2	Carbonized wood	—	>32.0	>35.9	1.00	Haynes, 1967	
—	UCLA-511	Tule Springs	—	B_2	Carbonized wood	—	>32.0	>35.9	1.00	Haynes, 1967	
—	UCLA-523	Tule Springs	—	B_2	Carbonized wood	—	>35.0	>40.0	1.00	Haynes, 1967	
—	UCLA-506	Tule Springs	—	B_2	Carbonized wood	—	>37.0	>41.6	1.00	Haynes, 1967	
—	UCLA-517	Tule Springs	—	B_2	Carbonized wood	—	>40.0	>43.6	1.00	Haynes, 1967	
—	UCLA-548	Eglington scarp	—	E_2	Carbonized wood	—	8.00±0.40	8.90±0.90	0.99	Haynes, 1967	
—	UCLA-551	Eglington scarp	—	E_2	Organic mat	—	9.35±0.20	10.69±0.51	1.00	Haynes, 1967	
—	UCLA-549	Eglington scarp	—	E_2	Organic mat	—	9.52±0.30	10.97±0.85	0.99	Haynes, 1967	
—	A-464	Eglington scarp	—	E_2	Organic mat	—	9.87±0.40	11.4±1.1	1.00	Haynes, 1967	
—	A-471	Eglington scarp	—	E_2	Tufa organics	—	10.16±0.16	11.76±0.49	0.94	Haynes, 1967	
								12.32±0.06	0.06		
—	UCLA-642	Eglington scarp	—	E_2	Tufa carbonate	C	11.80±0.25	13.69±0.61	1.00	Haynes, 1967	Same as A-471 but too old because of initial ^{14}C deficiency
—	UCLA-550	Eglington scarp	—	E_2	Organic mat	—	11.10±0.20	13.01±0.34	1.00	Haynes, 1967	
—	A-470	Eglington scarp	—	E_1	Tufa organics	—	13.40±0.23	16.11±0.71	1.00	Haynes, 1967	
—	UCLA-641	Eglington scarp	—	E_1	Tufa carbonate	C	15.00±0.30	18.20±0.65	1.00	Haynes, 1967	Same as A-470 because of initial ^{14}C deficiency
—	A-459b	Eglington scarp	—	E_1	Tufa organics	—	13.68±0.16	16.54±0.48	1.00	Haynes, 1967	
—	A-459a	Eglington scarp	—	E_1	Tufa carbonate	C	14.10±0.10	17.14±0.34	1.00	Haynes, 1967	Same as A-459b but too old because of initial ^{14}C deficiency
—	UCLA-529	Gilcrease Ranch	—	E_2	Organic mat	—	9.20±0.25	10.41±0.72	1.00	Haynes, 1967	
—	UCLA-537	Gilcrease Ranch	—	E_2	Organic mat	—	9.92±0.15	11.55±0.47	0.98	Haynes, 1967	
—	A-442	Gilcrease Ranch	—	E_2	Tufa organics	—	10.81±0.46	12.4±1.1	1.00	Haynes, 1967	
—	A-441	Gilcrease Ranch	—	E_2	Tufa carbonate	C	10.26±0.10	12.01±0.41	0.99	Haynes, 1967	Same as A-442
—	UCLA-539	Gilcrease Ranch	—	D	Carbonized wood	—	25.3±2.5	29.3±5.0	1.00	Haynes, 1967	
—	UCLA-542	Corn Creek flat	—	E_2	Organic mat	—	10.20±0.35	11.89±0.83	0.96	Haynes, 1967	
—	UCLA-530	Corn Creek flat	—	E_2	Organic mat	—	10.80±0.30	12.55±0.75	1.00	Haynes, 1967	
—	UCLA-541	Corn Creek flat	—	E_1	Organic mat	—	11.70±0.25	13.60±0.54	1.00	Haynes, 1967	
CSCarb-11a	A-2570	Lower Corn Creek flat	—	E_2	Black mat	A	6.22±0.25	7.05±0.52	1.00	Quade, 1986	Probably contaminated with modern rootlets

Appendix 1. Summary of radiocarbon ages obtained previously for the Las Vegas Formation.—Continued

[Uncertainties for the calibrated ages are given at the 95 percent (2σ) confidence level. All other uncertainties are given at the 68 percent (1σ) confidence level. Map units: Qsc, unit C; Qsd, unit D; Qse, unit E. Analyzed fractions: A, humins (insoluble in base); B, humates or humic acids (soluble in base); C, carbonate. no., number; AMS, accelerator mass spectrometry; ^{14}C, radiocarbon; ka, kilo-annum (thousands of years before present); cal, calibrated; P, probability of the calibrated age falling within the reported range as calculated by CALIB v.7.1html; –, not applicable; >, greater than; m, meter; ~, approximately; quad., quadrangle]

Sample no.	AMS no.	Location	Section	Unit	Material dated	Fraction analyzed	^{14}C age (ka BP)	Age (cal ka BP)[1]	P	Original source	Sample notes[2]
CS81Carb-11b	A-2571	Lower Corn Creek flat	—	E_2	Humates	B	8.64±0.15	9.79±0.38	1.00	Quade, 1986	Humic acids from A-2570
—	A-2545	Upper Tule Spring flat	—	E_2	Carbonized wood	—	9.37±0.21	10.70±0.53	1.00	Quade, 1986	
CS81Carb-3a	A-2585	upper Corn Creek flat	—	E_2	Black mat	A	10.09±0.16	11.70±0.49	0.98	Quade, 1986	
—	A-2465	Lower Corn Creek flat	—	E_2	Carbonized wood	—	10.98±0.27	12.90±0.53	0.98	Quade, 1986	
—	W-5643	Lower Corn Creek flat	—	E_1	Carbonized wood	—	12.60±0.30	14.85±0.94	0.99	Quade, 1986	
—	W-5646	Lower Corn Creek flat	—	E_1	Carbonized wood	—	12.63±0.30	14.90±0.97	1.00	Quade, 1986	
—	W-5653	Lower Corn Creek flat	—	E_1	Carbonized wood	—	13.83±0.40	16.7±1.1	1.00	Quade, 1986	
CSCarb-14b	W-5649	Lower Corn Creek flat	—	E_1	Carbonized wood	B	14.04±0.32	17.02±0.86	1.00	Quade, 1986	
Cac.Spr.Carb-2b	USGS-2213b	Cactus Springs	—	E_2	Organic layer	B	9.46±0.06	10.71±0.16	0.83	Quade and Pratt, 1989	Same layer as USGS-2212b, 200 m laterally
								11.01±0.06	0.17		
Cac.Spr.Carb-2b	USGS-2212b	Cactus Springs	—	E_2	Organic layer	B	9.68±0.10	10.99±0.26	1.00	Quade and Pratt, 1989	
—	USGS-2211b	Cactus Springs	—	B_2	Carbonized wood	B	42.6±1.6	46.2±3.0	1.00	Quade and Pratt, 1989	Possibly redeposited
—	Beta-45473	Eglington scarp	—	E_2	Black mat	—	9.82±0.10	11.34±0.28	0.92	DuBarton and others, 1991	
								10.91±0.05	0.06		
—	Beta-45472	Eglington scarp	—	E_2	Black mat	—	11.63±0.09	13.45±0.18	0.98	DuBarton and others, 1991	
—	A-4899	Corn Creek flat	—	D	Shell	C	28.4±1.1	32.6±2.0	1.00	Quade and others, 1995	
CSC87-8b	A-4901	Corn Creek flat	—	E	Carbonized wood	B	11.87±0.20	13.74±0.47	1.00	Quade and others, 1995	
CS81Carb-3b	A-4993	Corn Creek flat	—	E	Organic mat	B	10.14±0.13	11.72±0.46	0.98	Quade and others, 1995	Humic acids from A-2585
CSC87-1b	A-4996	Corn Creek flat	—	E	Organic mat	B	11.76±0.13	13.58±0.27	0.99	Quade and others, 1995	
CS81Carb-6b	A-4861	Corn Creek flat	—	E	Organic mat	B	9.22±0.18	10.39±0.49	0.96	Quade and others, 1995	
SCySCarb-1b	A-5222	South Coyote Springs	—	E_2	Organic mat	B	9.97±0.09	11.50±0.28	0.99	Quade and others, 1995	
NCySC-5b	A-5223	North Coyote Springs	—	E_2	Organic mat	B	9.50±0.28	10.94±0.79	0.99	Quade and others, 1995	
Cac.Spr.Carb-6b	A-5035	Cactus Springs	—	E_2	Organic mat	B	10.41±0.11	12.29±0.34	0.99	Quade and others, 1995	Referred to as “Indian Valley”
CSC87-5b	A-4987	Corn Creek flat	—	E_2	Black mat	B	6.34±0.26	7.16±0.53	1.00	Quade and others, 1998	
CSC87-9b	Beta-73963	Corn Creek flat	—	E_2	Black mat	B	8.76±0.06	9.75±0.20	0.94	Quade and others, 1998	
CSC87-7b	A-4995	Corn Creek flat	—	E_2	Black mat	B	10.20±0.13	11.89±0.50	0.99	Quade and others, 1998	
CS81Carb-13b	A-4537	Corn Creek flat	—	E_2	Black mat	B	10.22±0.21	11.90±0.64	1.00	Quade and others, 1998	
CSC87-6b	A-4994	Corn Creek flat	—	E_2	Black mat	B	10.39±0.15	12.19±0.48	1.00	Quade and others, 1998	
CSC87-2b	A-4862	Corn Creek flat	—	E_1	Carbonized wood	B	11.58±0.24	13.48±0.51	1.00	Quade and others, 1998	

Appendix 1. Summary of radiocarbon ages obtained previously for the Las Vegas Formation.—Continued

[Uncertainties for the calibrated ages are given at the 95 percent (2σ) confidence level. All other uncertainties are given at the 68 percent (1σ) confidence level. Map units: Qsc, unit C; Qsd, unit D; Qse, unit E. Analyzed fractions: A, humins (insoluble in base); B, humates or humic acids (soluble in base); C, carbonate. no., number; AMS, accelerator mass spectrometry; ^{14}C, radiocarbon; ka, kilo-annum (thousands of years before present); cal, calibrated; P, probability of the calibrated age falling within the reported range as calculated by CALIB v.7.1html; –, not applicable; >, greater than; m, meter; ~, approximately; quad., quadrangle]

Sample no.	AMS no.	Location	Section	Unit	Material dated	Fraction analyzed	^{14}C age (ka BP)	Age (cal ka BP)[1]	P	Original source	Sample notes[2]
CSWood1	Beta-73629	Corn Creek flat	—	E_1	Carbonized wood	A	11.54±0.05	13.37±0.09	1.00	Quade and others, 1998	
CSC87-3b	A-4988	Corn Creek flat	—	E_1	Black mat	B	11.80±0.18	13.67±0.39	1.00	Quade and others, 1998	
CSC-27b	Beta-84316	Corn Creek flat	OCI-11	E_1	Carbonized wood	B	12.10±0.06	13.95±0.17	1.00	Quade and others, 1998	
CSCarb-30b	Beta-73969	Corn Creek flat	186/187	E_1	Carbonized wood	B	12.18±0.11	14.16±0.41	1.00	Quade and others, 1998	
CSCarb-27b	Beta-73466	Corn Creek flat	186/187	E_1	Carbonized wood	B	12.40±0.06	14.50±0.36	1.00	Quade and others, 1998	
CSCarb-28a	Beta-73967	Corn Creek flat	186/187	E_1	Carbonized wood	A	12.41±0.06	14.52±0.36	1.00	Quade and others, 1998	
CSCarb-28b	Beta-73968	Corn Creek flat	186/187	E_1	Carbonized wood	B	12.49±0.05	14.67±0.37	1.00	Quade and others, 1998	
CSC-29b	Beta-84315	Corn Creek flat	OCI-11	E_1	Carbonized wood	B	12.81±0.06	15.31±0.22	1.00	Quade and others, 1998	
NCySC-4b	Beta-73960	North Coyote Springs	—	E_2	Black mat	B	6.67±0.05	7.54±0.08	0.99	Quade and others, 1998	
NCySC-6b	A-5224	North Coyote Springs	—	E_2	Black mat	B	7.79±0.09	8.60±0.19	0.93	Quade and others, 1998	
NCySC-8b	A-5625	North Coyote Springs	—	E_2	Black mat	B	8.15±0.08	9.14±0.19	0.91	Quade and others, 1998	
NCySC-3b	Beta-73959	North Coyote Springs	—	E_2	Black mat	B	8.16±0.07	9.15±0.17	0.98	Quade and others, 1998	
NCySC-9b	A-5626	North Coyote Springs	—	E_2	Black mat	B	8.40±0.07	9.39±0.14	1.00	Quade and others, 1998	
NCySC-7b	Beta-73961	North Coyote Springs	—	E_2	Black mat	B	8.88±0.08	9.95±0.25	1.00	Quade and others, 1998	
NCySC-2b	Beta-73958	North Coyote Springs	—	E_2	Black nmat	B	10.39±0.06	12.23±0.20	0.95	Quade and others, 1998	
Cac.Spr.Carb-7b	A-5881	Cactus Springs	—	E_2	Black mat	B	10.06±0.20	11.77±0.64	1.00	Quade and others, 1998	
—	Beta-61581	Tule Springs Park area		D	Charcoal	A	26.80±0.70	30.8±1.5	0.00	McVicker and Spaulding, 1993	
—	Beta-61580	Tule Springs Park area		D	Charcoal	A	27.58±0.65	31.9±1.3	0.00	McVicker and Spaulding, 1993	
TS-1	GX-23064	Tule Springs Park quad	—	Qts_e	Organic mud	—	13.18±0.48	15.6±1.5	1.00	Bell and others, 1998	
TS-2	GX-23065	Tule Springs Park quad	—	Qts_e	Mixed organics	—	12.23±0.56	14.5±1.5	1.00	Bell and others, 1998	Carbonized wood, organic mud
TS-3	GX-23066	Tule Springs Park quad	—	Qts_e	Large snail	C	15.71±0.12	18.99±0.28	1.00	Bell and others, 1998	
TS-8	GX-23070	Tule Springs Park quad	—	Qts_e	Mixed organics	—	14.29±0.44	17.3±1.1	1.00	Bell and others, 1998	Disseminated charcoal, Carbonized wood
TS-9	GX-23071	Tule Springs Park quad	—	Qts_c	Organics/inorganics	—	29.46±0.39	33.52±0.83	1.00	Bell and others, 1998	Small snails, gastropods, clams, organic mud
TS-11	GX-23073	Tule Springs Park quad	—	Qts_e	Mixed organics	—	11.90±0.35	14.04±0.96	1.00	Bell and others, 1998	Disseminated charcoal, Carbonized wood
TS-12	GX-23074	Tule Springs Park quad	—	Qts_e	Mixed organics	—	11.53±0.35	13.45±0.75	1.00	Bell and others, 1998	Disseminated peat, organic mud
TS-13	GX-23075	Tule Springs Park quad	—	Qts_d	Mixed inorganics	C	29.56±0.39	33.63±0.80	1.00	Bell and others, 1998	Small snails, clams
TS-14	GX-23076	Tule Springs Park quad	—	Qts_d	Large snails	C	20.1±2.1	23.8±4.4	1.00	Bell and others, 1998	

Appendix 1. Summary of radiocarbon ages obtained previously for the Las Vegas Formation.—Continued

[Uncertainties for the calibrated ages are given at the 95 percent (2σ) confidence level. All other uncertainties are given at the 68 percent (1σ) confidence level. Map units: Qsc, unit C; Qsd, unit D; Qse, unit E. Analyzed fractions: A, humins (insoluble in base); B, humates or humic acids (soluble in base); C, carbonate. no., number; AMS, accelerator mass spectrometry; ^{14}C, radiocarbon; ka, kilo-annum (thousands of years before present); cal, calibrated; P, probability of the calibrated age falling within the reported range as calculated by CALIB v.7.1html; –, not applicable; >, greater than; m, meter; ~, approximately; quad., quadrangle]

Sample no.	AMS no.	Location	Section	Unit	Material dated	Fraction analyzed	^{14}C age (ka BP)	Age (cal ka BP)[1]	P	Original source	Sample notes[2]
TS-15	GX-23077	Tule Springs Park quad	—	Qts_d	Mixed inorganics	C	20.±0.16	24.58±0.48	1.00	Bell and others, 1998	Small snails, gastropods, clams
TS-17	GX-23079	Tule Springs Park quad	—	Qts_e	Mixed organics	—	10.±0.15	12.47±0.37	1.00	Bell and others, 1998	Disseminated carbonized wood, organic mud
TS-18	GX-23080	Tule Springs Park quad	—	Qts_e	Organic mud	—	11.59±0.31	13.45±0.68	1.00	Bell and others, 1998	
TS-19	GX-23081	Tule Springs Park quad	—	Qts_e	Mixed organics	—	11.81±0.35	13.94±0.96	1.00	Bell and others, 1998	Detrital charcoal, carbonized wood
TS-20	GX-23082	Tule Springs Park quad	—	Qts_e	Mixed organics	—	10.79±0.18	12.73±0.35	0.96	Bell and others, 1998	Disseminated charcoal, Carbonized wood
TS-21	GX-23083	Tule Springs Park quad	—	Qts_e	Organic mud	—	10.10±0.17	11.73±0.51	0.97	Bell and others, 1998	
TS-28	GX-23089	Tule Springs Park quad	—	Qts_e	Mixed organics	—	11.47±0.45	13.6±1.2	1.00	Bell and others, 1998	Disseminated peat, organic mud
TS-31	GX-23987	Tule Springs Park quad	—	Qts_e	Organic mud	—	12.68±0.43	15.0±1.3	1.00	Bell and others, 1998	
TS-23	GX-23084	Corn Creek Springs quad	—	Qts_d	Large snails	C	24.8±4.7	29±10	1.00	Bell and others, 1999	
TS-24	GX-23085	Corn Creek Springs quad	—	Qts_e	Organic mud	—	12.12±0.41	14.3±1.1	1.00	Bell and others, 1999	
TS-25	GX-23086	Corn Creek Springs quad	—	Qts_e	Organic mud	—	12.97±0.73	15.5±2.0	1.00	Bell and others, 1999	
TS-26	GX-23087	Corn Creek Springs quad	—	Qts_e	Organic mud	—	9.92±0.28	11.53±0.88	0.99	Bell and others, 1999	
TS-27	GX-23088	Corn Creek Springs quad	—	Qts_e	Organic mud	—	10.23±0.39	11.8±1.0	1.00	Bell and others, 1999	
TS-35	GX-23073	Corn Creek Springs quad	—	Qts_e	Mixed	—	12.67±0.51	15.0±1.4	1.00	Bell and others, 1999	Organic mud/disseminated charcoal
TS-36	GX-23992	Corn Creek Springs quad	—	Qts_d	Small snails	C	28.07±0.29	32.03±0.74	1.00	Bell and others, 1999	
TS-37	GX-23993	Corn Creek Springs quad	—	Qts_e	Charcoal	—	12.65±0.18	14.89±0.69	1.00	Bell and others, 1999	
TS-39	GX-24249	Corn Creek Springs quad	—	Qts_d	Mixed	—	19.3±2.4	22.9±5.2	1.00	Bell and others, 1999	Disseminated carbonized wood, organic mud
TS-40	GX-24250	Corn Creek Springs quad	—	Qts_e	Mixed	—	12.14±0.35	14.28±0.97	1.00	Bell and others, 1999	Disseminated charcoal, organic mud
TS-41	GX-24251	Corn Creek Springs quad	—	Qts_d	Small snails	C	32.84±0.82	37.0±1.9	1.00	Bell and others, 1999	
TS-44	GX-24253	Corn Creek Springs quad	—	Qts_e	Organic mud	—	9.94±0.18	11.58±0.52	0.95	Bell and others, 1999	
TS-45	GX-24481	Corn Creek Springs quad	—	Qts_d	Organics/inorganics	C	34.37±0.42	38.9±1.0	1.00	Bell and others, 1999	Small shells, organic mud
NV94RMF86CL+CM	Beta-84781	Corn Creek flat	OCI-11	E_1	Terrestrial snail	C	12.80±0.08	15.31±0.29	1.00	Quade and others, 2003	*Vallonia cyclophorella*
NV94ED86BU	Beta-84780	Corn Creek flat	OCI-11	D	Aquatic snail	C	17.73±0.09	21.46±0.32	1.00	Quade and others, 2003	*Pisidium* sp.
NV94ED86BT	Beta-84776	Corn Creek flat	OCI-11	D	Aquatic snail	C	17.77±0.09	21.52±0.31	1.00	Quade and others, 2003	*Pisidium* sp.
CSC-25	Beta-86430	Corn Creek flat	OCI-11	D	Terrestrial snail	C	17.82±0.06	21.60±0.23	1.00	Quade and others, 2003	*Stagnicola* sp.
NV94ED86BT	Beta-84777	Corn Creek flat	OCI-11	D	Aquatic snail	C	18.33±0.10	22.17±0.26	1.00	Quade and others, 2003	*Pisidium* sp.

Appendix 1. Summary of radiocarbon ages obtained previously for the Las Vegas Formation.—Continued

[Uncertainties for the calibrated ages are given at the 95 percent (2σ) confidence level. All other uncertainties are given at the 68 percent (1σ) confidence level. Map units: Qsc, unit C; Qsd, unit D; Qse, unit E. Analyzed fractions: A, humins (insoluble in base); B, humates or humic acids (soluble in base); C, carbonate. no., number; AMS, accelerator mass spectrometry; ^{14}C, radiocarbon; ka, kilo-annum (thousands of years before present); cal, calibrated; P, probability of the calibrated age falling within the reported range as calculated by CALIB v.7.1html; –, not applicable; >, greater than; m, meter; ~, approximately; quad., quadrangle]

Sample no.	AMS no.	Location	Section	Unit	Material dated	Fraction analyzed	^{14}C age (ka BP)	Age (cal ka BP)[1]	P	Original source	Sample notes[2]
NV94ED86BT	Beta-84778	Corn Creek flat	OCI-11	D	Ostracodes	C	18.36±0.10	22.19±0.26	1.00	Quade and others, 2003	*Strandesia meadensis*
NV94ED86BY	Beta-91926	Corn Creek flat	OCI-11	D	Aquatic snail	C	18.84±0.07	22.70±0.22	1.00	Quade and others, 2003	*Pisidium* sp.
NV94RMF86BS+BT+BU	Beta-84779	Corn Creek flat	OCI-11	D	Terrestrial snail	C	19.38±0.11	23.32±0.32	1.00	Quade and others, 2003	*Vallonia* sp. + Pupillid
NV94RMF86AU+AT+AS	Beta-85981	Corn Creek flat	OCI-11	B_3	Terrestrial snail	C	33.78±0.28	38.03±0.82	1.00	Quade and others, 2003	*Vallonia* sp. + Pupillid
CSC-14	Beta-86425	Corn Creek flat	OCI-11	B_3	Aquatic snail	C	34.23±0.30	38.80±0.73	1.00	Quade and others, 2003	*Gyraulus parvus*
NV94RMF86AU+AT	Beta-85985	Corn Creek flat	OCI-11	B_3	Aquatic snail	C	34.87±0.27	39.38±0.65	1.00	Quade and others, 2003	*Pisidium* sp.
NV94RMF86AS	Beta-85984	Corn Creek flat	OCI-11	B_3	Aquatic snail	C	35.85±0.29	40.49±0.69	1.00	Quade and others, 2003	*Pisidium* sp.
CSC-16	Beta-86426	Corn Creek flat	OCI-11	B_2	Aquatic snail	C	33.52±0.25	37.75±0.79	1.00	Quade and others, 2003	*Gyraulus parvus*
NV94RMF86M+L	Beta-85986	Corn Creek flat	OCI-11	B_2	Terrestrial snail	C	35.84±0.29	40.48±0.69	1.00	Quade and others, 2003	*Vallonia* sp. + Pupillid
NV94RMF86AW	Beta-83993	Corn Creek flat	OCI-11	B_2	Terrestrial snail	C	37.39±0.69	41.7±1.1	1.00	Quade and others, 2003	*Vallonia* sp.
NV94RMF86AT	Beta-83994	Corn Creek flat	OCI-11	B_2	Terrestrial snail	C	37.39±0.73	41.6±1.2	1.00	Quade and others, 2003	*Vallonia* sp.
NV94RMF86AW	Beta-84784	Corn Creek flat	OCI-11	B_2	Aquatic snail	C	37.54±0.90	41.7±1.5	1.00	Quade and others, 2003	*Pisidium* sp.
NV94RMF86AT	Beta-84783	Corn Creek flat	OCI-11	B_2	Aquatic snail	C	39.0±1.1	43.0±1.7	1.00	Quade and others, 2003	*Pisidium* sp.
NV94RMF86M+L	Beta-84782	Corn Creek flat	OCI-11	B_2	Aquatic snail	C	40.4±1.3	44.1±2.0	1.00	Quade and others, 2003	*Pisidium* sp.
NV94RMF86AE+AF	Beta-84774	Corn Creek flat	OCI-11	B_2	Aquatic snail	C	40.7±1.3	44.3±2.1	1.00	Quade and others, 2003	*Pisidium* sp.
NV94RMF86AE+AF	Beta-84775	Corn Creek flat	OCI-11	B_2	Terrestrial snail	C	41.8±1.5	45.5±2.7	1.00	Quade and others, 2003	*Vertigo berryi +vallonia* sp.
RMF93NV1d,-0.25m	Beta-74329	Corn Creek flat	LPM-34	D	Aquatic snail	C	16.39±0.07	19.79±0.22	1.00	Quade and others, 2003	*Pisidium* sp.
RMF93NV1d,-0.25m	Beta-76433	Corn Creek flat	LPM-34	D	Terrestrial snail	C	16.85±0.10	20.31±0.27	1.00	Quade and others, 2003	*Vallonia* sp.; Age listed as 18,850±100 ^{14}c years in table 1
RMF93NV1g,-0.75m	Beta-76434	Corn Creek flat	LPM-34	D	Terrestrial snail	C	25.34±0.18	29.41±0.51	1.00	Quade and others, 2003	*Vallonia* sp.
RMF93NV1f,-1.00m	Beta-74330	Corn Creek flat	LPM-34	D	Aquatic snail	C	26.62±0.16	30.84±0.25	1.00	Quade and others, 2003	*Pisidium* sp.
Cac.Spr.Carb-8	Beta-86427	Cactus Springs	LPM-35	E_2	Carbonized wood	—	10.03±0.06	11.52±0.25	0.99	Quade and others, 2003	
Cac.Spr.QUADE90-100	Beta-86429	Cactus Springs	LPM-35	E_1	Terrestrial snail	C	12.30±0.06	14.35±0.30	1.00	Quade and others, 2003	Succineidae
Cac.Spr.QUADE45-55	Beta-86428	Cactus Springs	LPM-35	E_1	Aquatic snail	C	12.89±0.06	15.41±0.23	1.00	Quade and others, 2003	*Gyraulus circumstriatus*
NV94RMF84O	Beta-83992	Cactus Springs	LPM-35	E_1	Terrestrial snail	C	13.35±0.06	16.05±0.21	1.00	Quade and others, 2003	*Pupilla muscorum*
NV94RMF84N	Beta-83995	Cactus Springs	LPM-35	E_1	Terrestrial snail	C	13.69±0.08	16.54±0.30	1.00	Quade and others, 2003	*Euconulus fulvus*
NV94RMF84N	Beta-83991	Cactus Springs	LPM-35	E_1	Terrestrial snail	C	13.27±0.26	15.93±0.77	1.00	Quade and others, 2003	*Pupilla muscorum*
NV94RMF84N	Beta-83988	Cactus Springs	LPM-35	E_1	Terrestrial snail	C	13.42±0.06	16.14±0.21	1.00	Quade and others, 2003	*Vertigo berryi*
NV94RMF84M	Beta-83989	Cactus Springs	LPM-35	E_1	Terrestrial snail	C	13.63±0.06	16.44±0.24	1.00	Quade and others, 2003	*Euconulus fulvus*
NV94RMF84M	Beta-83990	Cactus Springs	LPM-35	E_1	Terrestrial snail	C	13.56±0.06	16.35±0.23	1.00	Quade and others, 2003	*Pupilla muscorum*
GPSW-1	252832	Gass Peak SW quad	—	E_2	Charcoal	A	6.98±0.07	7.81±0.13	1.00	Ramelli and others, 2011	
GPSW-2	294464	Gass Peak SW quad	—	E_2	Charcoal	A	7.77±0.05	8.53±0.10	1.00	Ramelli and others, 2011	

Appendix 1. Summary of radiocarbon ages obtained previously for the Las Vegas Formation.—Continued

[Uncertainties for the calibrated ages are given at the 95 percent (2σ) confidence level. All other uncertainties are given at the 68 percent (1σ) confidence level. Map units: Qsc, unit C; Qsd, unit D; Qse, unit E. Analyzed fractions: A, humins (insoluble in base); B, humates or humic acids (soluble in base); C, carbonate. no., number; AMS, accelerator mass spectrometry; ^{14}C, radiocarbon; ka, kilo-annum (thousands of years before present); cal, calibrated; P, probability of the calibrated age falling within the reported range as calculated by CALIB v.7.1html; –, not applicable; >, greater than; m, meter; ~, approximately; quad., quadrangle]

Sample no.	AMS no.	Location	Section	Unit	Material dated	Fraction analyzed	^{14}C age (ka BP)	Age (cal ka BP)[1]	P	Original source	Sample notes[2]
GPSW-3	289513	Gass Peak SW quad	—	E_2	Charcoal	A	9.40±0.05	10.63±0.12	1.00	Ramelli and others, 2011	
GPSW-4	269140	Gass Peak SW quad	—	E_2	Black mat	A	9.79±0.07	11.22±0.14	0.96	Ramelli and others, 2011	
GPSW-5	279304	Gass Peak SW quad	—	E_2	Charcoal	A	10.48±0.06	12.35±0.23	1.00	Ramelli and others, 2011	
GPSW-6	297878	Gass Peak SW quad	—	E_2	Charcoal	A	11.53±0.05	13.37±0.09	1.00	Ramelli and others, 2011	
GPSW-7	279305	Gass Peak SW quad	—	E_1	Charcoal	A	12.43±0.06	14.56±0.38	1.00	Ramelli and others, 2011	
GPSW-8	279251	Gass Peak SW quad	—	E_1	Charcoal	A	12.84±0.06	15.35±0.22	1.00	Ramelli and others, 2011	
GPSW-9	279306	Gass Peak SW quad	—	E_1	Charcoal	A	13.39±0.06	16.10±0.21	1.00	Ramelli and others, 2011	
GPSW-10	178778	Gass Peak SW quad	—	E_0	Charcoal	A	14.78±0.04	17.98±0.15	1.00	Ramelli and others, 2011	
GPSW-11	264965	Gass Peak SW quad	—	E_0	Charcoal	A	16.30±0.07	19.71±0.22	1.00	Ramelli and others, 2011	
GPSW-12	279250	Gass Peak SW quad	—	E_0	Charcoal	A	16.41±0.07	19.80±0.22	1.00	Ramelli and others, 2011	
GPSW-13	272512	Gass Peak SW quad	—	E_0	Charcoal	A	16.82±0.07	20.28±0.22	1.00	Ramelli and others, 2011	
GPSW-14	297880	Gass Peak SW quad	—	E_0	Charcoal	A	17.30±0.08	20.87±0.26	1.00	Ramelli and others, 2011	
GPSW-15	282792	Gass Peak SW quad	—	E_0	Charcoal	A	17.37±0.06	20.96±0.24	1.00	Ramelli and others, 2011	
GPSW-16	252833	Gass Peak SW quad	—	D	Organic sediment	A	20.31±0.12	24.45±0.39	1.00	Ramelli and others, 2011	
GPSW-17	268971	Gass Peak SW quad	—	D	Black mat	A	25.95±0.17	30.18±0.52	1.00	Ramelli and others, 2011	
GPSW-18	268972	Gass Peak SW quad	—	D	Black mat	A	27.85±0.18	31.68±0.47	1.00	Ramelli and others, 2011	
GPSW-19	264964	Gass Peak SW quad	—	D	Charcoal	A	31.10±0.24	35.04±0.50	1.00	Ramelli and others, 2011	

[1]Calibrated ages were calculated using CALIB v.7.1html, IntCal13.14C dataset; limit 50.0 calendar ka BP. Calibrated ages are reported as the midpoint of the calibrated range. Uncertainties are calculated as the difference between the midpoint and either the upper or lower limit of the calibrated age range, whichever is greater (reported at the 95 percent [2σ] confidence level). Multiple ages are reported when the probability of a calibrated age range exceeds 0.05.

[2]The notes included here were taken verbatim from the original manuscripts.

Appendix 2. Summary of Thermoluminescence Ages Obtained Previously for the Las Vegas Formation

[Data from Page and others, 2005. Map units: Qso, old fine-grained spring deposits; Qsab, units A and B (undifferentiated); Qfw, fine-grained deposits of Whitney Mesa; Qse, unit E; Qsc, unit C; Qsd, unit D; Qsa, unit A; Qsb, unit B. no., number; N, north; W, west; TL, thermoluminescence;ka, kilo-annum (thousands of years before present)]

Sample no.	Latitude (°N)	Longitude (°W)	Unit	Minimum TL age (ka)	Maximum TL age (ka)
LV-1[1]	36.26722	115.06222	Qso	226	399
LV-3	36.28547	115.12958	Qsab	99	120
LV-6	36.08158	115.06342	Qfw	232	379
LV-14	36.34842	115.28753	Qse	11	17
LV-15	36.34842	115.28753	Qse	10	15
LV-16	36.34967	115.28575	Qsc	24	36
LV-17	36.31853	115.19619	Qsd	24	41
LV-18	36.31933	115.19847	Qsc	35	56
LV-19	36.31914	115.19108	Qsa	131	225
LV-20	36.31914	115.19108	Qsb	89	144

[1]Sample age originally reported as 433–226 ka by Lundstrom and others, 1998.

Appendix 3. Summary of Sample Information and Optically Stimulated Luminescence Ages From This Study

[Uncertainties for all dose parameters are given at the 68 percent (1σ) confidence level interval, and ages are given at the 95 percent (2σ) confidence level. ID, identifier; %, percent; K, potassium; U, uranium; Th, thorium; ppm, part per million; Gy, gray (unit of measure for luminescence dose); ka, kilo-annum (thousands of years before present); OSL, optically stimulated luminescence; n/a, not applicable]

Sample ID	Section	Easting[1]	Northing[1]	Member/ bed	Water content (%)[2]	K (%)	U (ppm)	Th (ppm)	Cosmic dose addition (Gy/ka)[3]	Total dose rate (Gy/ka)[4]	Equivalent dose (Gy)[4]	Age (ka)
OSL19	D-1	654819	4022979	D_2	0 (24)	1.23±0.02	2.40±0.07	4.69±0.13	0.19±0.02	2.20±0.06	66±3	30±3
OSL10	B-5	664317	4020174	B_3	1 (66)	1.08±0.01	1.83±0.03	4.81±0.05	0.22±0.02	1.68±0.03	63±6	37±7
OSL7	B-4	663221	4020539	B_3	3 (63)	0.85±0.01	2.49±0.04	3.92±0.05	0.14±0.01	1.50±0.03	61±2	40±4
OSL9	B-5	664317	4020174	B_2	3 (68)	1.01±0.01	2.02±0.03	4.57±0.05	0.19±0.01	1.63±0.03	70±3	43±4
OSL6	B-4	663221	4020539	B_2	2 (27)	0.60±0.01	2.98±0.04	2.54±0.04	0.13±0.01	1.49±0.02	68±5	46±7
OSL12	B-8	661875	4020878	B_2	0 (64)	1.04±0.02	1.81±0.04	4.88±0.13	0.15±0.01	1.59±0.06	63±3	40±5
OSL18	B-3	659274	4022359	B_1	0 (15)	0.68±0.01	1.21±0.03	3.22±0.12	0.19±0.02	1.35±0.06	76±4	56±8
OSL8	B-5	664317	4020174	B_1	2 (61)	0.76±0.01	1.66±0.03	3.70±0.04	0.17±0.01	1.29±0.02	78±4	60±7
OSL17	B-2	660255	4021627	$B_{1\text{-wet}}$	1 (34)	0.58±0.01	1.32±0.04	3.32±0.12	0.16±0.01	1.15±0.05	97±6	84±13
OSL5	B-4	663221	4020539	B_1	5 (25)	0.88±0.01	1.70±0.03	4.36±0.05	0.11±0.01	1.58±0.02	137±6	87±7
OSL2	A-4	664281	4020284	A	1 (50)	0.77±0.01	1.04±0.03	3.28±0.04	0.14±0.01	1.17±0.02	Saturated	n/a
OSL4	A-1	664555	4020071	A	1 (110)	0.76±0.01	1.87±0.03	3.16±0.04	0.16±0.01	1.11±0.02	Saturated	n/a
OSL1	A-4	664281	4020284	A	2 (91)	0.57±0.01	1.97±0.03	2.22±0.04	0.09±0.01	0.95±0.02	Saturated	n/a
OSL15	A-5	663075	4020598	A	1 (40)	0.33±0.01	0.84±0.04	2.11±0.09	0.16±0.01	0.76±0.04	Saturated	n/a
OSL3	A-1	664555	4020071	X	1 (46)	0.35±0.01	1.22±0.03	1.24±0.04	0.12±0.01	0.73±0.03	Saturated	n/a

[1]Universal Transverse Mercator coordinates are all in zone 11S.

[2]Field moisture (complete sample saturation). Ages were calculated using 50 percent of saturation values.

[3]Cosmic doses and attenuation with depth were calculated following Prescott and Hutton (1994). See the text in the section “Luminescence Dating Methods” for details.

[4]Dose rate and equivalent doses for fine-grained (180–90 millimeter) quartz OSL. A linear + exponential (exponential only) fit was used to calculate the equivalent dose for OSL.

Support provided by the Science Publishing Network,
Denver Publishing Service Center

For more information concerning the research in this report, contact the
Center Director, USGS Geosciences and Environmental
Change Science Center

Box 25046, Mail Stop 980
Denver, CO 80225
(303) 236-5344

Or visit the Geosciences and Environmental Change Science Center
website at https://gec.cr.usgs.gov/

USGS

Springer and others—**The Las Vegas Formation**—Professional Paper 1839

ISSN 1044-9612 (print)
ISSN 2330-7102 (online)
https://doi.org/10.3133/pp1839

ISBN 978-1-4113-4237-8